CSIRO LIBRARY NETWORK SYSTEM
3 9009 00250538 2



C.S.I.R.O. ATMOSPHERIC RESEARCH
2 DEC 1988
LIBRARY

THE SCIENTIFIC APPLICATION OF BASELINE OBSERVATIONS OF ATMOSPHERIC COMPOSITION

ASPENDALE, AUSTRALIA

7-9 November, 1984.

EXTENDED ABSTRACTS

DIVISION OF ATMOSPHERIC RESEARCH.

Historical note :

In 1953 the CSIRO Division of Atmospheric Research (then much smaller, and known as the 'Section of Meteorological Physics) was re-located from Highett to its present site at Aspendale, a bayside Melbourne suburb named after a racing mare.

The Aspendale site, originally part of the ancient Carrum Swamp and once used as farmland and a public racecourse, provided space for growth and was close to the Edithvale field station used for the Division's micro-meteorological programmes.

During recent years an increase in buildings, facilities and staff numbers has been necessary to support the increasing diversity of the Divisional research effort.

Aspendale has changed from a sparsely-settled holiday area to a residential suburb, many of whose residents commute daily to the city by rail or road.

H. S. Goodman.
Oct. 1984.

Workshop: The Scientific Application of Baseline Observations of Atmospheric Composition held at the CSIRO Division of Atmospheric Research, Aspendale, Australia, November 7-9, 1984.
Jointly funded by the CSIRO and the Bureau of Meteorology.

Convenor, G. I. Pearman.
Secretary, V. Jemmeson.

Extended abstracts published by Balcombe D. & R. Service Pty. Ltd. Mordialloc, 3195 Australia.

C.S.I.R.O. ATMOSPHERIC RESEARCH
2 DEC 1988
LIBRARY

P R E F A C E

Dear Participant,

Welcome to Melbourne and to our Conference on the Scientific Application of Baseline Observations of Atmospheric Composition. For more than ten years now, members of the Division of Atmospheric Research have been working towards the establishment of an observatory for the measurement of the composition of background air. We are pleased that a facility has been constructed for this purpose at Cape Grim, Tasmania and already provides scientists with important information concerning background concentrations of atmospheric constituents in a region of the world relatively devoid of research institutes and observational programs. However, there are heavy responsibilities that follow from the establishment of the station. We must ensure both the continuity of the existing projects as well as the evolution of a program dedicated to providing data which meet the requirements of the global scientific community for the resolution of a wide spectrum of problems. Initially, Cape Grim, and for that matter some of the other similar observatories around the world, was founded particularly to document the changes in the atmospheric composition that were potentially significant in climatic stability. This remains an important objective. But, the last decade has seen a major advancement in knowledge of atmospheric chemistry. It has become clear that background observations of the composition of the atmosphere are of much wider general importance.

There is the need to improve our understanding of the natural processes that result in the circulation of chemical elements through the atmosphere, oceans and biosphere if we are to be able to assess the large-scale environmental consequences of human activities on the planet. The atmosphere is, for many of these elements a reservoir whereby global dispersion is achieved, or a reaction vessel wherein chemical transformations occur. Many measurement programs already underway relate to the establishment of a sound understanding of cycles of elements such as carbon, nitrogen and sulphur. Much more remains to be done.

Further, fluid dynamicists are advancing our ability to represent in numerical form, the dynamical and physical behaviour of the global atmosphere. In this area there is the exciting possibility of exchange of information between the dynamicists and the atmospheric chemists. On the one hand, some chemical constituents are useful tracers of atmospheric motions and as such are valuable in the evaluation of transport models. On the other, the chemist who studies compounds or aerosols with lifetimes of more than a few hours is confronted by the interaction of chemistry, air-surface exchanges and transport and the need to adequately account for transport in any interpretation. In the SABOAC meeting we are fortunate to have present people interested in both approaches and I am sure this will prove to be most profitable.

It is the breadth of this potential application of the Cape Grim facility and other similar observatories which we hope to explore through this Conference. We hope that the meeting will serve to demonstrate the exciting diversity of applications for baseline data and the rapidly evolving nature of the measurement requirements.

It is necessary for me to apologize in advance for the fullness of the program. The response to the meeting has been such that the number of participants is about three times greater than originally planned. Our lecture theatre is not really designed for such large groups. We will do everything possible to ensure that the length of the sessions and the number of people in the theatre doesn't become too trying. We do not pretend that twenty minutes is a reasonable time to present a high quality paper, but we hope you will agree that the advantage of having the opportunity to meet and hear such a wide range of excellent speakers will make up for these short-comings.

I wish to acknowledge the financial support of the CSIRO and the Bureau of Meteorology and the assistance of my colleagues, in particular Val Jemmeson, in the preparation of this meeting.

Graeme Pearman.

C O N T E N T S

LOCALITY GUIDES :	Maps	viii
	Floor Plan - Div. of Atmos. Research, CSIRO.	ix
MEETING GUIDE	....	x
LIST OF PARTICIPANTS	....	xii
PROGRAMME SUMMARY.	....	xvi

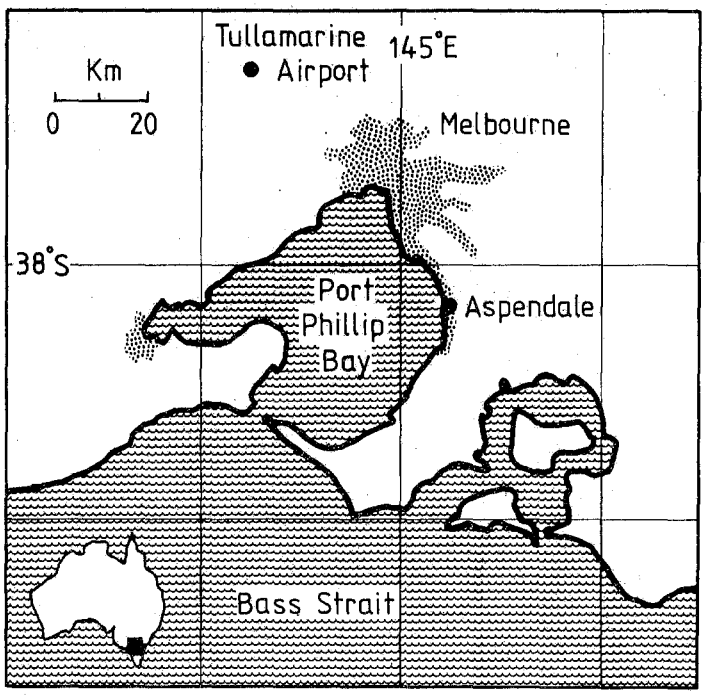
EXTENDED ABSTRACTS

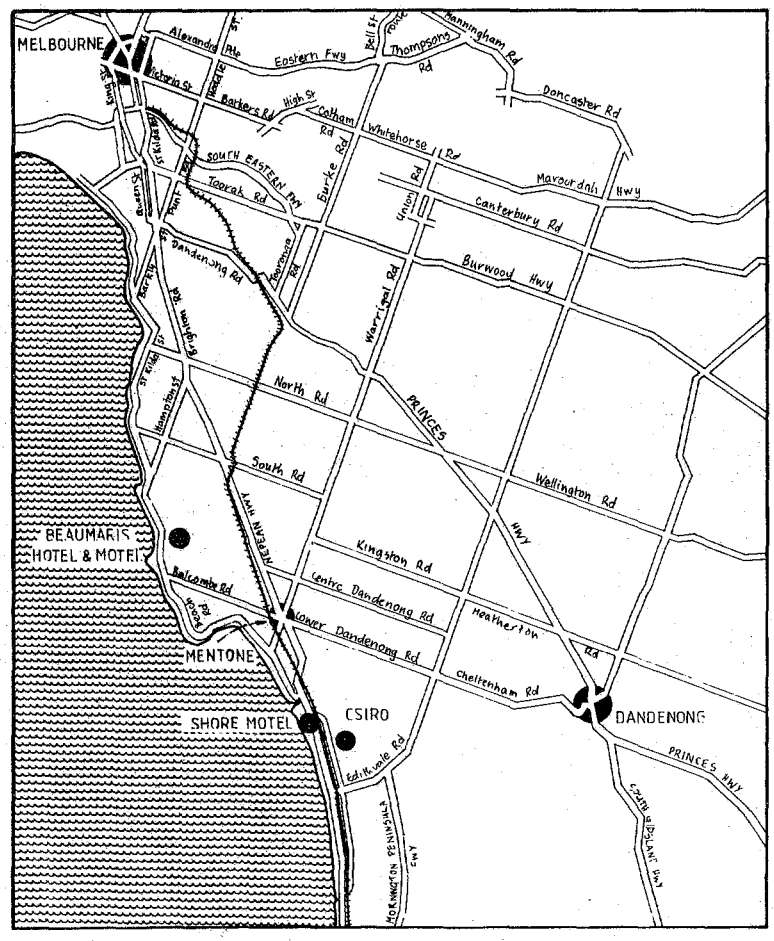
Alyea, F.	Implications for large scale transport from 5 years of ALE data.	1
Ayers, G., J.P.Ivey and H.S. Goodman.	Excess sulfate and methanesulfonate in aerosol samples from Cape Grim.	2
Barrie, L.	* Features of the atmospheric cycle of aerosol trace elements and sulphur dioxide revealed by baseline research studies in Canada.	
Bigg, E.K.	Baseline observations of cloud condensation nuclei at Cape Grim, Tasmania.	3
Bodhaine, B.	The GMCC aerosol monitoring program.	4
Cunnold, D.	Fluorocarbons lifetime and releases from 5 years of ALE data.	7
Duce, R.A.	Aerosol species at the SEAREX north and south Pacific sites.	9
Dutton, E. and J.DeLuisi	Interpretation of apparent atmospheric transmission using solar photometer precipitable water measurements.	12
Ehhalt, D. and J.Rudolph	Light non methane hydrocarbons in the background troposphere.	15
Enting, I. G.	Preliminary studies with a two-dimensional model using transport fields from a GCM.	18
Fehsenfield, F. C. et al	Background ozone and anthropogenic impact in the Colorado mountains.	23
Fraser, P.J. and P.Hyson and R.A. Rasmussen.	Methane and carbon monoxide in the southern hemisphere.	26

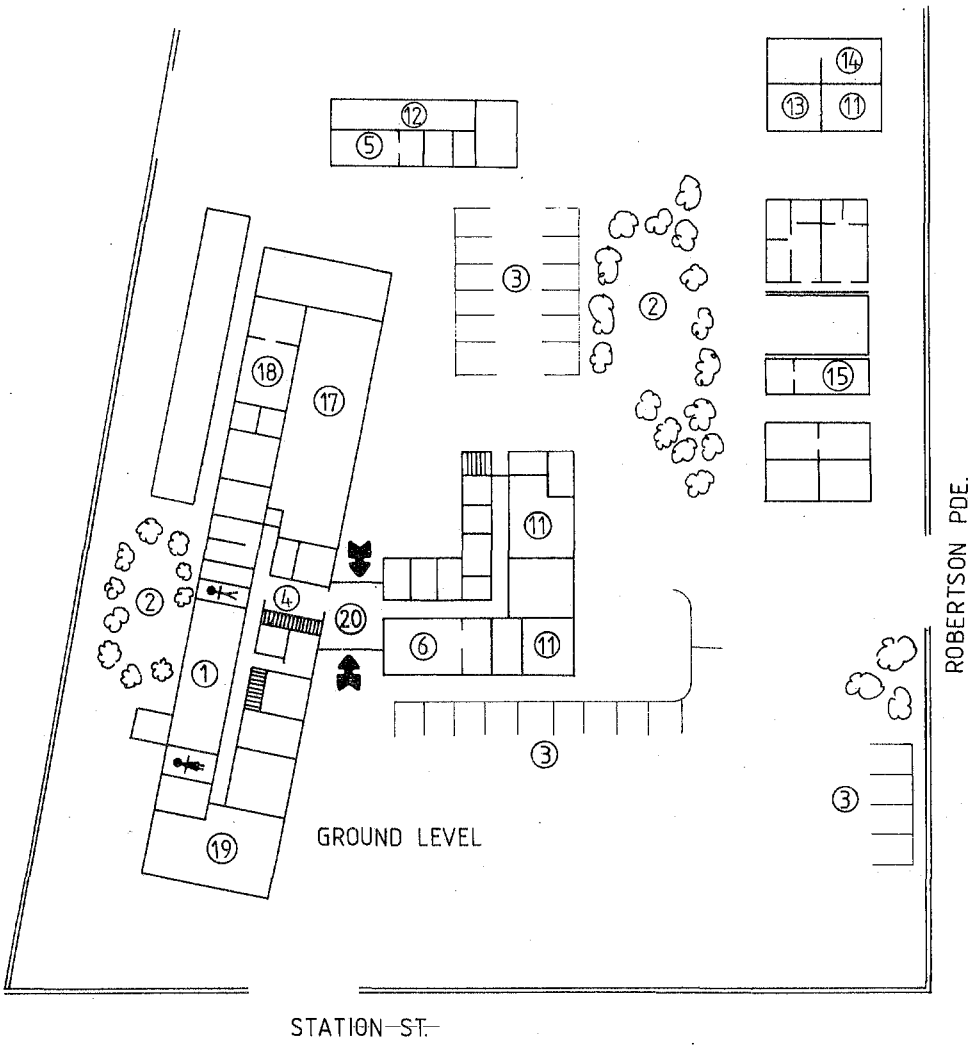
Fung, I. et al	On the variability of CO_2 exchange between the atmosphere and the biosphere.	28
Galbally, I.E.	Long term changes in atmospheric nitrous oxide.	31
Gammon, R. et al	The 1982/83 ENSO event: the response of the global atmospheric CO_2 distribution.	32
Gras, J. and A.Adriaansen.	Concentration and size variation of condensation nuclei.	34
Heinzenberg, J.	What can we learn from aerosol measurement at baseline stations?	38
Herbert, G.A. and J.Harris.	Trajectory representation of flow conditions.	41
Hov, Ø and Ivar S.A.Isaksen	Interpretation of trace gas measurements at high northern latitudes and other remote locations.	44
Ito, T.	Study of background aerosols in the Antarctic troposphere.	46
Jaenicke, R. et al	Information about atmospheric aerosols dormant in measuring series - four examples.	49
Keeling, C. and W.G. Mook.	Sources and sinks of atmospheric carbon dioxide deduced from $^{13}C/^{12}$ ratio.	52
Likens, G. et al.	The chemistry of precipitation in Katherine, Australia.	56
Logan, J.A.	Tropospheric ozone, seasonal patterns and trends.	59
Mendonca, R. et al.	Atmospheric transmission decreases and stratospheric warming at Mauna Loa during the two years after the El Chichon volcanic eruption.	62
Noller, B. et al.	Acidity of rainfall in the Alligator Rivers region, Northern Territory, Australia.	66
Pearman, G. and P. Hyson	Global transport and interreservoir exchange of CO_2 with particular reference to the effect on concentration and isotopic distribution.	67

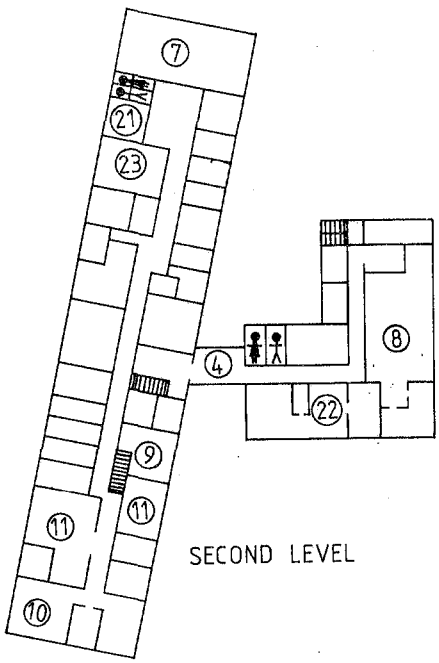
Pearman, G. et al.		Interannual variations of atmospheric CO_2 concentration.	70
Peterson, J.		Measurements of atmospheric CO_2 at Barrow, Alaska from the U.S. NOAA/GMCC program.	72
Platt, C.M.R.		The interpretation of atmospheric turbidity measurements.	75
Plumb, R.A.		The zonally-averaged transport characteristics of a GCM and a test of the validity of "K-Theory" as a parameterization of eddy transport.	77
Prather, M.		Simulations of chlorofluorocarbons with a three-dimensional model.	79
Prinn, R.G. and A.Golombek		A global three-dimensional model of the circulation and chemistry of $CFCl_3$, CF_2Cl_2, CH_3CCl_3, CCl_4 and N_2O.	83
Rasmussen, R.	*	Atmospheric isoprene: global significance.	
Rowland, S. and D. Blake	*	World-wide increase in tropospheric methane, 1978-1984.	
Seiler, W.	*	Results on measurements of several trace substances at Cape Point, South Africa.	
Shaw, G.	*	The microphysical and chemical properties of the Arctic haze and its relation to air mass systems and transport pathways.	
Steele, P et al.	*	Global distribution of atmospheric methane and aspects of interpretation of these data.	
Watson, R.	*	How baseline observations are utilised and needed in order to understand tropospheric and stratospheric chemistry.	
Whittlestone, S.		Radon measurements as an aid to interpretation of atmospheric monitoring.	84

* Abstracts not available at date of printing.
(Late abstracts may be available as loose-leaf inserts).


Tullamarine
Airport
145°E
Km
0
20
Melbourne
38°S
Port
Phillip
Bay
Aspendale
Bass Strait


MELBOURNE
Alexandra Pde
Eastern Fwy
Bell St
Thompsons Rd
Cunningham Rd
Victoria St
Hoddle St
Barkers Rd
High St
Cotham Rd
Doncaster Rd
Whitehorse Rd
Burke Rd
SOUTH EASTERN FWY
Toorak Rd
Union Rd
Mavoorndn Hwy
Canterbury Rd
Queens St
Punt Rd
Dandenong Rd
Tooronga Rd
Burwood Hwy
Warrigal Rd
St Kilda
Nepean Hwy
North Rd
PRINCES
South Rd
Wellington Rd
HWY
BEAUMARIS
HOTEL & MOTEL
Kingston Rd
Balcombe Rd
Centre Dandenong Rd
Heatherton Rd
MENTONE
Lower Dandenong Rd
Cheltenham Rd
SHORE MOTEL
CSIRO
DANDENONG
Edithvale Rd
PRINCES HWY
MORNINGTON PENINSULA HWY
SOUTH GIPPSLAND HWY





LEGEND

TOILETS

STAIRS

1. CANTEEN
2. GARDEN AREAS
3. CARPARKING AREAS
4. PHOTOCOPIERS
5. CSIDA ROOM
6. OFFICE
7. LECTURE THEATRE
8. LIBRARY
9. CONFERENCE ROOM
10. CHIEF'S OFFICE
11. CHEMISTRY LABORATORIES
12. COMPUTING CENTRE
13. RADIATION LABS.
14. LIDAR ROOM
15. WIND TUNNEL
16. STORE
17. MECHANICAL WORKSHOP
18. CARPENTER WORKSHOP
19. GFD LABORATORY
20. FOYER / MAIN ENTRANCE
21. GRAPHICS
22. ELECTRONICS WORKSHOP
23. PHOTOGRAPHY

FLOOR PLAN OF CSIRO DIVISION OF ATMOSPHERIC RESEARCH NOVEMBER 1984

MEETING GUIDE

Venue : The talks will be held in the Lecture Theatre of the CSIRO Division of Atmospheric Research with closed circuit video coverage available in the Conference Room.

Talks: 30 Minutes has been allowed for each participant. We appreciate that this is too short for adequate presentation of a complete paper. However, it is absolutely essential to keep to this time so that everyone has equal time. Chairmen are advised to insist on 20 minutes for the presentation of the paper and 10 minutes for discussion.

Slides should be handed to the projectionist at least one half day before your talk is scheduled. All other aids are available but please ensure your requirements are known by contacting either Mr. David Whillas, the projectionist or the Conference Secretary, well ahead of time.

Publications:

1. Extended Abstracts will be distributed before the Conference.
2. Manuscripts should be handed to the Secretary as soon as possible after arrival. This will assist the Editor to quickly select referees (possibly from other meeting participants) and hasten the publication process.

Morning/Afternoon Coffee and Lunches: Refreshments will be taken in the Canteen on the ground floor. There will be no charge.

Lunches will be provided as the Aspendale shopping center has very limited facilities. A charge of $2.50 per head will be levied.

Accommodation: As stated previously, accommodation is limited due to the demand from golfers and other sports enthusiasts. It will be necessary for you to check immediately with your motel/hotel to ascertain whether they can provide for you after the 10th November. Should there be a problem it can be quickly resolved by taking an extra nights accommodation further down the 'Bay' in Frankston. If in doubt about accommodation contact the Secretary.

Transport: There will be sufficient vehicles to collect participants from the major accommodation houses at 8 a.m. In addition, if you require help to move from one place to another please make this known to the Secretary who will endeavour to assist you.

Cape Grim Visit: Please confirm with the Secretary your intention to join the group visiting Cape Grim on Saturday, 10th November, 1984. It is envisaged that this trip will leave around 9 a.m. returning at approximately 5.00 p.m. The cost will be around <$100. Firm numbers will be required by 7th November, 1984.

Tourist Information: Tourist information and maps will be in your satchel. Please make known to the Secretary, specific needs.

Entertainment: An 'Icebreaker' function will be held on Wednesday evening the 7th November, 1984 in the canteen, immediately following the last paper. Weather permitting, a 'sausage sizzle' will be held at the Division on Friday evening. Cost $5. Local sight-seeing will be informally organised.

Local Eating Houses:

Expensive (but good)
~~Aspendale, Nepean Highway. "Le Coq au Vin" (French). Licensed.~~
~~(Select your own lobster from live lobster tank) Telephone 580 2085~~
"Chandelier Room" Beaumaris Hotel, Beaumaris. Licensed.
Mentone Hub Restaurant, Mentone, Nepean Highway. Licensed.

Medium Price Range.
"Dragon Garden" Mordialloc, (Close by Post Office) Nepean Highway, Mordialloc. (Chinese). BYO
"King Yuen" (Rear of 'Nautilus'), Balcombe Rd., Mentone, Mentone. BYO (Chinese)
"Billabong" Restaurant, Royal Oak Hotel, Nepean Highway, Mentone. Licensed.
"Spinnaker" Restaurant, Mordialloc Hotel, Nepean Highway, Mordialloc. Licensed.
"Bistro" Beaumaris Hotel, Beach Road, Beaumaris. Licensed.

Take-away Food.
All suburbs have a variety of inexpensive 'take-away' food shops.

Note:
Hotels close at 10.15 p.m. unless a meal is being served. General stores or "milk bars" are often open until 9 p.m.

Telephone Calls.
Local calls may be made from the Division by dialling "0".
Overseas calls need to be placed through the Receptionist by dialling "9".

Photocopying.
Please contact the General Office.

Travel.
The Divisional Staff Travel Clerk in the General Office will be pleased to assist you.

Banking.
Banks in Australia are open from 9.30 a.m. until 4 p.m. Monday to Thursday and 9.30 a.m. until 5 p.m. Friday. Please ensure that you have your passport and identification papers with you when changing money.

Suburban Travel.
A number of schemes exist for travelling on the suburban rail line, e.g. 'off-peak' The cost of a daily 'travel card' from Aspendale to Melbourne is $3.50. This also allows for travel on suburban trams. Trains run approximately every 20 minutes.

PARTICIPANTS

Dr. F.N. Alyea,
CAP Incorporated,
417 Chestnut Ridge Drive
ATLANTA. Georgia. 30338 U.S.A.

Dr. G. Ayers,
CSIRO Div. of Atmos. Res.,
Private Mail Bag No. 1.,
MORDIALLOC. VIC. 3195 Australia

Dr. E.K. Bigg,
CSIRO Div. of Atmos. Res.,
Cloud Phys. lab.,
P.O. Box 134,
EPPING. N.S.W. 2121 Australia

Dr. L. Barrie,
Atmos. Env. Service,
Dept. of Environment,
DOWNSVIEW. ONTARIO. Canada

Prof. H. Bloom,
C/- Dept. of Chemistry,
Univ. of Tasmania,
HOBART. TAS. 7001 Australia

Dr. B. Bodhaine
NOAA ERL/Air Resources Lab.,
GMCC,
BOULDER. CO. 80303 U.S.A.

Mr. Harry Burton
Antarctic Division,
KINGSTON. TAS. 7150 Australia

Dr. T. Clarkson,
N.Z Met. Service,
P.O. Box 722
WELLINGTON. N.Z.

Dr. R. Crawford
Oregon Graduate Centre,
19600 N.W. Walker Road,
BEAVERTON. OREGON. 97006 U.S.A.

Dr. D.M. Cunnold,
CAP Incorporated
4170 Chestnut Ridge Drive
ATLANTA. GEORGIA 3038 U.S.A.

Dr. R. Dubs
CSIRO Inst. of Phys. Sciences,
P.O. Box 225,
DICKSON. A.C.T. 2602 Australia

Dr. R.A. Duce,
Graduate School of Oceanography,
Box 3, Univ. of Rhode Is.,
KINGSTON. R.I. 02881 U.S.A.

Dr. E. Dutton,
NOAA ERL/Air Resources Lab.,
GMCC,
BOULDER. CO. 80303 U.S.A.

Dr. A.J. Dyer,
61 Barmah Street,
MOUNT ELIZA. VIC. 3930 Australia

Dr. D.H. Ehhalt,
Inst. for Atmos. Chemistry,
Kernforschungsanlage Julich,
Postbox 1913,
D-5170 JULICH. F.R.G.

Dr. I.G. Enting,
CSIRO Div. of Atmos. Res.,
Private Mail Bag No. 1
MORDIALLOC. VIC. 3195 Australia

Dr. F.C. Fehsenfeld,
Aeronomy Lab., RE/AL4,
ERRL NOAA,
BOULDER. CO. 80303 U.S.A.

Dr. B. Forgan,
Director,
Australian Baseline Air Pollution
Station,
SMITHTON. TAS. 7330 Australia

Dr. Paul Fraser,
CSIRO Div. of Atmos. Res.,
Private Mail Bag No. 1,
MORDIALLOC. VIC. 3195 Australia

Dr. R. Francey,
CSIRO Div. of Atmos. Res.,
Private Mail Bag No. 1,
MORDIALLOC. VIC. 3195 Australia

Dr. I. Fung,
Goddard Inst. for Space Studies,
2880 Broadway,
NEW YORK, N.Y. 10025 U.S.A.

Mr. I.E. Galbally,
CSIRO Div. of Atmos. Res.
Private Mail Bag No. 1
MORDIALLOC. VIC. 3195 Australia

Dr. R. Gammon,
NOAA ERL/Air Resources lab.,
GMCC
BOULDER. CO. 80303 U.S.A.

Dr. D.J. Gauntlett,
Director, Res. & Systems,
Bur. of Meteorology
P.O. Box 1289K,
MELBOURNE. VIC. 3001 Australia

Dr. W. Gibbs,
48 The Ridge,
BLACKBURN. VIC. 3130 Australia

Mrs. H.S. Goodman,
CSIRO Div. of Atmos. Res.
Private Bag No. 1,
MORDIALLOC. VIC. 3195 Australia

Dr. J. Gras,
CSIRO Div. of Atmos. Res.,
Private Mail Bag No. 1,
MORDIALLOC. VIC. 3195 Australia

Prof. J. Heintzenberg,
Dept. of Meteorology,
Univ. of Stockholm,
Arrhenius Lab.,
S-106 91 STOCKHOLM. Sweden

Dr. G. Herbert,
NOAA ERL/Air Resources Lab.,
GMCC,
BOULDER. CO. 80303 U.S.A.

Dr. Ø. Hov,
Norwegian Inst. For Air Res.,
P.O. Box 130, N-2001,
LILLESTROM. Norway.

Mr. Peter Hyson,
CSIRO Div. Atmos. Res.,
Private Bag No. 1,
MORDIALLOC. VIC. 3195 Australia

Dr. T. Ito,
1-1 Nagamine, Yatabe,
IBARAKI 305 JAPAN

Mr. J. Ivey,
Aust. Gov. Analy. Lab.,
P.O. Box 84,
KINGSTON. TAS. 7150 Australia

Prof. R. Jaenicke,
Inst. for Meteorology,
Univ. of Mainz,
SAARSTR. 21,
D-6500 Mainz. F.R.G.

Mrs. V. Jemmeson,
CSIRO Div. of Atmos. Res.,
Private Mail Bag No. 1
MORDIALLOC. VIC. 3195 Australia

Dr. P.V. Johnson,
DSIR, Phys & Eng Lab.,
Atmospheric Station,
Private Bag,
OMAKAU. Central Otago. N.Z.

Prof. C.D. Keeling,
Scripps Inst. of Oceanography,
Univ. of California
2314 Ritter Hall A-020,
LA JOLLA. CAL. 92093 U.S.A.

Dr. J. King,
School of Geophysical Scs.,
Georgia Tech.,
GEORGIA. U.S.A.

Dr. G. Likens, Director,
The New York Botanical Garden,
Institute of Ecosystem Studies,
Box AB., MILLBROOK. N.Y. 12545 U.S.A.

Dr. J.A. Logan,
Harvard University,
Centre for Earth & Planetary Physics,
Pierce Hall, 29 Oxford Street,
CAMBRIDGE, MA 02138 U.S.A.

Mr. Low Pak Sum,
Centre of Environmental Studies
University of Tasmania
Box 252C, G.P.O.
HOBART. TAS. 7001 Australia

Dr. M. Manning
DSIR,
Institute of Nuclear Science,
Private Bag,
LOWER HUT. N.Z.

Dr. B. Mendonca,
NOAA ERL/Air Resources Lab.,
GMCC,
BOULDER. CO. 80303 U.S.A.

Prof. W.J. Megaw,
Chairman, Dept. of Physics,
York University,
4700 Keele Street,
DOWNSVIEW. ONTARIO M3J 1P3.

Mr. B. Noller,
Office of Supervising Scientist,
Jabiru Lab.,
P.O. East Jabiru,
NORTHERN TERRITORY. 5796 Australia

Dr. G.I. Pearman,
CSIRO Div. of Atmos. Res.,
Private Mail Bag No. 1
MORDIALLOC. VIC. 3195 Australia

Dr. J.T. Peterson,
NOAA ERL/Air Resources Lab.,
GMCC,
BOULDER, CO. 80303 U.S.A.

Dr. C.M.R. Platt,
CSIRO Div. of Atmos. Res.,
Private Mail Bag No. 1
MORDIALLOC. VIC. 3195 Australia

Dr. R.A. Plumb,
CSIRO Div. of Atmos. Res.
Private Bag No. 1,
MORDIALLOC. VIC. 3195 Australia

Mr. P. Pohl,
DSIR, Institute of Nuclear Sci.,
Private Bag,
LOWER HUTT. N.Z.

Prof. M. Prather,
Harvard University,
The Centre for Earth & Planetary,
Pierce Hall,
CAMBRIDGE. MA. 02138 U.S.A.

Dr. C.H.B. Priestley,
Flat 2,
862 Malvern Road,
ARMADALE. VIC. 3143 Australia

Dr. R.G. Prinn,
Prof. of Meteorology,
Mass. Inst. Tech.
CAMBRIDGE 02168, U.S.A.

Dr. R.A. Rasmussen,
Dept. of Environmental Sciences,
Oregon Graduate Centre,
19600 N.W. Walker Road,
BEAVERTON. OREGON. 97006 U.S.A.

Dr. R. Rosen,
Atmos. & Environ. Research Inc.,
840 Memorial Drive,
CAMBRIDGE. MA 02139 U.S.A.

Prof. F. Sherwood Rowland,
Department of Chemistry
University of California, Irvine,
IRVINE CA. 92717 U.S.A

Prof. Dr. W. Seiler,
Max-Planck-Institut fur Chemie,
Postach 3060
D-6500 MAINZ. F.R.G.

Dr. G. Shaw,
Geophysical Institute,
University of Alaska,
FAIRBANKS. ALASKA. U.S.A.

Dr. P.G. Simmonds,
"Rushwater",
39 Avon Castle Drive,
RINGWOOD. DORSET. BH 24 2 BB U.K.

Dr. P. Steele,
NOAA ERL/Air Resources lab.,
GMCC,
BOULDER. CO 80303 U.S.A.

Dr. Mary-Lou Thompson,
CSIRO Div. of Atmos. Res.,
Private Mail Bag No. 1
MORDIALLOC. VIC. 3195 Australia

Dr. G.B. Tucker
CSIRO Div. of Atmos. Res.,
Private Mail Bag No. 1
MORDIALLOC. VIC. 3195 Australia

Ms. M. Voice,
Bureau of Meteorology,
P.O. Box 1289K,
MELBOURNE. VIC. 3001 Australia

Dr. R.T. Watson,
Manager, Upper Atmosphere Res.
NASA.,
WASHINGTON. D.C. 20546 U.S.A.

Dr. S. Whittlestone,
AAEC,
Private Mail Bag,
SUTHERLAND. N.S.W. 2232 Australia

Dr. J. Zillman, Director
Bureau of Meteorology,
MELBOURNE. VIC. 3001 Australia

PROGRAM

WEDNESDAY

815 - 1030

WELCOME: Dr. G.B. Tucker

NON-REACTIVE GASES (1)

Chairman: Dr. D. Ehhalt

1. P. Steele, P. Fraser, R. Rasmussen and M. Khalil. Global distribution of atmospheric methane and aspects of interpretation of these data.
2. P. Fraser, P. Hyson and R. Rasmussen. Methane and carbon monoxide in the Southern Hemisphere.
3. S. Rowland and D. Blake. World-wide increase in tropospheric methane 1978-1984.

REFRESHMENTS

1100 - 1300

NON-REACTIVE GASES (2)

5. D. Ehhalt and J. Rudolph. Light non methane hydrocarbons in the background troposphere.
6. D. Cunnold. Fluorocarbon life-times and releases from 5 years of ALE data.
7. I. Galbally. Long term changes in atmospheric nitrous oxide.
8. R. Watson. How baseline observations are utilized and needed in order to understand tropospheric and stratospheric chemistry.

LUNCH

1400 - 1530

REACTIVE GASES (1)

Chairman: Dr. O. Hov.

1. W. Seiler. Results on measurements of several trace substances at Cape Point, South Africa.
2. R. Rasmussen. Atmospheric isoprene: global significance.
3. J. Logan. Tropospheric ozone: Seasonal patterns and trends.

REFRESHMENTS

1600 - 1730

REACTIVE GASES (2)

4. F. Fehsenfeld and S. Liu. Tropospheric oxone.
5. O. Hov and I. Isaksen. Interpretation of trace gas measurements at high northern latitudes and other remote locations.
6. J. Gras and A. Adriaansen. Concentration and size variation of condensation nuclei at Mawson, Antarctica.

THURSDAY

TRANSPORT (1)

Chairman: A. Plumb

1. M. Prather. Interpretation of trace gas measurements with a GCM.
2. R. Prinn. A global three-dimensional model of the circulation and chemistry of $CFCl_3$ CF_2Cl_2, CH_3CCl_3, CCl_4 and N_2O.
3. A. Plumb. The zonally-averaged transport characteristics of a GCM and a test of the validity of "K-theory" as a parameterization of eddy transport.
4. I. Enting. Preliminary studies with a two-dimensional model using transport fields from a GCM.

TRANSPORT (2)

5. F. Alyea. Implications for large-scale transport from 5 years of ALE data.
6. I. Fung. On the variability of CO_2 exchange between the atmosphere and the biosphere.

PARTICULATES (1)

Chairman: Dr. G. Shaw

1. T. Ito. Study of background aerosols in the Antarctic troposphere.
2. B. Bodhaine. The GMCC aerosol monitoring program.

PARTICULATES (2)

3. K. Bigg. Baseline observations of cloud condensation nuclei at Cape Grim, Tasmania.
4. R. Duce. Aerosol species at the SEAREX north and south Pacific sites.
5. G. Shaw. The microphysical and chemical properties of the Arctic haze and its relation to air mass systems and transport pathways.

PARTICULATES (3)

6. L. Barrie. Features of the atmospheric cycle of aerosol trace elements and sulphur dioxide revealed by baseline research studies in Canada.
7. G. Ayers, J. Ivey and H. Goodman. Excess sulphate and methanesulphonate in aerosol samples from Cape Grim.
8. J. Heinzenberg. What can we learn from aerosol measurements at baseline stations?

FRIDAY

RADIATION

Chairman: R. Jaenicke.

1. E. Dutton and J. DeLuisi. Interpretation of apparent atmospheric transmission using solar photometer precipitable water measurements.
2. M. Platt. The interpretation of atmospheric turbidity measurements.
3. G. d'Almeida, L. Helmes and R. Jaenicke. Information about atmospheric aerosols dormant in measuring series-four examples.
4. B. Mendonca, J. DeLuisi and E. Dutton. Atmospheric transmission decreases and stratospheric warming at Mauna Loa during the two years after the El Chichon volcanic eruption.

RADIATION (2)

5. G. Herbert and J. Harris. Trajectory representation of flow conditions.

CARBON DIOXIDE (1)

Chairman: Dr. J. Peterson.

1. C. Keeling and W.G. Mook. Sources and sinks of atmospheric carbon dioxide deduced from $^{13}C/^{12}C$ ratio measurements.
2. G. Pearman and P. Hyson. Global transport and interreservoir exchange of CO_2 with particular reference to the effects on concentration and isotopic distributions.
3. R. Gammon. The 1982/83 ENSO Event: The Response of the Global Atmospheric CO_2 Distribution.

CARBON DIOXIDE (2)

4. G. Pearman, M. Thompson, I. Enting and P. Hyson. Interannual variations of atmospheric CO_2 concentration.
5. J. Peterson. Measurements of atmospheric CO_2 at Barrow, Alaska from the U.S. NOAA/GMCC program.

PRECIPITATION CHEMISTRY (1)

Chairman: Dr. G. Likens.

1. B. Noller er al. Acidity of rainfall in the northern Alligator River region of N.T., Australia.

PRECIPITATION CHEMISTRY (2)

2. G. Likens, W. Keene, J. Miller and J. Galloway. The Chemistry of precipitation in Katherine, Australia.
3. S. Whittlestone. Radon measurements as an aid to interpretation of atmospheric monitoring.

IMPLICATIONS FOR LARGE SCALE TRANSPORT FROM 5 YEARS OF ALE DATA

F. N. Alyea

Georgia Institute of Technology and CAP, Incorporated
Atlanta, Georgia

The ALE network of ground stations has collected daily measurements of nitrous oxide and four halocarbon species ($CFCl_3$, CF_2Cl_2, CCl_4, CH_3CCl_3) at each of its sites for more than five years. While the network includes only five globally distributed stations, the data is such that a number of inferences can be made concerning large scale atmospheric transport times. Analysis of the fluorocarbons $CFCl_3$ and CF_2Cl_2 are most useful for this purpose since their known sources are anthropogenic, fairly well documented, and confined primarily to the northern hemisphere. Transport is the only important physical/chemical process which affects the distribution of these long-lived species (time constants $\sim$ 100 years) in the troposphere over time periods of several years.

As a tool for understanding the ALE data base and for calculating species lifetimes, simple box model concepts have been used in the past (see, for example, the ALE papers, particularly ALE 3, J. Geophys. Res., 88, 8379-8400, 1983). However, we now invert the process to analyze not for lifetimes but for global scale transport time constants assuming known annual release rates.

In the simplest case, a four box configuration is used to estimate the long term and annual cycle transport components. This process, however, assumes constant release rates for each calendar year as given by industry sources. Thus, any annual variability in the actual releases will show up in the form of errors in the calculated transport times. To get around this problem, an alternate configuration of the four-box model is employed to estimate potential release rate variability.

EXCESS SULFATE AND METHANESULFONATE IN AEROSOL SAMPLES FROM CAPE GRIM.

*1. *2 *1.
G. P. Ayers, J. P. Ivey and H.S. Goodman

*1. CSIRO Division of Atmospheric Research
Private Bag No.1, Mordialloc, Vic. 3195 Aust.

*2 Aust.Govt. Analy.Lab., Kingston, Tas.

Aerosols collected by high volume sampling over approximately monthly periods since late 1976 at Cape Grim have been analysed for excess sulfate and methanesulfonate. The results are discussed in terms of our current understanding of the atmospheric sulfur cycle in clean maritime air.

" " "

BASELINE OBSERVATIONS OF CLOUD CONDENSATION NUCLEI AT CAPE GRIM, TASMANIA

E. K. BIGG

Cloud Physics Laboratory, Division of Atmospheric Research, CSIRO,
P.O. Box 134, Epping, NSW, 2121

Measurements of cloud condensation nuclei (CCN) have been made at supersaturations of 0.25, 0.5, 0.75, 1.0 and 1.25% at Cape Grim, Tasmania for more than three years using a thermal gradient counter. Number N (cm^{-3}) and supersaturation S are related by the equation $N = C\ S^k$ within this range of supersaturations in clear air, C being 80% of total particle concentrations and k having a value near 0.5. As the total concentration of particles in the air increases, the relationship only holds for supersaturations above 0.5%, C becomes a smaller percentage of all particles and k increases slightly. The measurements show that for most natural clouds in this area the droplet concentrations would be largely determined by CCN rather than by the rate of cooling. The measurement is therefore a useful one for predicting the extent of possible climatic changes that would be associated with variation in CCN concentrations.

Size distributions obtained from diffusion batteries or electron microscope measurements of collected particles agree in predicting quite a different type of relationship between N and S if it is assumed that the particles are wholly composed of a simple inorganic salt. Possible reasons for this discrepancy include incorrect chemical assumptions, the presence of surface-active agents on the particles or the failure of sizing methods to resolve a very narrow peak in the size distribution. It is suggested that the use of a CCN counter having a working vapour other than water might help resolve these difficulties and lead to a better understanding of the nature of the particles. Experience with an experimental counter using ethanol as its working vapour is described.

It is proposed that higher priority than has been given in the past should be given by the baseline monitoring programs to measurements of particles active in modifying either the ability of clouds to precipitate, their lifetime or their radiative properties, for most forms of terrestrial life depend on precipitation, are harmed by the temperature extremes that occur in the absence of clouds and are sensitive to changes in mean temperature.

THE GMCC AEROSOL MONITORING PROGRAM

Barry A. Bodhaine

Geophysical Monitoring for Climatic Change, NOAA
325 Broadway, Boulder, CO 80303

1. INTRODUCTION

The NOAA-GMCC program operates four background monitoring stations located at Barrow, Alaska; Mauna Loa, Hawaii; Cape Matatula, American Samoa; and South Pole. The mission of the program is to detect any long-term trends in gaseous and aerosol species which may be caused by anthropogenic or natural sources, and to assess climatic effects that may result from these changes. A description of the GMCC monitoring program may be found in the series of GMCC annual reports; see, for example, Harris and Bodhaine (1983). The aerosol program, in particular, was described by Bodhaine (1983).

Condensation nuclei (CN) concentration and aerosol scattering extinction (σ_{sp}) are measured continuously at the four GMCC sites. This report summarizes the CN and σ_{sp} data records at these stations.

2. INSTRUMENTATION

Condensation nuclei concentration is measured continuously at all stations using General Electric CN counters. Daily calibration points are provided by Pollak CN counters which act as on-site standards. The operation and calibration of the CN instruments have been described by Bodhaine and Murphy (1980).

Aerosol scattering extinction is measured at all stations using four-wavelength nephelometers similar to the design of Ahlquist and Charlson (1969). Operation at the four wavelengths, 450, 550, 700, and 850 nm, allows detection of the aerosol that is the major contributor to the atmospheric scattering of visible radiation. Operation and calibration of the GMCC nephelometers were described by Bodhaine (1979).

3. DISCUSSION OF DATA

Monthly means of CN and σ_{sp} data for the four GMCC stations are presented in Fig. 1, and daily means for a selected year for each station are presented in Fig. 2. The Barrow σ_{sp} data exhibit an annual cycle which reaches a maximum in the winter/spring and a minimum in the summer. The Arctic haze event is clearly seen in the data each March and was studied during the Arctic Gas and Aerosol Sampling Program in 1983 (Schnell, 1984).

The Mauna Loa σ_{sp} data exhibit a strong annual cycle with a maximum in April/May and a minimum in winter. The spring maximum is caused by the transport of Asian dust in the upper troposphere. The Mauna Loa CN data show no annual cycle and appear to be representative of the background troposphere.

The Samoa σ_{sp} and CN data are representative of a clean marine aerosol and show no obvious annual cycle.

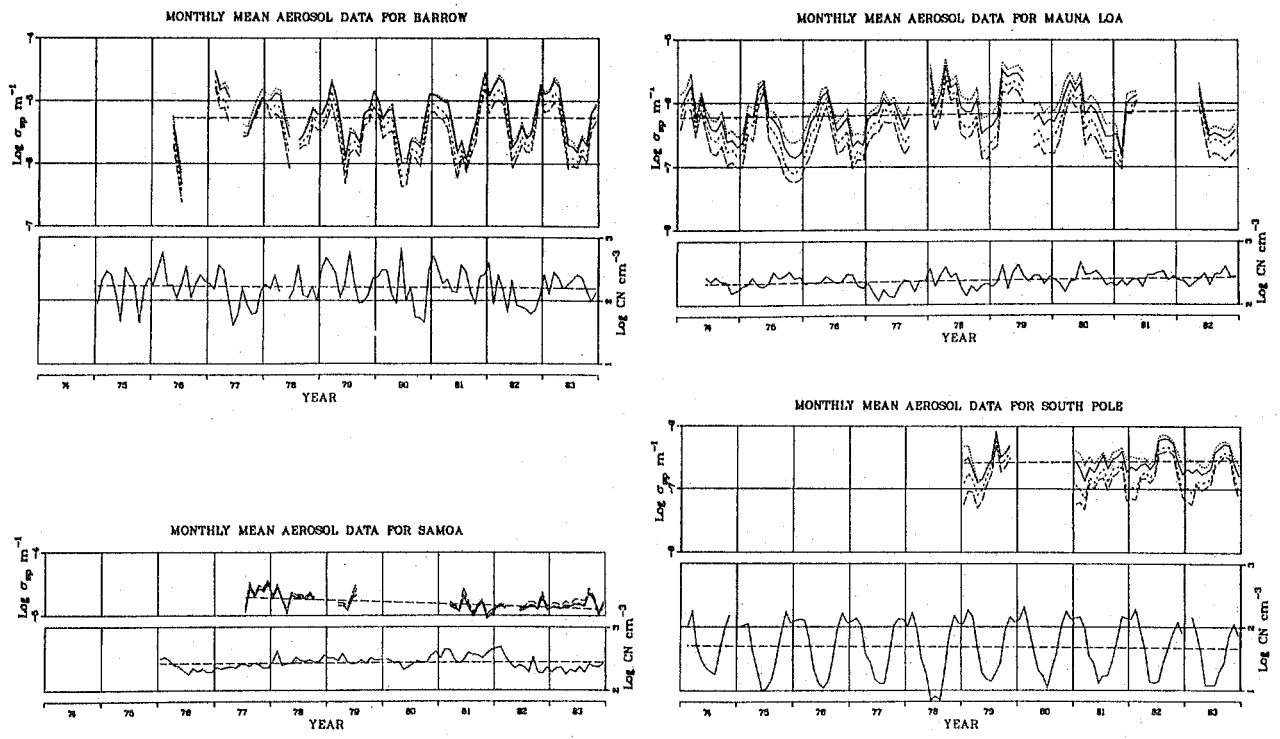


Fig. 1 Monthly means of σ_{sp} and CN data at Barrow, Mauna Loa, Samoa, and South Pole. Only 0000-0800 LST data were used for Mauna Loa. Light-scattering data (upper) are for 450 (dotted), 550 (solid), 700 (dashed), and 850 nm (long-dashed).

The South Pole σ_{sp} data show an annual cycle which is relatively high in the austral summer, reaches a minimum in about April, and is dominated by sea salt events during the austral winter. The South Pole CN data show an annual cycle different from the σ_{sp} data with a maximum in austral summer and a minimum in austral winter.

4. CONCLUSIONS

Long-range transport is a theme common to Barrow, Mauna Loa, and South Pole. The Barrow record clearly shows the regular appearance of the Arctic haze, believed to be caused by the tropospheric transport of anthropogenic aerosol particles from midlatitude pollution sources. The Samoa record is dominated by sea salt aerosol and does not appear to show signs of long-range transport. The Mauna Loa record shows the regular appearance of Asian dust, transported in the troposphere during April or May. The Asian deserts were proven conclusively by aerosol chemistry and long-distance trajectory analysis to be the source. The South Pole record shows a series of sea salt events during austral winter which are transported in the troposphere from coastal regions to the interior of the Antarctic continent during large storms. None of the data records shows a significant long-term trend.

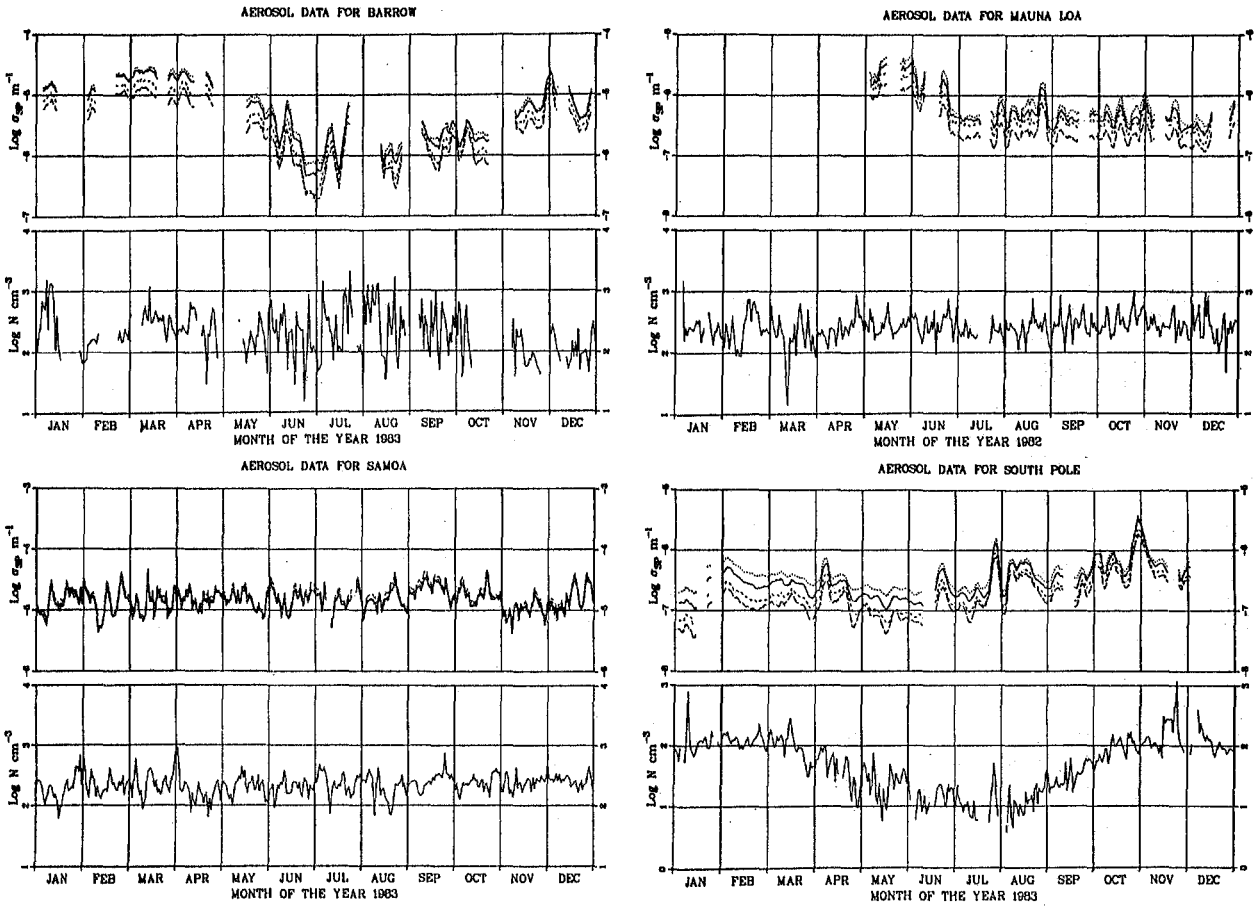


Fig. 2 Daily geometric means of σ_{sp} and CN data for selected years at Barrow, Mauna Loa, Samoa, and South Pole (as in Fig. 1).

5. REFERENCES

Ahlquist, N. C. and R. J. Charlson, 1969: Measurement of the Wavelength Dependence of Atmospheric Extinction Due to Scatter, Atmos. Environ., 3, 551-564.

Bodhaine, B. A., 1979: Measurement of the Rayleigh Scattering Properties of Some Gases with a Nephelometer, Appl. Opt., 18, 121-125.

Bodhaine, B. A., 1983: Aerosol Measurements at Four Background Sites, J. Geophys. Res., 88, 10753-10768.

Bodhaine, B. A. and M. E. Murphy, 1980: Calibration of an Automatic Condensation Nuclei Counter at the South Pole, J. Aerosol Sci., 11, 305-312.

Harris, J. M. and Bodhaine, B. A. (eds.), 1983: Geophysical Monitoring for Climatic Change No. 10, Air Resources Laboratory, NOAA, Boulder, Colo.

Schnell, R. C., 1984: Arctic Haze and the Arctic Gas and Aerosol Sampling Program (AGASP), Geophys., Res. Lett., 11, 361-364.

FLUOROCARBON LIFETIMES AND RELEASES FROM 5 YEARS OF ALE DATA

D. M. Cunnold

Georgia Institute of Technology and CAP, Incorporated
Atlanta, Georgia

Five years of data on $CFCl_3$, CF_2Cl_2, CH_3CCl_3 and CCl_4 taken at the ALE global network of ground stations has been analyzed. Preliminary lifetime estimates have been made assuming a 5% increase in release in 1983 over 1982 - industry estimates of release for 1983 are not yet available. The $CFCl_3$ lifetime estimate based on the temporal trend in the ALE data is 72 years, a result which differs insignificantly from the "3 year" lifetime estimate. For CF_2Cl_2 the lifetime estimates (based on the trend technique) are 769 years, 85 years and 68 years based respectively on 3, 4, and 5 years of ALE data.

It is suspected that this substantial variation in the CF_2Cl_2 lifetime estimates is indicative of atmospheric inputs of CF_2Cl_2 which are different from the estimates by industry (CMA, 1983). Using a two-dimensional (9-box) model of the atmosphere together with the ALE data, the atmospheric inventory of CF_2Cl_2 (and $CFCl_3$) has been estimated as a function of time assuming that the only atmospheric loss process is stratospheric photodissociation. Table 1 compares the resulting release estimates with those of industry.

ANNUAL ATMOSPHERIC RELEASES OF FLUOROCARBONS

(Million Kilograms)

	$CFCl_3$			CF_2Cl_2	
Year (July 1-June 30)	CMA Estimates	ALE Estimates F11S	F11P	CMA Estimates	ALE Estimates
1978-1979	285	255	291	387	478
1979-1980	270	266	264	390	370
1980-1981	265	271	271	402	390
1981-1982	262	258	248	418	351
1982-1983	?	265	259	?	421

The substantial differences for CF_2Cl_2 could be caused by substantial (a factor of more than 2) variation in the stratosphere-troposphere exchange rate from year to year. However, the agreement exhibited for $CFCl_3$ suggests the existence of real differences in the CF_2Cl_2 release estimates. Since Eastern Europe is believed to account for a significant proportion of the CF_2Cl_2 release, but not $CFCl_3$, the differences are probably at least partially the result of a lack of information about release there.

The 3 year ALE data set resulted in significant uncertainties in the CH_3CCl_3 lifetime because of apparent inconsistencies between the atmospheric inventory of CH_3CCl_3, its temporal trend and the latitudinal gradient. These differences were expected to result from uncertainties in the data record (the

ALE instruments were not optimized for CH_3CCl_3) and perhaps from uncertainties in the atmospheric release of CH_3CCl_3. ALE release estimates for CH_3CCl_3 will be presented at the meeting. Based on 4 years of ALE data, the differences narrowed as a result of reductions in the trend lifetime estimates at the two Southern Hemisphere sites. At Samoa, the estimate dropped from 111 to 17 years while at Tasmania it dropped from 15 to 11 years. The 5-station average trend lifetime estimate was reduced to 8.8 years as a result.

Although the original purpose of the ALE experiment was the determination of atmospheric lifetimes, the data provides information on the rates of release of fluorocarbons into the atmosphere, transport rates and local atmospheric variability. Relevant to determining all these parameters is a consideration of errors. Short term (less than 6 months) variability in the data has been studied using empirical orthogonal functions. This analysis indicates that much of the short term variability is common to several of the species at an individual station and is consistent with expected time-scales of atmospheric variability. For July-December 1981 at Barbados, for example, $CFCl_3$(S), $CFCl_3$(P) and CF_2Cl_2 possess common variability between 5 and 15 days. Interpreting differences in variability as instrumentally produced, instrumental variations predominate on time scales shorter than 1 day and longer than 30 days (during the 6 month period).

The principal utility of the ALE data is for deriving long term ($\gtrsim$ 3 month) variations. In deriving long term parameters the shorter term variability discussed in the previous paragraph may generally be averaged out (except at locations such as Adrigole where pollution events are common). Uncertainties in the parameters are therefore usually dominated by variations on the time scale of several months to several years. One way to estimate the measurement uncertainties for each species is to examine the variations of the temporal trends about those calculated from the best-fit two-dimensional model. The fact that differences between the trends of $CFCl_3$ on the two columns at each site are of comparable magnitude suggests that, indeed, this procedure is estimating measurement uncertainties and not two-dimensional model deficiencies. This procedure indicates, for example, that the ALE release estimates in Table 1 possess a precision (1σ) of approximately $\pm$ 5%.

Reference

Chemical Manufacturers Association, World production and release of chlorofluorocarbons 11 and 12 through 1982, Rep. of the Fluorocarbon Program Panel, Washington, D.C., 1983.

AEROSOL SPECIES AT THE SEAREX NORTH AND SOUTH PACIFIC SITES

Robert A. Duce

Center for Atmospheric Chemistry Studies
Graduate School of Oceanography
University of Rhode Island
Kingston, RI 02881 USA

1. THE SEAREX PACIFIC OCEAN NETWORK

As part of the Sea/Air Exchange (SEAREX) Program, a network of island stations in the Pacific Ocean region has been operated for the collection of aerosol species and precipitation. Initial objectives of this network are to evaluate the temporal and geographical variability of such substances as mineral dust, sea salt, nitrate, sulfate, selenium, and ^{210}Pb over the Pacific Ocean, to evaluate the sources and atmospheric transport paths for these substances, and to evaluate their exchange rates with the ocean. In the North Pacific region seven island stations are located from 50°N to 4°N. These include Shemya, Midway, Oahu, Guam, Enewetak, Belau, and Fanning. In the South Pacific region an additional seven island stations are located from 1°S to 34°S. These include Nauru, Funafuti, American Samoa, New Caledonia, Rarotonga, Norfolk, and Cape Reinga New Zealand. The stations in the North Pacific were initiated in 1981 and those in the South Pacific in early 1983. All are manned by volunteer personnel on the islands. The network is operated jointly by the University of Miami and the University of Rhode Island.

Aerosol particle samples are collected for one week intervals using high-volume air sampling systems (~1.1 m^3/min) and 20x25 cm Whatman 41 filters. The sampling systems at the sites are located on windward coasts as close to the ocean as possible and at elevations ranging from 2 to 200 meters above sea level. The air sampler is controlled by a wind monitoring system to minimize the possibility of contamination from local sources. The acceptance angle of each wind direction monitor is set to a sector facing the ocean, with the pumping system only operating when the wind comes from the sea. The aerosol sample filters are usually changed the same day at all stations so that synoptic comparisons can be made. Filter blank samples are taken regularly.

Total deposition samples are collected at the North Pacific sites continuously over two week sampling intervals using a conical polyethylene collector and a four liter acid-washed deflatable polyethylene container. The collectors are placed in close proximity to the air-sampling systems. Washing of the dry deposition material into the container is dependent upon rain. On arrival at the analytical laboratory, a deposition sample is immediately passed through a 20 μm mesh nylon screen to eliminate the largest particles and local debris (e.g., insects and plant tissues). The sample is then adjusted to 0.15 N nitric acid. If the amount of liquid in a sample is less than 300 g, the sample is combined with the sample collected during the following period. As a blank control solution during storage, handling and chemical analysis, several 300 g aliquots of distilled deionized water are treated in the same manner as samples.

2. MINERAL DUST

Atmospheric mineral particle concentrations are based on the aluminum concentrations in the aerosol and deposition samples, assuming the mineral material is 8 percent aluminum. Aluminum is determined by neutron activation analysis at the University of Rhode Island. In the North Pacific, a strong seasonal transport pattern has been found at most of the island sites, with high atmospheric dust concentrations from February to June (the high-dust season) and low concentrations from July to January (the clean season). When combined with observa- tions of dust storms in Asia and isentropic trajectory analysis, it is clear that in the high-dust season the dust over the North Pacific is transported from the arid desert regions in central and eastern Asia by the upper level westerly winds. In some cases atmospheric transport paths of over 10,000km are observed. During the clean season trajec- tories to the tropical and sub-tropical sites are often from the Americas.

Mean atmospheric mineral dust concentrations during the high dust season range from 3 to 10 times those during the clean season, except at the near-equatorial Fanning site, where little difference with season was observed. Within the high-dust season, several particularly high concentration events with durations of a few days to a week or two are observed each year. These events are correlated with specific dust storms in China. Even though the periods of extremely high dust concentrations during the high dust season are infrequent, they contribute the major fraction of the annual dust flux to the North Pacific Ocean. There is a latitudinal gradient in the atmospheric concentrations, with the highest concentrations being observed at Midway and Shemya and the lowest at Fanning. The quantity of dust transported from Asia to the marine atmosphere over the central North Pacific during the February to June period represents 70-90 percent of the annual dust load in this region.

The atmospheric dust fluxes to the Pacific Ocean surface measured at Midway and Oahu (60 and 40 $\mu g\ cm^{-2}\ yr^{-1}$, respectively) were comparable to the present-day downward flux of mineral particles in the water column of the North Pacific measured by sediment traps east of Hawaii (50 $\mu g\ cm^{-2}\ yr^{-1}$). It is clear that Asian deserts are major sources for both the suspended mineral matter in the water column and the non-biogenic component of marine sediments in the North Pacific. From the total deposition samples it is estimated that ~20 x 10^{12}g per year of mineral matter is deposited to the area covered by the net- work in the North Pacific (0-50°N, 150°E-130°W).

To date mineral aerosol data are only available for approximately one year at the South Pacific sites. From this limited data set it appears that there is a strong temporal cycle at Norfolk, with high dust concentrations during the November-April period. This is the time of maximum occurrence of fires and dust storms in Australia. Meteorological conditions are also most favorable for transport from Australia to Norfolk during this period. Mean mineral dust concentrations at New Caledonia are about half those at Norfolk. Concentrations at Rarotonga and American Samoa were seven to ten times lower than New Caledonia.

3. SULFATE AND NITRATE

Concentrations of aerosol nitrate and non-sea-salt (NSS) sulfate are measured by ion chromatography at the University of Miami. Analysis of the samples for nitrate and NSS sulfate reveals a number of significant trends in their areal distribution and temporal variability. Over a vast region of the North Pacific (temperate and sub-tropical), significant quantities of these two constituents appear to be derived from Asia. During the February to June (high-dust) period mean NSS sulfate concentrations range from 0.49 to 0.78 $\mu g/m^3$(STP) and mean nitrate concentrations range from 0.31 to 0.40 $\mu g/m^3$. In contrast, from July through January the mean NSS sulfate concentrations are nearly a factor of two lower than during the high-dust season, 0.28 to 0.31 $\mu g/m^3$; the mean nitrate concentrations are also somewhat lower, 0.25 to 0.32 $\mu g/m^3$. NSS sulfate and nitrate are not signifi- cantly correlated with atmospheric sea salt at any of the sites. The highest NSS sulfate concentrations are found at Shemya, likely related to transport of pollution-derived sulfate (or sulfate precursors) from Asia. Annual mean nitrate concentrations show much less geographical variability than NSS sulfate.

The equatorial Pacific and the tropical and sub-tropical areas of the South Pacific constitute a major region in which natural marine and/or global atmospheric sources appear to supply the majority of the nitrate and NSS sulfate. Throughout this region mean nitrate concen- trations are in the range of 0.1 to 0.15 $\mu g/m^3$, being somewhat higher over the equatorial North Pacific than the South Pacific. Mean NSS sulfate concentrations vary from 0.36 to 0.68 $\mu g/m^3$. The mean NSS sulfate concentration at Fanning is somewhat higher than in the sub- tropical latitudes north and south of the equator, suggesting the possible importance of biological sources for gas-phase reduced sulfur species in the equatorial upwelling region. Nitrate concentrations are significantly correlated with ^{210}Pb, even at the equatorial Fanning site. ^{210}Pb is derived from ^{222}Rn, whose primary source is soils in continental regions. This suggests that nitrate or nitrate precur- sors measured in this region may have an important continental source. The highest nitrate concentrations at Fanning are also associated with qualitative observations of filter "grayness", an indication of elemental carbon, perhaps from biomass burning. During this period (fall) at Fanning trajectories indicate transport from northern South America and Central America, areas with extensive biomass burning. These regions also have the greatest frequency of lightning discharge in the world during this time of year.

4. SELENIUM

Concentrations of selenium are measured by neutron activation analysis at the University of Rhode Island. The distribution of par- ticulate selenium at the North and South Pacific sites parallels to a great extent that of NSS sulfate. In particular, the high concentration of selenium near 50°N and near the equator suggest that contributions from both anthropogenic and marine biological sources are probably important. Concentrations range from ~400 pg/m^3 at Shemya and Fanning to ~100 pg/m^3 at Samoa.

INTERPRETATION OF APPARENT ATMOSPHERIC TRANSMISSION USING SOLAR PHOTOMETER PRECIPITABLE WATER MEASUREMENTS

Ellsworth Dutton and John DeLuisi

NOAA Air Resources Laboratory, Geophysical Monitoring for Climatic Change, Boulder, CO

1. INTRODUCTION

Pyrheliometeric measurements of direct normal solar radiation at the NOAA Geophysical Monitoring for Climatic Change (GMCC) observatory at Mauna Loa, Hawaii (MLO) have been used to determine long-term (since 1958) variations in clear-sky atmospheric transmission (Ellis and Pueschel, 1971, and others). The established procedure is to calculate a daily apparent atmospheric transmission factor (ATF) by ratioing pyrheliometeric measurements made at specific solar zenith angles during the course of a clear morning. The ATF is independent of the pyrheliometer calibration, some voltage measurement biases, and the extraterrestrial solar constant. Changes in the ATF are due entirely to changes in atmospheric composition along the path of view, and are most significantly affected by water vapor, aerosols, and ozone. The sensitivity and long-term accuracy of the ATF are on the order of 0.001 equivalent optical depth units. The principal interest in the ATF has been the aerosol contribution to the variations in the atmospheric transmission. Aerosol studies using the MLO ATF were subject to assumptions about precipitable water because appropriate direct measurements of water vapor were not available. In this paper we present results of an investigation on the relationship between the MLO ATF and precipitable water, which were measured nearly coincident in time and space.

2. PRECIPITABLE WATER MEASUREMENT

The water vapor measurement record, beginning in 1978, was obtained with a solar infrared dual-channel photometer that operates simultaneously with the pyrheliometer. The calibration and measurement procedures for solar water vapor photometers are extensively discussed in the literature by Volz (1974) and others. The calibration of the MLO instrument was transferred from a GMCC standard photometer, the calibration of which is detailed in Bodhaine and Harris (1982). Water vapor measurements obtained from a solar photometer are particularly well suited for interpreting pyrheliometer measurements, not only because they are made at the same time and along the same atmospheric path, but also because the measured water vapor variations are due to radiatively effective water vapor variations. The pyrheliometer responds to the radiatively effective water vapor amount rather than the actual amount in which the attenuation efficiency varies with temperature and pressure.

3. MODELING

Hoyt (1979) presented a method of using the U. S. Air Force atmospheric transmission model, LOWTRAN, to model the ATF. The ATF is defined by

$$ATF = \frac{1}{3} \sum_{i=3}^{5} \frac{I_i}{I_{i-1}}$$

where I is the direct normal solar intensity at a given integer relative air mass (i) from 2 to 5. Hoyt demonstrated the effect of variable water vapor and aerosol parameterizations on the ATF. We used LOWTRAN5 to calculate a water vapor normalization expression, which when evaluated for a measured precipitable water amount and applied to an observed ATF value yields a water-vapor-independent ATF. The water vapor normalization expression is somewhat dependent on the magnitude and spectral dependence of the aerosol optical depth. Information on the spectral dependence of aerosol optical depth is not contained in the ATF, so independent spectral optical depth data of Shaw (1982) for MLO were used to specify the aerosol in LOWTRAN5. The effect of varying the spectral dependence of aerosol optical depth on the water vapor normalization expression will be discussed in the full-length version of this paper.

The water vapor normalization expression generated from LOWTRAN5 is in the form of an ATF adjustment, which is a function of precipitable water. The adjustment is added to a measured ATF, normalizing it to a constant water vapor amount, which was chosen to be 0.30 cm for this investigation. The remaining day-to-day variability in the normalized ATF is then assumed to be due entirely to aerosols. The aerosol residual in the ATF can be derived by subtracting a constant value, which is equal to the normalized ATF when no aerosols are present in the atmosphere. Since it is not known if this "zero aerosol" ATF value has ever been observed, LOWTRAN5 was used to model it. Using the LOWTRAN tropical atmosphere starting at an elevation of 3.4 KM, 0.30 cm water (actual), and 238 m-atm-cm ozone, we find this zero aerosol ATF value is 0.941.

LOWTRAN5 was also used to show that the range of total ozone variation at MLO has no significant effect on the ATF.

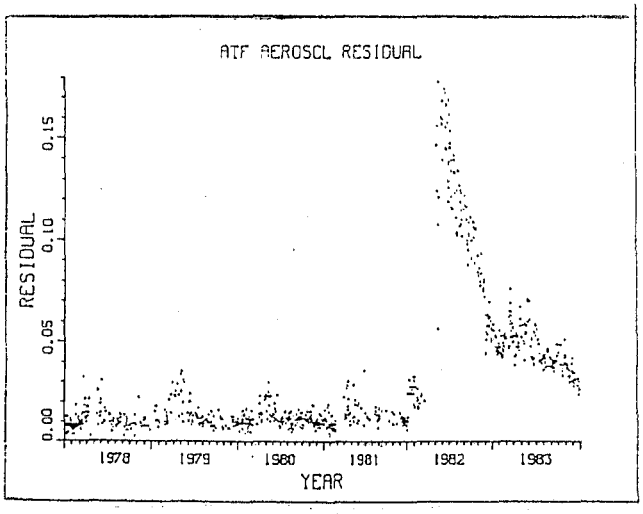


Fig. 1 Aerosol influence on the changes in daily atmospheric transmission as deduced from the Mauna Loa pyrheliometeric record and corrected for precipitable water. Units for the residual are given in text.

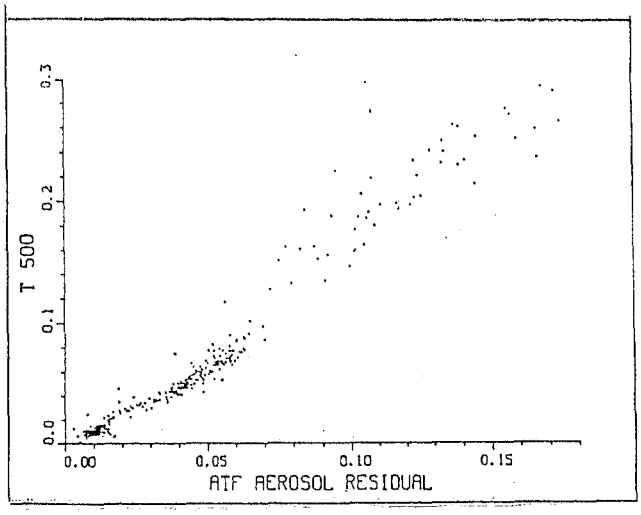


Fig. 2 Comparison of pyrheliometrically derived aerosol (ATF units) and direct aerosol optical depth measurements at 500 nm.

4. RESULTS

Figure 1 shows the aerosol residual for the MLO ATF from 1978 through 1983. The three notable features from Fig. 1 are that (1) our pre-1982 values agree well with estimates of aerosol optical depth made by Mendonca et al. (1979) and others (not shown) from the MLO ATF except we have daily resolution and reduced uncertainty relative to water vapor, (2) there is an annual spring aerosol maximum, and (3) the residual dramatically increases following the 1982 eruption of El Chichon. The aerosol residual values, which are proportional and approximately equal to base e optical depth units at 500 nm for the period before El Chichon, are not valid approximations to 500 nm optical depth after El Chichon. Figure 2 shows a comparison between directly measured 500 nm aerosol optical depth at MLO and the aerosol residual from Fig. 1 for 1980, 1982, and 1983. Work is in progress to derive the relationship between the aerosol residual following El Chichon and an absolute measure of aerosol optical depth. The El Chichon event is, however, very unusual and transient. The water vapor normalization procedure presented here permits more precise interpretation of background-level aerosol effects on the MLO ATF on time scales as short as 1 day.

5. REFERENCES

Bodhaine, B. A. and J. M. Harris, editors, 1982: Geophysical Monitoring for Climatic Change, No. 10: Summary Report 1981, available from NOAA/ERL, Boulder, CO.

Ellis H. T. and R. F. Pueschel, 1971: Solar radiation: Absence of air pollution trends at Mauna Loa, Science, 172, 845-846.

Hoyt, D. V., 1979: Apparent atmospheric transmission using the pyrheliometric ratioing technique, App. Optics, 18, 2530-2531.

Mendonca, B. G., J. J. DeLuisi, K. J. Hanson, and J. T. Peterson, 1979: Signatures in Atmospheric Transmission Variations at Mauna Loa Observatory, Hawaii, Proceedings, WMO Technical Conference on Regional and Global Observations of Pollution Relative to Climate, 20-24 August 1979, Boulder, CO.

Shaw, G. E., 1982: Solar spectral irradiance and atmospheric transmission at Mauna Loa Observatory, App. Optics, 21, 2006-2011.

Volz, F. E., 1974: Economical multispectral sunphotometer for measurements of aerosol extinction from 0.44 m to 1.6 m and precipitable water, App. Optics, 13, 1732-1733.

LIGHT NON METHANE HYDROCARBONS IN THE BACKGROUND TROPOSPHERE

D.H. Ehhalt and J. Rudolph

Institut für Chemie 3: Atmosphärische Chemie
Kernforschungsanlage Jülich GmbH, P.O. Box 1913, D-5170 Jülich, FRG

1. INTRODUCTION

Measurements of light non methane hydrocarbons (NMHC) have shown that these compounds are present in the non urban troposphere at mixing ratios of several ppt to a few ppb (see Rudolph and Ehhalt, 1981). Despite the fact that they are more than three orders of magnitude less abundant than methane, the other hydrocarbons are of considerable interest for the photochemistry, because they react much faster with OH radicals than methane. In addition some hydrocarbons - the alkenes - also react with ozone. Thus, in total, the NMHC may reach similar photochemical conversion rates as methane. Their global importance depends on their global distribution. In this paper we present global NMHC data what were obtained during the "STRATOZ II" flight of the French Caravelle research aircraft. The flight track is shown in Figure 1.

It was completed between 20. April and 10. May 1980. The plane landed about every 3000 km which allowed to take vertical profiles during the approach to the air-ports, whose positions are indicated by the dots. Because of the expected pollution close to the air-ports no samples were taken below 800 mb pressure altitude.

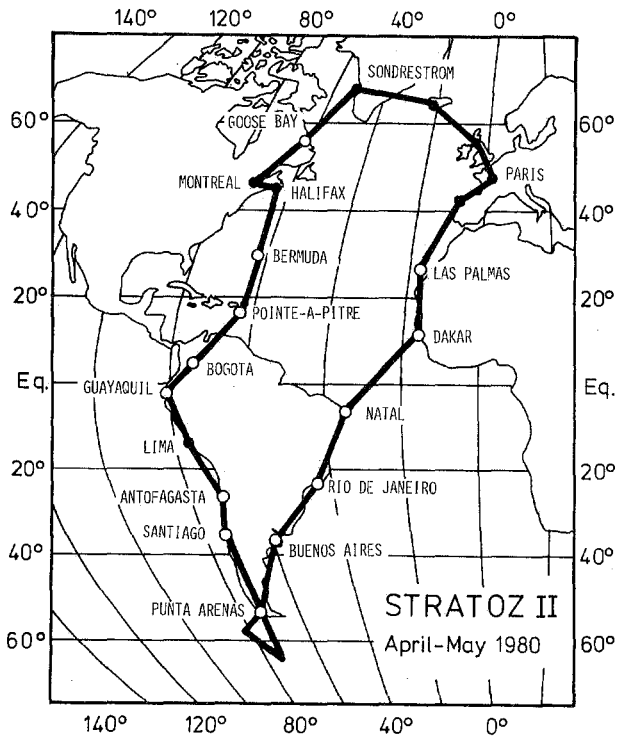


Fig. 1: Flight track of the STRATOZ II experiment.

2. EXPERIMENTAL

The air samples were collected by grab sampling in special stainless steel containers of 2 l volume. They were analyzed in the laboratory by flame-ionization gaschromatography after hydrocarbon enrichment on a precolumn. Details of the analytical technique and the sample containers are described by Rudolph et al. (1981). The samples were analyzed for ethane, ethene, acetylene, propane, propene, n-butane, i-butane, n-pentane and i-pentane. The detection limits were between 20 ppt and 50 ppt, depending on the available sample volume and the individual compound. Neither the sample containers nor the analytical procedure caused detectable blank values. The sample containers allowed storage during several months without detectable changes of the mixing ratios of these light hydrocarbons.

3. RESULTS

The results are summarized in form of latitude - altitude cross sections. The latter are divided into a southbound flight segment leading from Greenland to Puntas Arenas, and a northbound leg from Puntas Arenas to Paris, and from Paris to Greenland. Figure 2 presents the meridional distribution of C_3H_8 as an example. For clarity the figure does not contain the individual data points, but rather the isolines of constant mixing ratio interpolated between them.

4. DISCUSSION

The meridional distribution C_3H_8 shows a number of characteristic features which are repeated in the distributions of the other trace gases as well. We note a mean latitudinal gradient at all altitudes, the mixing ratio decreasing as we go from mid-north latitudes to the equator and into the southern hemisphere. The data exhibit also generally a clear vertical decrease of mixing ratio with altitude. There is however one conspicuous exception. There is a definite cell of maximum mixing ratios around 50° N latitude and about 10 km altitude in the southbound flight. It must be caused by upward mixing of boundary layer air, as can be demonstrated from the pattern in the abundance distribution of the NMHC measured. Plausible trajectories will be discussed. Another maximum - although much less pronounced - is also present over the tropics during the northbound flight. The maximum at 50°N causes a very steep vertical gradient towards the tropopause. It also influences the isolines further south in the sense that they run more of less trapezoidal with the exception of some wiggles probably superimposed by air mass movements. These are the regular distribution features which can be extracted from Figure 2. At the same time we note substantial variability which is expressed in the bends and folds of the lines of constant mixing ratio. They are caused by large scale advection. We further note that the south and northbound cross sections differ significantly indicating at least temporary zonal variations: Generally the northbound leg over the African Coast shows lower mixing ratios than the southbound leg.

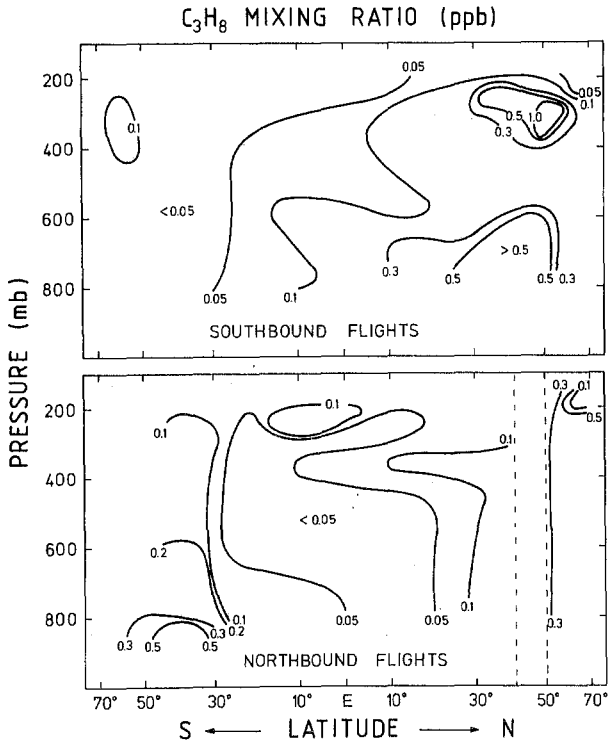


Fig. 2: Latitude-altitude cross section of the C_3H_8 mixing ratios obtained during STRATOZ II. The contours of constant mixing ratio are given in ppb.

5. REFERENCES

Rudolph, J. and Ehhalt, D.H., 1981: Measurements of C_2 - C_5 Hydrocarbons over the North-Atlantic, J. Geophys. Res., 86, pp. 11959-11964.

Rudolph, J., Ehhalt, D.H., Khedim, A. and Jebsen, C., 1981: Determination of C_2 - C_5 Hydrocarbons in the Atmosphere at Low Parts per 10^9 to High Parts per 10^{12} Levels., J. Chromatography, 217, pp. 301-310.

Ehhalt, D.H. and Rudolph, J., 1984: On the importance of light hydrocarbons in multi-phase atmospheric systems, Berichte der Kernforschungsanlage Jülich, No. Jül-1942, 5170 Jülich, FRG.

PRELIMINARY STUDIES WITH A TWO-DIMENSIONAL MODEL USING TRANSPORT FIELDS FROM A GCM

I.G. Enting

CSIRO, Division of Atmospheric Research
Private Bag 1, Mordialloc, Vic 3195 Australia.

There have been a relatively large number of two-dimensional models developed for describing the distribution of minor constituents of the atmosphere. The distributions of such atmospheric tracers have been modelled in terms of atmospheric transports and sources and sinks for the various tracers. A major difficulty in setting up a two-dimensional model is the choice of appropriate transport fields. The transports are usually represented as due to a combination of zonal mean advection and a set of diffusion processes that purport to represent the effects of both transient eddies and standing eddies that can not be represented directly in a two-dimensional formulation.

There are several possible ways in which transport fields can be obtained. The main ways are

i) Direct observations,
ii) Theoretical inferences from direct observations,
iii) Calibration of transport fields from observations of tracer distributions,
iv) Numerical determination of effective transport coefficients from calculations using general circulation models.

Each of these approaches suffers from severe limitations and in practice some combination is generally used. Direct observations are generally possible only for the advective transports and even in this case there is relatively little data for the southern hemisphere. More importantly, direct observations determine an Eulerian mean for the zonal mean advection. The use of Eulerian means is only correct if the diffusive transports are represented by tensors that are asymmetric, thus creating additional problems for other aspects of determining transport fields.

The approach of using theoretical inferences to estimate transport coefficients has mainly been used in the determination of diffusive transports by assuming some fixed relation between the effective diffusion and certain statistical properties of the variablity of the wind fields. This approach is of doubtful theoretical validity and has not been subjected to any validation studies on a global scale.

The use of tracer distributions to determine the transport coefficients (or to tune a set of initial estimates) suffers from the limitation that this calibration problem is severely underdetermined. In particular, there are very few atmospheric constituents for which the sources and sinks are known sufficiently well to form the basis for this sort of calibration. There is a real danger of developing circular arguments when it becomes necessary to use observations of a single tracer to deduce both the transport coefficients and the sink strengths.

The use of transport coefficients derived from a general circulation model provides a possible way of escaping from these limitations and it is

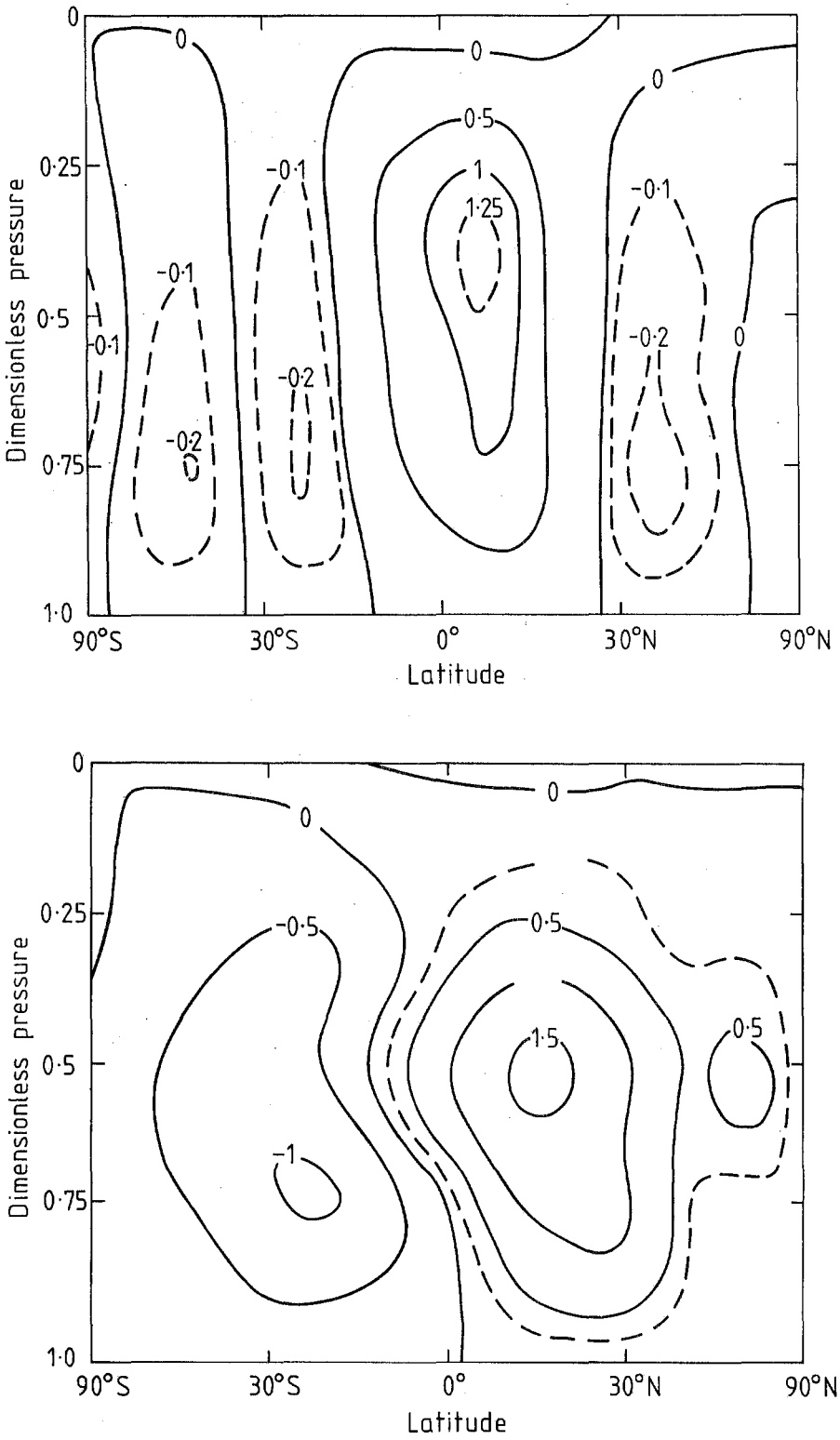


Figure 1. Comparison of mass stream functions for advective transport. Units are atmospheric masses per year. Plots are zonal means for February.
(a) Eulerian mean based on Oort (1983).
(b) Effective transport circulation from GCM calculations obtained by adding antisymmetric part of diffusion tensor to the Eulerian mean stream function.

this approach that is investigated in this paper. The transport coefficients were derived by Plumb and Mahlman from the GFDL (Princeton) GCM/tracer model (Mahlman and Moxim, 1978). Figure 1 shows a comparison of the Eulerian mean stream function obtained from observations (Oort,1983) compared to the effective transport circulation derived from the GCM calculations. This effective transport circulation treats the antisymmetric contributions to the diffusion tensor as advective transports. A comparison between Figures 1.a and 1.b shows how the transport circulation has embodied many near-cancellations between the eddy fluxes and the Eulerian mean circulation.

Plumb (this meeting) describes a number of studies that test how well a two-dimensional representation can reproduce the result of experiments performed using the original GCM. The present paper investigates the question of how well the two-dimensional representation can reproduce observed distributions of minor atmospheric constituents. The use of a two-dimensional representation is not the only way of using GCM transport fields in the study of tracer distributions. The transport fields from GCMs have been used to study tracer distributions in three-dimensional models by Fung et al. (1983) and Fung (1984), see also Fung, this meeting, Prather this meeting,and Prinn, this meeting).

The advantages of using a two-dimensional model compared to three-dimensional models are that with a smaller model it becomes practical to perform a systematic investigation of a much larger range of mechanisms for the sources and sinks of particular tracers.

The present paper describes a number of studies for particular tracers. These studies are preliminary investigations designed to assess the general validity of using the transport fields from the GCM. CCl_3F is studied, primarily as a check on the amount of interhemispheric transport in the model. It is found that the interhemispheric gradient is slightly underestimated, indicating that the transports are too large.

The seasonal variation of carbon dioxide is also investigated. This problem is more complicated because no attempt is made to model the surface sources and sinks. In the model the surface concentrations are forced to follow a smoothed representation of the observed behaviour and the sources are deduced as described by Enting (1984).

The seasonal variations above the surface are used as a check on the validity of the transport formalism. In addition this calculation provides a way for estimates of the surface source strengths as a function of latitude and time to be calculated directly (as opposed to the iterative procedures used by Pearman and Hyson, 1980). The results of the present calculation are shown in Figure 2.

Finally the model is used to investigate the transport of the products of nuclear testing from the stratosphere to the tropsphere. While many of the radionuclide distributions can be represented adequately by the model, the seasonal variations of ^{14}C over the period 1962-1966 are anomalous. There have been a number of conflicting explanations of this seasonal behaviour by various workers of the last 20 years. While the present calculations can exclude some of these possibilities, it has not been possible to obtain a satisfactory model for the behaviour of ^{14}C.

The overall conclusion is that the transport fields derived from the GCM

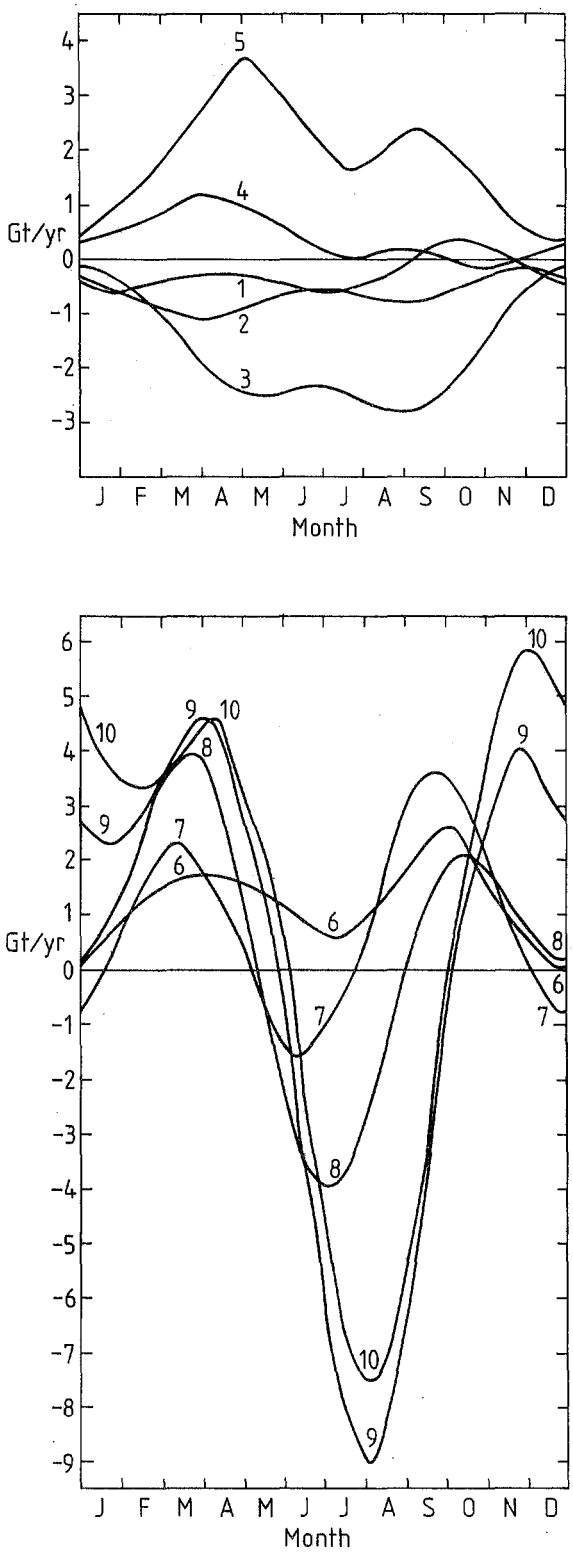


Figure 2. CO_2 source strengths in Gigatons of carbon per year for equal area zones 1 (south) to 10 (north) deduced by using 2-D model with transports based on GCM calculations and smoothed observations of surface CO_2 concentrations used to define surface boundary condition of model.

give a good basis for two-dimensional modelling the distribution of atmospheric constituents, but that the resolution of various minor anomalies is likely to require some tuning of the transport coefficients as well as a refined treatment of the sources and sinks of the tracers.

REFERENCES

Enting, I.G. 1984. Techniques for determining surface sources from surface observations of atmospheric constituents. Division of Atmospheric Research Paper No. 5. (CSIRO, Australia) 30 pp.

Fung, I. Analysis of the seasonal and geographic patterns of atmospheric CO_2 distributions with 3-D tracer model. To appear in "The Global Carbon Cycle: Analysis of the Natural Cycle and Implications of Anthropogenic Alterations for the Next Century" proceedings of the 6th Oak Ridge National Laboratory Life Sciences Symposium. Knoxville, Tennessee, Oct. 31 - Nov.2, 1983.

Fung, I., Prentice, K., Mathews, E., Lerner, J. and Russell, G. 1983 Three-dimensional tracer model study of atmospheric CO_2: Response to seasonal exchanges with the terrestrial biosphere. J. Geophys. Res. 88C: 1281-1294.

Mahlman, J.D. and Moxim, W.J. 1978 Tracer simulation using a global general circulation model: Results from a mid-latitude instantaneous source experiment. J. Atmos. Sci. 35: 1340-1374.

Oort, A.H., 1983 Atmospheric Circulation Statistics, 1958-1973 NOAA Professional Paper 14. (U.S. Govt. Printing Office, Washington, D.C.) 180 pp. plus microfiche.

Pearman, G.I. and Hyson, P. 1980 Activities of the global biosphere as reflected in atmospheric CO_2 records. J. Geophys. Res. 85C: 4468-4474.

Background Ozone and Anthropogenic Impact in the Colorado Mountains

F. C. Fehsenfeld, S. C. Liu, D. D. Parrish, P. C. Murphy,
D. W. Fahey, M. Trainer, and D. L. Albritton

Aeronomy Laboratory
Environmental Research Laboratories
National Oceanic and Atmospheric Administration
Boulder, Colorado 80303

1. INTRODUCTION

Before it is possible to assess the anthropogenic influence on the atmospheric ozone concentration and, thus, the subsequent environmental impact of increased ozone levels on vegetation, it is necessary to determine the ozone levels at the surface that can be attributed to the natural background. The evidence for a natural background level of ozone comes mostly through the analysis of long-term ozone measurements in rural and remote locations. However, most of these locations are under the influence of diluted anthropogenic emissions. Since there is observational evidence that significant O_3 is produced photochemically when its precursor NO_x ($NO+NO_2$) is as low as 0.5 ppbv (Fehsenfeld et al., 1983), it is difficult to derive the level of natural background surface ozone.

Between June 1980 and October, 1981, O_3, NO, NO_2, HNO_3, particulate NO_3, and SO_4, CO, several aromatic hydrocarbons, terpenes, solar UV flux, H_2O, temperature, and wind speed and direction were measured (continuously for most of them) at a rural site in the Colorado mountains. The purpose of these measurements is to study the photochemistry of O_3. In the following sections, we will show that the extensive data on O_3 and NO_x can be used to derive the background O_3 level.

There is argument (e.g., Fishman et al., 1979) claiming that the northern hemispheric background O_3 level has already been elevated significantly due to anthropogenic emissions of CO and NO_x. If this is true, the background O_3 level derived in the following would not be the natural background level but the "elevated background" level.

2. LOCATION AND MEASUREMENTS

The measurements were obtained at the research site (40° 2'N; 105° 32'W, 3.05 km elevation) in a forest clearing located approximately 200 m below treeline. The site is located 80 km northwest of metropolitan Denver, which has an elevation of approximately 1.6 km. The prevailing winds at the site blow from the west. This air is normally free of anthropogenic pollution. However, there are frequent occasions when the wind is from the east. These easterlies (i.e., upslopes) can transport anthropogenic pollution from the metropolitan area to the research site. As a consequence of this meteorology, the measurements show large variation in concentration associated with anthropogenic pollution.

Ozone was measured by a UV-absorption instrument (Dasibi, Inc., Model 1003-AH) that has a detection limit of 3 ppbv and an estimated uncertainty of less than 10%. Nitric oxide is measured using a chemiluminescence technique, while NO_2 is first photolyzed to NO, which is then measured. This instrument has a detection limit for a 10 sec averaging time of 0.002 ppbv for NO and approximately 0.01 ppbv for NO_2.

3. RESULTS AND DISCUSSION

Since NO_x together with hydrocarbons (HC) and CO are precursors for photochemically generated O_3 in the troposphere, it is expected that O_3 correlates with NO_x, HC, and CO, especially in the summer when photochemistry is most intense. Figures 1a, and 1b show respectively the morning and afternoon relationship between O_3 and NO_x in the summer. Because of the photochemical production of O_3 during the day, O_3 mixing ratio increases with NO_x up to about 3 ppbv, especially in the afternoon. When NO_x is higher than 3 ppbv there is a slight decrease in O_3. However, there are not enough data points to establish this trend. There is a greater standard deviation when NO_x is greater than 0.5 ppbv. We believe most of the deviation is due to the presence of clouds that reduce the production of O_3 as discussed by Fehsenfeld et al. (1983).

When NO_x is less than 0.15 ppbv, the data asymptote toward a constant O_3 level of about 43 ± 9 ppbv. This strongly suggests that 43 ppbv is the summer background O_3 level at Niwot Ridge. The disappearance of daytime variation in O_3 implies that the photochemical production of O_3 is slow relative to the transport processes that maintain the O_3 level. Our model calculations gave a net O_3 production of about 2 ppbv per day under clear sky conditions when NO_x is at 0.1 ppbv, too small to give any detectable diurnal variation. In addition, with this net production rate the doubling time for O_3 is about 20 days. If we allow for the probability of cloudiness, the doubling time would be even longer. The westerlies at 500 mb is about 10 ms^{-1} which will transport air masses from the Pacific to Niwot Ridge in about 3 days. Since air masses from the Pacific can probably be considered as natural background air as far as NO_x and O_3 are concerned (Liu et al., 1983), therefore we conclude that the background O_3 level at Niwot Ridge is probably also the natural background O_3 value.

After establishing the summer natural background O_3 level, one can evaluate the anthropogenic effect on the day time ozone level by subtracting 43 ppbv from all the points in Figures 1a and 1b, and calculating the average difference. The same processes are applied to other seasons. As expected, anthropogenic impacts on O_3 in other seasons are smaller than the summer value due to smaller photochemical production.

4. REFERENCES

Fehsenfeld, F. C., M. J. Bollinger, S. C. Liu, D. D. Parish, M. McFarland, M. Trainer, D. Kley, P. C. Murphy, D. L. Albritton, and D. H. Lenschow, 1983: A study of surface ozone in the Colorado Mountains, J. of Atmospheric Chemistry, 1, 87-105.

Fishman, J., S. Solomon, and P. J. Crutzen, 1979: Observational and theoretical evidence in support of a significant in situ photochemical source of tropospheric ozone, Tellus, 31, 632-446.

Liu, S. C., M. McFarland, D. Kley, O. Zafiriou, and B. Huebert, 1983: Tropospheric NO_x and O_3 budgets in the equatorial Pacific, J. Geophys. Res., 88, 1360-1368.

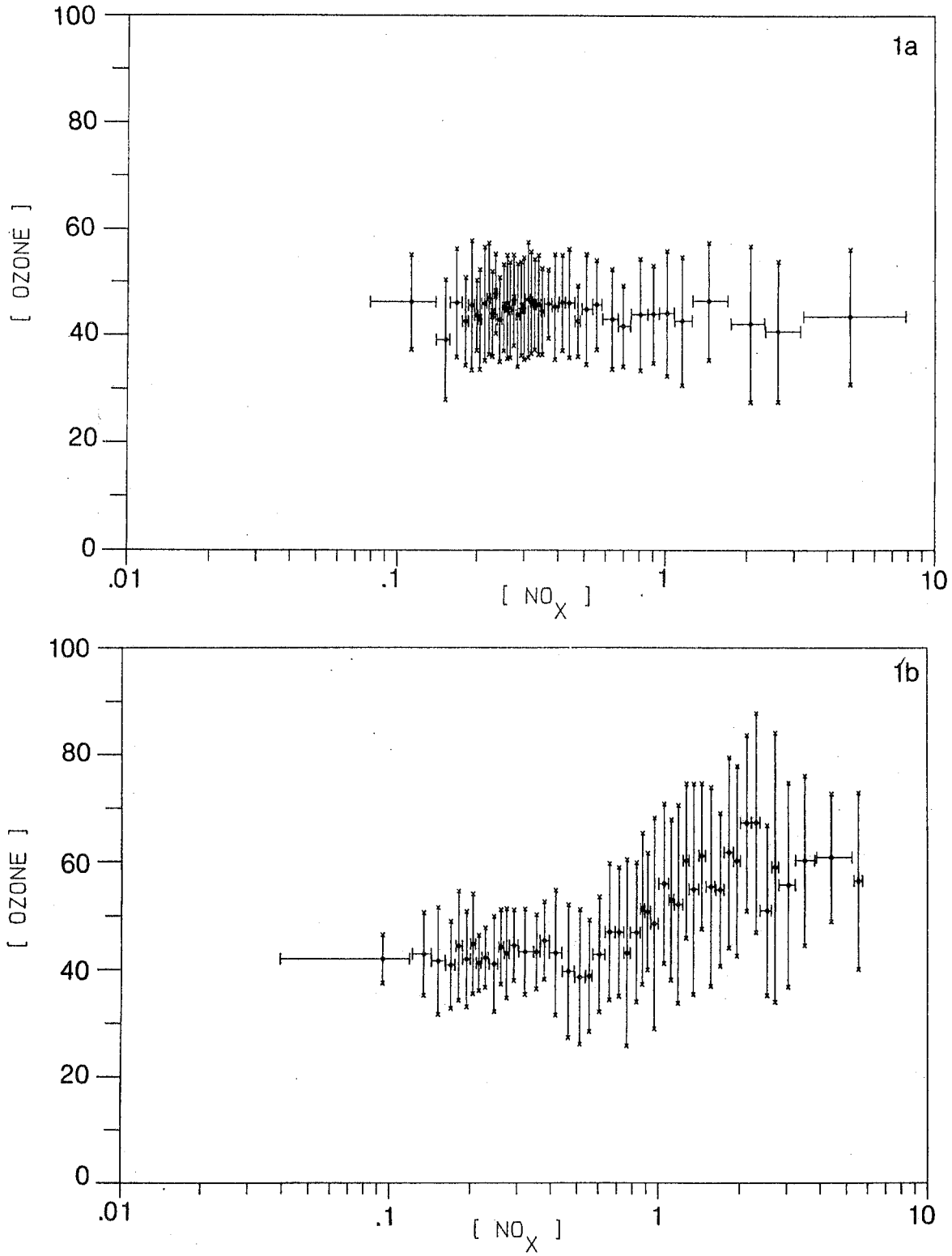


Fig. 1a Correlation of O_3 and NO_x mixing ratios (ppbv) between 7 a.m. MST and 12 Noon MST for the period June 1, 1981 and August 31, 1981 at Niwot Ridge, Colorado. Each point represents the average of twenty measurements, the vertical bar indicates the standard deviation of the O_3 mixing ratios, and the horizontal bar is the span of NO_x mixing ratios for each set of data.

Fig. 1b Same as 1a except the measurements were made between 3 p.m. MST and 8 p.m. MST.

METHANE AND CARBON MONOXIDE IN THE SOUTHERN HEMISPHERE

P.J. Fraser, P. Hyson

CSIRO, Division of Atmospheric Research,
Private Bag 1, Mordialloc, Vic. 3195 Australia.

and

R.A. Rasmussen

Department of Chemical, Biological and Environmental Sciences,
Oregon Graduate Centre,
19600 NW Walker Road, Beaverton, Oregon 97006, U.S.A.

Methane (CH_4) is an important component of the background atmosphere, not only because of its significant contribution to total infrared opacity, but also because of its major roles in both stratospheric and tropospheric chemistries. Carbon monoxide (CO) and CH_4, together with ozone (O_3), water vapour (H_2O) and ultra violet radiation are believed to control the levels of hydroxyl radicals (OH) in the background marine troposphere (Crutzen, 1982). Unfortunately there is currently a lack of direct, quantitative data available on the distribution of OH in the troposphere. However the major atmospheric sinks for CH_4, CO and methylchloroform (CH_3CCl_3) are reaction with OH and, provided their sources can be independently evaluated, the spatial and temporal variablitiy of these gases in the background atmosphere can be used to assess the behaviour of background OH levels as predicted by photochemical models.

In this paper we report CH_4, CO and CH_3CCl_3 data from Cape Grim, Tasmania (41°S, 145°E), CH_4 and CO from Mawson, Antarctica (68°S, 63°E), CH_4 from aircraft over SE Australia (34°S - 41°S, 130°E - 150°E) and from ships between the Australian mainland and the Antarctic coast (40°S - 68°S, 62°E - 155°E). The data are analysed for seasonal cycles and long term trends, which are evident in all species, except CO at Cape Grim, which does not show any significant long term changes in concentration.

The CH_4, CO and CH_3CCl_3 concentrations observed at Cape Grim are simulated using a global two-dimensional transport model (Hyson et al., 1980), tuned to reproduce the global distribution of trichlorofluoromethane (CCl_3F; Fraser et al., 1983). We use published sources of CH_4 (Khalil and Rasmussen, 1983), CO (Logan et al., 1981) and CH_3CCl_3 (Prinn et al., 1983). Sinks for all species involve reaction with OH (De More et al., 1982) as well as a soil sink for CO (Logan et al., 1981). OH fields are derived from Crutzen (1982).

The global distributions of CH_4, CO and CH_3CCl_3 obtained from the model are compared to the observations reported in this paper and from other locations around the globe (CH_4: Khalil and Rasmussen, 1983; Fraser et al, 1984; Steele et al., this meeting; CO: Khalil and Rasmussen, 1984; CH_3CCl_3, Prinn et al., 1983).

The relative contributions of OH chemistry and transport to the observed variability of CH_4, CO and CH_3CCl_3 at Cape Grim are assessed.

REFERENCES

Crutzen, P.J., 1982, The global distribution of hydroxyl,in E.D. Goldberg (ed.), Atmospheric Chemistry, Springer-Verlag, Berbin, pp 313-328.

De More, W.B., Watson, R.T., Golden, D.M., Hampson, R.F., Kurylo, M., Howard, C.J., Molina, M.J. and Ravishankara, A.R., 1982, Chemical kinetics and photochemical data for use in stratospheric modelling. Evaluation number 5. JPL Publication 82-57, Jet Propelsion Laboratory, California Institute of Technology, Pasadena, California.

Fraser, P.J., Hyson, P., Enting, I.G. and Pearman, G.I., 1983, Global distribution and southern hemispheric trends of atmospheric CCl_3F, Nature, 302, 692-695.

Fraser, P.J., Khalil, M.A.K., Rasmussen, R.A. and Steele, L.P., 1984, Tropospheric methane in the mid-latitudes of the southern hemisphere, J. Atmospheric Chemistry, 1, 125-135.

Hyson, P., Fraser, P.J. and Pearman, G.I., 1980, A two-dimensional transport simulation model for trace atmospheric constituents, J. Geophys. Res., 85, 4443-4455.

Khalil, M.A.K. and Rasmussen, R.A., 1983, Sources, sinks, and seasonal cycles of atmospheric methane, J. Geophys. Res., 88, 5131-5144.

Khalil, M.A.K. and Rasmussen, R.A., 1984, Carbon monoxide in the earth's atmosphere: increasing trend, Science, 224, 57-56.

Logan, J.A., Prather, M.J., Wofsy, S.C. and McElroy, M.B., 1981, Tropheric chemistry: a global perspective, J. Geophys. Res. 86, 7210-725Y.

Prinn, R.G., Rasmussen, R.A., Simmonds, P.G., Alyea, F.N., Cunnold, P.M. Lane, B.C., Cardelino, C.A. and Crawford, A.J., 1983, The Atmospheric Lifetime Experiment; 5. Results of CH_3CCl_3 based on three years of data, J. Geophys. Res., 88, 8415-8426.

ON THE VARIABILITY OF CO_2 EXCHANGE BETWEEN THE ATMOSPHERE AND THE BIOSPHERE

Inez Y. Fung
NASA Goddard Space Flight Center, Institute for Space Studies
New York, New York 10025 USA
and
Lamont-Doherty Geological Observatory of Columbia University
Palisades, New York 10964 USA

C. J. Tucker
NASA Goddard Space Flight Center
Greenbelt, Maryland 20771 USA

Katharine C. Prentice
Department of Geography, Columbia University
New York, New York 10027 USA

1. INTRODUCTION

The terrestrial biota plays a major role in the geographical and temporal variations of atmospheric CO_2. The seasonal exchange of CO_2 exchange between the atmosphere and the biosphere, via photosynthesis and soil release, is the primary cause of the annual oscillations found in the records of atmospheric CO_2 (see e.g., Machta, 1972; Keeling, 1983). Analyses of the atmospheric CO_2 measurements show that the annual oscillations exhibit interannual variations and the amplitudes of the cycles have been increasing in time (Pearman and Hyson, 1981; Keeling, 1983). One of the possible contributing factors to the interannual and long-term variations is enhanced summer assimilation by the biosphere, although there is little field evidence to confirm the hypothesis.

Simulations of atmospheric CO_2 concentrations at a few remote marine stations have been used to estimate the magnitude of this seasonal exchange (e.g., Junge and Czeplak, 1968; Machta, 1972; Pearman and Hyson, 1980; Fung et al., 1983). Because of the differences in the atmospheric transport models, the biospheric exchange functions that provided best fit to the observations differed by at least a factor of two. Furthermore, because the exchange functions are based on simple assumptions, they cannot be used to evaluate the year-to-year changes in biospheric activity or the contributions of these changes to the interannual variations of atmospheric CO_2. In this paper, we present a new method, using satellite and field data, to study the seasonal exchange of CO_2 between the atmosphere and the terrestrial biota.

2. METHOD

(1) Uptake of carbon: Global distributions of the 'normalized difference vegetation index' (NVI), derived as a combination of channel 1 (0.5-0.7μm) and channel 2 (0.7-1.1 μm)

radiances measured by the Advanced Very High Resolution Radiometer (AVHRR) aboard the polar-orbiting satellites of NOAA, have been obtained for April 1982 to March 1984. At each location, the phasing of the CO_2 uptake is assumed to be directly proportional to the phasing of the NVI, and the annual Net Primary Productivity (NPP) based on the Matthews vegetation map (1983).

(2) Release of carbon: Empirical relationships between environmental conditions and the soil release of carbon have been derived for the major biomes or biome groups. These relationships are coupled with surface climate observations and the NPP map to yield the monthly distribution of release of carbon due to soil respiration.

The monthly distributions of the net flux of carbon between the atmosphere and the biosphere thus derived reflect the spatial complexity as well as the temporal behavior of the terrestrial biota. These prescriptions of the biosphere-atmosphere exchange of CO_2 have been used as inputs to the 3D tracer transport model (cf. Fung et al., 1983) which uses winds generated by a 3D general circulation model (Hansen et al., 1983) to advect CO_2 as an inert constrituent in the atmosphere.

3. DISCUSSION

The annual cycles of CO_2 simulated at the locations of the measurements are found to be in reasonable agreement with those observed. The differences between the simulated and observed CO_2 cycles are within the natural variability of the observations. This result supports the model of biospheric exchange of CO_2 based on satellite and field data.

Analysis of the carbon uptake derived from the NVI shows that the amount of carbon assimilated during 4/83-3/84 is approximately 15 percent less than that assimilated during 4/82-3/83, probably as a result of the severe El-Nino event. This could be partial explanation for the decreased amplitudes of CO_2 oscillations in 1983 compared to those in 1982. However, to quantify the contributions of the different factors affecting the interannualvariations of the atmospheric CO_2 cycles, the variations in soil respiration and in atmospheric circulation must be included.

4. REFERENCES

Fung I., K. Prentice, E. Matthews, J. Lerner and G. Russell, 1983: Three-dimensional tracer model study of atmospheric CO_2: Response to seasonal exchange with the terrestrial biosphere, J. Geophys. Res., 88, 1281-1294.

Hansen, J., G. Russell, D. Rind, P. Stone, A. Lacis, S. Lebedeff, R. Ruedy and L. Travis, 1983: Efficient three dimensional global models for climate studies: Models I and II, Mon. Wea. Rev., 111, 609-662.

Junge, C. and G. Czeplak, 1968: Some aspects of the seasonal variation of carbon dioxide and ozone, Tellus, 20, 422-434.

Keeling, C.D., 1983: The global carbon cycle: What we know and could know from atmospheric, biospheric and oceanic observations, In Proceedings: Carbon Dioxide Research Conference, Science and Consensus. September 19-23, 1982, Berkeley Springs, West Virginia, U.S. Dept. of Energy CONF-820970.

Machta, L., 1972: Mauna Loa and global trends in air quality, Bull. Am Meteorol. Soc., 53, 402-420.

Matthews, E., 1983: Global vegetation and land use: new high-resolution data bases for climate studies, J. Climate and Appl. Meteor., 22, 474-487.

Pearman G. and P. Hyson, 1980: Activities of the global biosphere as reflected in atmospheric CO_2 records, J. Geophys. Res., 85, 4468-4474.

Pearman G. and P. Hyson, 1981: The annual variation of atmospheric CO_2 concentration observed in the northern hemisphere, J. Geophys. Res., 86, 9839-9843.

LONG TERM CHANGES IN ATMOSPHERIC NITROUS OXIDE

I. E. Galbally

CSIRO, Division of Atmospheric Research
Private Bag 1, Mordialloc, Vic. 3195 Australia.

Measurements in surface air at Cape Grim, Tasmania, (40^{o}S) made since 1978 show a slow increase in the mixing ratio of N_2O. Similar observations at other locations have been reported.

Various authors have attributed the increase in atmospheric N_2O to either anthropogenic emissions of N_2O from fossil fuel combustion or enhanced N_2O emissions from agricultural activities.

A simple model of atmospheric N_2O based on measured emission ratios from various ecosystems, historical changes in the areas of these ecosystems, other natural and anthropogenic sources and a simple concentrated department sink (simulated statistical manoeuvre) is presented.

The calculated rate of change of atmospheric N_2O during the last decade is presented and the trend of the last decade is compared with observations.

THE 1982/83 ENSO EVENT: THE RESPONSE OF THE GLOBAL ATMOSPHERIC CO_2 DISTRIBUTION.

R. Gammon, W. Komhyr, L. Waterman, T. Conway, K.Thoning and D. Gillette

Geophysical Monitoring for Climatic Change, ERL/NOAA, Boulder, Colorado 80302

From the established correlation of the Southern Oscillation Index with anomalies in the CO_2 growth rate (Bacastow, 1976, Bacastow et al., 1980), it was expected that the extreme ENSO event which began in mid-1982 would measurably perturb the global atmospheric CO_2 distribution. This CO_2 anomaly was first reported in analyses of the NOAA/GMCC global CO_2 records by Gammon et al (1983), who documented an anomalously low observed rate of CO_2 increase in mid 1982 and predicted a post-ENSO maximum in the CO_2 year-to-year increase for late 1983/early 1984 of 2-3 ppm yr^{-1}. This prediction has been confirmed in the latest results from the GMCC/NOAA network (Figure 1).

More detailed analyses of the recent NOAA CO_2 data summarized below have been presented at the DOE Symposium on the Global Carbon Cycle in Knoxville, November 1983 (Gammon et al., 1983) at the AGU Chapman Conference on National Variations in CO_2 and the Global Carbon Cycle in Tarpon Springs, Florida, January, 1984 (Gammon et al. 1984a), and research findings to appear in the Department of Energy State-of-the-Art Report to Congress on the CO_2 question (Gammon et al., 1984b).

The globally averaged year-to-year change in atmospheric CO_2 plotted by season (Figure 1) clearly shows the effect of the 1982/83 ENSO event on the global atmospheric burden of CO_2 over at least a two-year period, from mid-1982 to mid-1984. The fall of 1982 relative to the fall of the previous year showed no increase (0.0 ± 0.3 ppm yr^{-1}) in global CO_2 which means that the equivalent of approximately 5×10^9 tons of fossil carbon burned during that interval was removed from the atmospheric reservoir for (temporary) storage in the near surface ocean, and (probably) in the land biosphere as well. Now, more than a year after the minimum in the Southern Oscillation Index (1/83), this missing 5 Gtons of carbon seems to have been returned to the atmosphere; the year-to-year CO_2 increase peaked in early 1984 at 2.2 ± 0.3 ppm yr^{-1}, well above the mean growth rate of 1.4 ppm yr^{-1} over the past decade. Recall that the past 5 years has been a period of nearly constant global production of fossil fuel (~5 Gton yr-1), so that the observed large interannual variations in atmospheric CO_2 are clearly not the result of changing rates of fossil fuel usage..

Previous investigators have focussed interpretations on the high CO_2 growth phase, which lags the SOI minimum by a few seasons, depending on the latitude of the CO_2 monitoring station (Bacastow et al., 1980); however, the precursor phase of low CO_2 growth is equally prominent in the 1982/83 event, and may offer predictive possibilities for future ENSO events. There is also the distinct possibility that the El Chichon eruption (4/82) is somehow linked to the subsequent atmospheric circulation anomalies in the Spring/Summer of 1982, which marked the unusually phased beginning of this ENSO event. If, in addition to the well established stratospheric heating, tropospheric cooling could be clearly attributed to the El Chichon dust veil, such a cooling might

have deepened the mid 1982 CO_2 slow-growth dip. One hope in unravelling the interwined effects of El Chichon/El Niño upon global circulation, and upon the global carbon cycle, rests in the inherently longer timescale of the climatic signal of the volcanic stratospheric dust. As the circulation and SST anomalies attributable to the 82/83 ENSO event fade, the residual and more persistent volcanic signal, and its global climatic and carbon cycle signature, may emerge.

Probably more important than the complicating effects of El Chichon is the very large uncertainty in assessing the global response of the land biosphere to the altered temperature and predcipitation patterns which accompany a major El Niño event. While regional crop failures, floods and droughts are well documented, the globally integrated response and its effect on the atmospheric CO_2 level is harder to estimate. There is some recent evidence from satellite monitoring of the"vegetation index" of land plant antivity that 1982 was a better growing season globally than was 1983 (Tucker et al., 1984). This suggests that some fraction of the 5 Gtons of carbon missing from the global atmosphere in the Fall of 1982 may have been temporarily stored in the annually recycled biosphere.

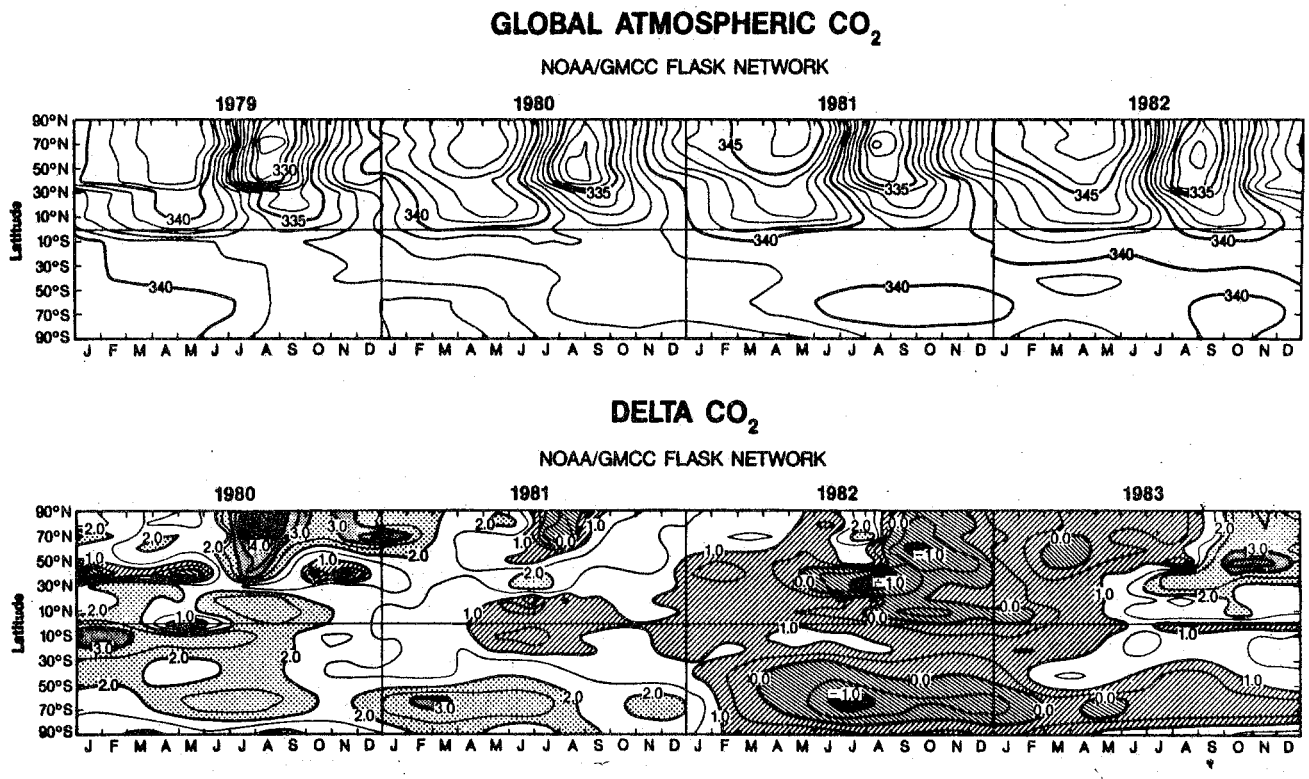


Figure 1(a)Zonally averaged CO_2 concentration for 1979-82 as determined from the GMCC/NOAA global flask network(Gammon et al , 1984). Resolution of the original data is approximately 10^o in latitude, biweekly in time.

Figure 1(b)Year-to year difference of the concentration surfaces of Figure 1(a), plotted in the forward year. Growth rate anomalies less than 1.0 ppm yr^{-1} (hatched) or greater than 2.0 ppm yr^{-1} (dotted) indicate the latitude and time dependence of the 1982/83 El Niño-Southern Oscillation perturbation.

CONCENTRATION AND SIZE VARIATION OF CONDENSATION NUCLEI AT MAWSON, ANTARCTICA

J.L. Gras and A. Adriaansen

Cloud Physics Laboratory, Division of Atmospheric Research, CSIRO
P.O. Box 134, Epping, NSW, 2121

Few data sets with sufficiently long periods to satisfactorily determine the seasonal variation of condensation nucleus (CN) concentration are available for the Antarctic continent. Even fewer give information on the size distribution. Such data however promise to be of help in understanding the complex process of natural particle production and transport over a vast area of Antarctica and the surrounding Southern Ocean. In this paper we present a number of observations from the first of a new series of CN measurements made at Mawson, on the Antarctic coast, commencing in 1981 and comprising approximately three annual cycles in CN concentration and eight months of preliminary size distribution data.

Annual variation in CN concentration

Condensation nucleus concentrations have been measured at Mawson using a (Pollak) replica 1957 photoelectric nucleus counter (Pollak and Metnieks 1960), for approximately three annual cycles. Although in routine analysis the Mawson data have been edited to the extent that essentially only occasions where air arriving at the station has an immediately "continental" trajectory are included, there is virtually no difference in the form of variation of the median when all the data are included. The form of the annual variation at Mawson is clearly dominated by the concentration of particles in the cold boundary layer of air which almost continually flows down from the central plateau region (Mather 1969). The concentration from October to March remains relatively constant in the range 300 to 400 cm^{-3} and then falls very rapidly during April-May to typical levels of some tens of particles per cubic centimetre. There is some indication that concentrations may rise slightly over winter although the most rapid rise, back to summer concentrations, occurs in September with a time constant very similar to the autumn decline. There are many points in common in the annual variation at Mawson and at the South Pole as discussed in detail by Bigg et al. (1984). The close similarity of the form of this annual variation in particle concentrations and the annual variation in solar radiation at a number of remote southern hemisphere sites, and the asymmetry of the particle variation around the winter solstice as shown by Bigg et al., variation in condensation nuclei over the Antarctic continent is dominated by the availability of solar radiation during the autumn-winter-spring

period and that the source of these nuclei is photochemical. This line of reasoning indicates a mean lifetime of 20 to 30 days for Antarctic aerosol, a value similar to that deduced by Shaw (1982) from the variation of optical depth across the continent. A slight increase in particle concentrations during July-August at Mawson and at Syowa but which is less evident at South Pole does not appear to be photochemical in origin but is more likely associated with the penetration of maritime air from off-shore cyclonic disturbances. In winter intrusions of low-level, relatively warm moist air at Mawson and Syowa associated with off-shore cyclonic disturbances are accompanied by sustained period of high particle concentration (to around 500 cm^{-3}) lasting from several hours to over a day.

Variation in size distribution, winter-summer 1982-1983

A manually operated eight-stage screen diffusion battery similar in design to that described by Sinclair and Hoopes (1975) was used in conjunction with the station Pollak counter to derive size distribution information over the period June 1982 to February 1983. Data obtained during the winter period, when concentrations are exceedingly low (10 to 20 cm^{-3}), are obviously exceedingly difficult to size by this (or any) method; however, there is a clear indication that the typical size is very small, as shown on several occasions when virtually all particles were lost on passing the first stage of the diffusion battery (50% transmission for r = 0.0075 μm). From late winter in 1982 total particle concentrations rose relatively steadily until about the end of spring, when a marked decrease occurred. This is similar to the summer variation of CN at South Pole. The concentration of particles penetrating up to stage 2 of the diffusion battery (50% transmission at r = 0.019 μm) were similar to the total concentration. For larger particles, for example those penetrating stage 6 (maximum transmission, 42% at r = 0.30 μm), the variation in concentration bears little relation to the variation of total particle concentration, exhibiting two broad increases - one in late winter and the other over summer. These penetration variations appear to suggest a complicated seasonal variation in particle size distributions consistent with a large particle increase in late winter followed by an increase in both concentration and relative size, initially in spring in smaller size ranges and later in summer in large sizes (penetrating up to stage 6).

The majority of distributions, obtained by inverting the penetration data, have a single mode and are approximately log-normal, but bimodal distributions were indicated on approximately 30% of occasions. Bimodal size distributions obtained on July 16 and 18 correspond with a period of enhanced particle concentration similar in nature to the "events" reported by Ito and Iwai (1981). These authors, after Hogan and Barnard (1978), tentatively classified events as due to either subsidence of dry air associated with upper frontal passage during summer or advection of warm moist air from lower latitudes with low-level frontal activity. Examination of the meteorological data for the period around the particle enhancement shows a concomitant increase in moisture (although little change in temperature), suggesting the advection of oceanic air, in which case it is probable that the larger size mode is sea-salt. It should be noted however that when the air arrived at Mawson its trajectory was south-east or "continental".

By considering the larger mode of the bimodal distributions to be independent of the remaining small particle mode a general seasonal trend in modal diameter of the small particle mode is evident. Typical values range from less than 0.01 μm in winter increasing to around 0.03 to 0.04 μm in summer. Within the limitations of the sizing technique this summer value for typical size agrees quite well with the typical size of about 0.025 μm observed for the fine particle sulfate mode in maritime air at southern mid-latitudes by Gras and Ayers (1983). The very small typical size of the winter aerosol and its persistence over the sunless part of the winter can be understood in view of the low concentrations and the consequent weak thermal coagulation. Bigg et al. (1984) have argued that the time constant for the decay of aerosol concentrations over the Antarctic continent is 20 to 30 days, which implies a mid-tropospheric source or reservoir. Assuming for example that the source of particles is at 500 mbar and the number concentration is 50 cm^{-3} (numerically similar to the Mawson (sea level) winter value but significantly greater than South Pole winter concentrations), then for particles typically 0.01 μm radius coagulation only accounts for a number decrease of around 10% in two weeks. Growth to much larger sizes even with a 20- to 30-day lifetime will clearly be inhibited while concentrations are as low as this. The increase in typical size from winter to summer is consistent with a photochemical source of the fine particle fraction and a shift from mainly new particle nucleation in spring to heterogeneous growth during summer, as suggested by Bigg et al. (1984). This is possibly most clearly indicated in the penetration data, where the initial springtime increase in particle concentrations occurs for particles removed before stage 4 of the diffusion battery (50% transmission at 0.07 μm) and the increase in larger particles as shown by the number penetrating stage 6 of the battery only occurs once the total concentration has reached its typical summer value and is levelling off.

Diurnal variation in CN concentration

Systematic diurnal variation in CN concentrations was investigated by examining the percentage variation at a given sampling time of four-weekly median concentrations. A similar procedure was followed for wind strength which has a known, pronounced diurnal variation (Streton 1962; Mather 1969). This revealed an early morning maximum and later afternoon minimum in wind strength, as reported by Streton for the summer period. As well, a weak diurnal variation (<4%) with a maximum around local mid-day was present in the years studied. By comparison the CN concentrations showed little consistent variation with respect to time of day or season and hence also wind strength. There is some suggestion of a more pronounced and organized diurnal variation during winter, although the noise level clearly dictates a longer data period to establish this trend with certainty. It is evident therefore that the influence of the strength of the katabatic wind on particle concentrations, via mechanisms such as particle losses to blowing snow, is very weak in an average sense. It is also apparent that the diurnal variation in the inversion strength and depth has very little significant effect on particle concentrations in the surface layer.

References

Bigg E.K., J.L. Gras and C. Evans. Origins of Aitken particles in remote regions of the Southern Hemisphere. J.Atmos.Chem., I, 203-214, 1984.

Gras J.L., and G.P. Ayers. Marine aerosol at southern mid-latitudes. J.Geophys.Res., 88, 10661-10666, 1983.

Hogan A. and S. Barnard. Seasonal and frontal variation in Antarctic aerosol concentrations. J.Appl.Meteorol., 17, 1458-1465, 1978.

Ito T. and K. Iwai. On the sudden increase in the concentration of Aitken particles in the Antarctic atmosphere. J.Meteorol.Soc. Japan, 59, 262-271, 1981.

Mather K.B. The pattern of surface wind flow in Antarctica. Pageoph., 75, 332-354, 1969.

Pollak L.W. and A.L. Metrieks. Intrinsic calibration of the photo-electric condensation nucleus counter model 1957 with convergent light beam. Technical (scientific) note No. 9, School of Cosmic Physics, Dublin Institute for Advanced Studies, Eire, 1960.

Shaw G.E. On the residence time of the Antarctic Ice Sheet aerosol. J.Geophys.Res., 87, 4309-4313, 1982.

Sinclair D. and G.S. Hoopes. A novel form of diffusion battery. Am.Ind. Hyg.Assoc.J., 36, 39-42, 1975.

Streton N.A. Notes on weather conditions in Antarctica (with particular reference to the western part of the Australian Antarctic Territory), Aust.Meteorol.Mag., 37, 1-20, 1962.

WHAT CAN WE LEARN FROM AEROSOL MEASUREMENTS AT BASELINE STATIONS?

Jost Heintzenberg

Department of Meteorology, University of Stockholm
Arrhenius Laboratory, S-106 91 Stockholm, Sweden

1. INTRODUCTION

Aerosol measurements are an integral part of atmospheric monitoring at all baseline stations. Their degree of sophistication varies from single parameters, such as total particle counts (CN) and total aerosol filter samples, to multi-wavelength nephelometry, turbitity measurements, and size-segregated aerosol sampling and chemical analyses. In view of the fact that aerosols are relatively short-lived and comprise only small mass fractions as compared to other atmospheric trace substances, such as CO_2, the questions arise: How do aerosol measurements fit into the initial rationale of atmospheric baseline monitoring and how can they contribute to long-term monitoring for climatic changes on regional (thousands of kilometers) scales and on a global scale (ten thousands of kilometers)? In this paper present possibilities of baseline aerosol monitoring are discussed. They are compared to the extent of implementation and data evaluation within the framework of existing baseline monitoring programs. Recommendations for extensions and reductions of baseline aerosol measurements are given.

2. EVALUATION OF EXISTING BASELINE AEROSOL RECORDS

In both hemispheres 3-8 year aerosol records are available at polar and low-latitude stations. The results of a synthesis of published aerosol results, from 3 stations, concerning average annual variations of different aerosol parameters are discussed below. Each station allows the monitoring of specific regional or natural components. Possibly, hemispheric or global baseline values are observed during part of the year. As an example for a regional anthropogenic aerosol component the spring occurence of Arctic haze is shown in Fig. 1 in terms of particulate sulphate concentrations on Spitsbergen. The spring events of Asian dust at the Mauna Loa observatory are shown in Fig. 2 in terms of particle light scattering coefficients as an example for the monitoring of a regional natural aerosol component. Northern hemispheric and upper tropospheric baseline levels are recorded at the 2 stations during summer and fall, respectively. Finally, the annual variation of total aerosol number concentration (CN) at the South Pole observatory is plotted in Fig. 3, interpreted as showing global tropospheric baseline levels for an illuminated and a dark atmosphere.

3. POSSIBILITIES OF EXTENDING BASELINE AEROSOL MONITORING

Recent aerosol field experiments and the present state of aerosol science in general suggest many valuable extensions (and some reductions) in present monitoring programs. Parametric,

size segregated aerosol sampling for chemical analyses greatly increases the information content of the aerosol records. The Asian dust events have been identified by chemical analyses of sequential filter samples. Such filter samples can be analysed for many anthropogenic and natural components on identical particulate samples. Soot or particulate elemental carbon (PEC) is one such aerosol component for which sequential samples can be collected and analysed by simple means. In Fig. 4 the PEC-results of 3 pilot experiments at baseline stations in the northern and southern hemisphere are collected. The data cover 3 years and show between 2-3 times less PEC in the southern hemisphere.

In Fig. 5a,b examples are given showing the limitations in interpreting certain existing aerosol data sets. Long and continuing 4λ-nephelometer + CN records exist at 4 baseline stations. However, their information content is insufficient for the retrieval of aerosol size distributions: The observations can be explained either by very broad size distributions or by unrealistically narrow bimodal distributions.

4. CONCLUSIONS

Aerosol measurements at baseline stations have proven to be valuable sources of information about atmospheric burdens of particulate matter on regional and hemispheric scales. They need to be augmented by long-term chemical sampling programs to support the interpretation. Chemical sampling programs should include the light absorbing aerosol material and multi-element analyses allowing for the monitoring of chemical signatures of specific natural and anthropogenic source regions.

FIGURE CAPTIONS

Fig. 1 Annual course of $SO_4^{=}$-S 1979-1983 at Ny-Ålesund, Spitsbergen.

Fig. 2 Annual course of 550 nm - light scattering coefficients 00-08 local time 1979-1981 at Mauna Loa observatory.

Fig. 3 Annual course of condensation nuclei concentrations 1974-1981 at South Pole Observatory.

Fig. 4 Northern and southern hemisphere baseline values of aerosol light absorption at 550 nm.

Fig. 5a Maximum possible (——) and minimum necessary (---)
5b aerosol size distributions causing March 1979 and July 1976 4λ-nephelometer + total particle count data at Mauna Loa observatory.

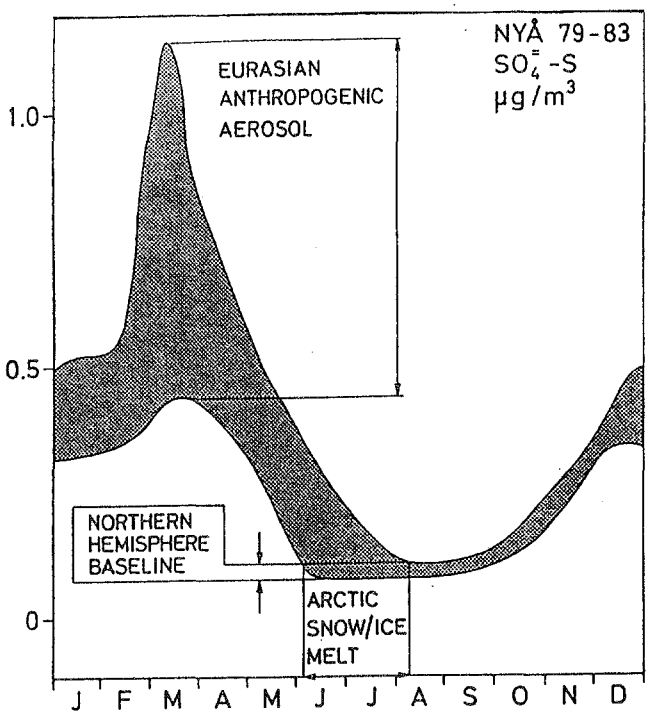


Fig. 1

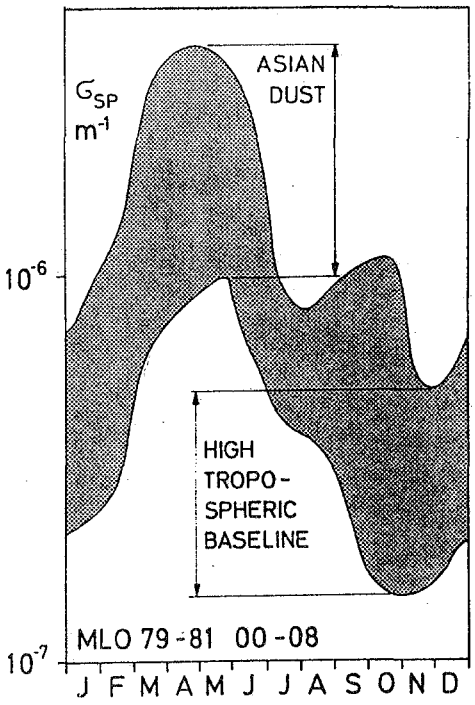


Fig. 2

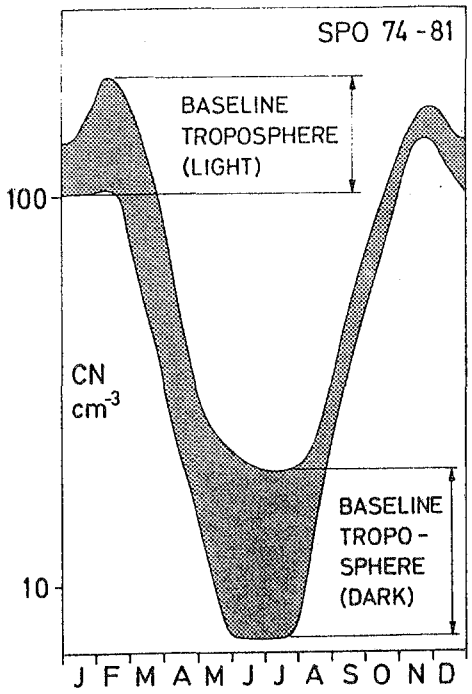


Fig. 3

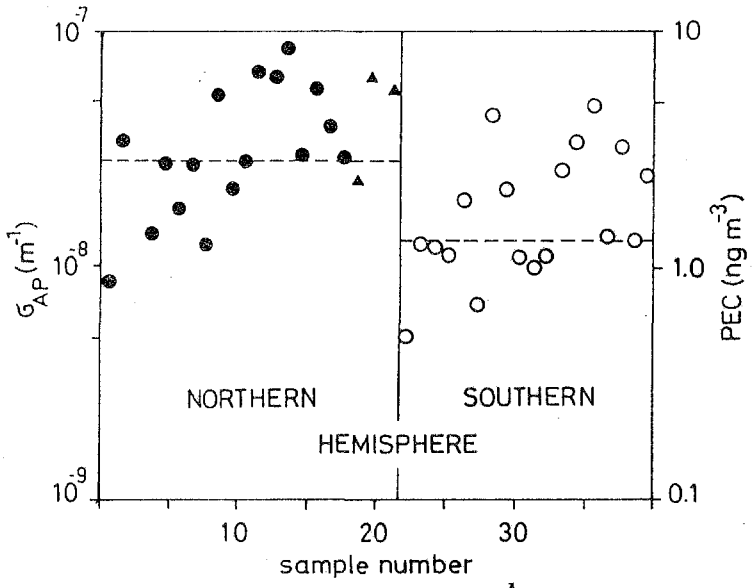


Fig. 4

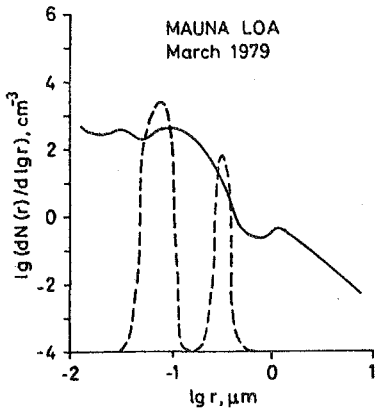
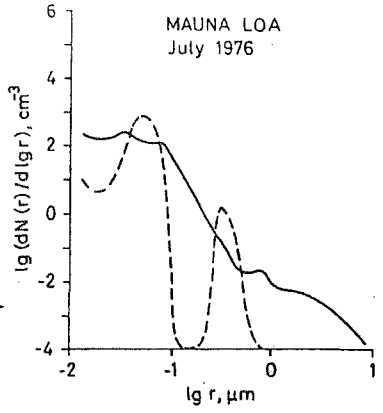


Fig. 5a

Fig. 5b



TRAJECTORY REPRESENTATION OF FLOW CONDITIONS

G. A. Herbert and J. M. Harris

Geophysical Monitoring for Climatic Change, NOAA
325 Broadway, Boulder, Co 80303

THE TRAJECTORY MODEL

For the past 4 years the staff of the Geophysical Monitoring for Climatic Change Division (GMCCD) has been developing and testing computer models to plot back trajectories from receptor locations of interest. The trajectories are plotted on isobaric and isentropic surfaces representative of the receptor site. The model is an adaptation of the Air Resources Laboratory model described by Pack et al. (1978). The program computes trajectories up to 10 days in duration beginning at 00 or 12 CUT on mandatory pressure levels to any location in the Northern Hemisphere (Harris, 1982). The source data consist of a gridded representation of the wind field in component form that is derived from the routine analysis of the U. S. National Meteorological Center. The data consist 65 x 65 grid points distributed over the Northern Hemisphere. In the past, trajectories have been used to track the movement of large plumes for long distances in the midtroposphere.

THE MLO DUST SIGNATURE

The transport of Asian dust to the central Pacific ocean region has received considerable attention since the dramatic duststorm of late April 1979 at MLO, first reported by Shaw (1980). The relative importance of the spring dust events at MLO in 1979 can be seen in the plot of the concentration of aluminum measured during downslope (nighttime) wind conditions (Figure 1). In discussing these data, Parrington et al. (1963) computed the concentration for February through June to be an order of magnitude greater than that observed during the remainder of the year. They also showed a pronounced decrease in the aluminum concentration from 1979 to 1980 and beyond, in agreement with Figure 1. In an effort to understand the causes for such pronounced changes, air mass back trajectories for the months of April-May were computed; see Figure 2. This period represents the peak of the dust season. Studies show that the 500 mb level best represents midtropospheric flow during this season.

The ensemble of back trajectories shown in Figure 2 can be subdivided into three general classes. More than half of the 122 trajectories arrive at MLO after meandering around the mid-Pacific basin for the previous 10 days. The remainder can be tracked to Hawaii on a pronounced westerly flow, some curving in from the south, others with a definite cyclonic curvature off the Asian continent. It is these trajectories that most commonly carry dust to MLO. Especially interesting are the two trajectories that pass over southern Alaska. They arrived in Hawaii on April 25, at the time of the occurrence of the peaks in Figure 1. In 1980 and subsequent years, the majority of the trajectories from the west originate further south in the nondesert regions. The midtropospheric region is zonal much of the time. The reduced occurrence of curved trajectories off the Asian continent indicates a lower frequency of storms for this period. The trajectory ensembles for 1980 through 1982 clearly indicate fewer storms and longer transit paths to Hawaii originating

to the south of the main Asian deserts. These three features are related, and can explain the decrease in the dust concentration that occurred in 1980 and subsequent years.

The large decrease in the aluminum concentration in the spring of 1983 deserves special comment. While in previous years, a number of the weekly filter samples exhibited concentrations in excess of 100 ng m^{-3}, this was not the case in 1983, when the largest concentration was only 37 ng m^{-3}. A review of the trajectories for this season shows a complete absence of curvature. Zonal flow prevails in accord with the general situation in the mid-Pacific caused by the ENSO event and unusually cold water in the north Pacific. An unusually strong zonal flow existed at all altitudes during the winter and spring of 1983. This unusual flow pattern drastically affected the sampling conditions at MLO. In particular, few Pacific storms passed, no rain fell in the months of January-March and very little dust was measured. The 1983 spring dust season is only slightly above background periods of previous years.

CAPE GRIM CLIMATOLOGY

The general wind flow over Cape Grim, Tasmania, was analyzed using back trajectories. The wind field representation known as the Global Grid, with a resolution of 2.5° x 2.5° of latitude and longitude was used. Ten-day back trajectories were computed at 12-hour intervals for 1982. The significant gaps in the data occurred in February for a week, all of July and for a week in August. Trajectories were computed at the 1000-, 850-, and 700-mb levels. The resulting analysis is in terms of the starting point locations at 1 (1000 mb only), 3 and 10 days previous.

As expected, the majority of the trajectories, regardless of length, begin in the western quadrant, at all levels. There is also excellent agreement at the individual levels between 3-day and 10-day starting points. While the trajectories cross sectors in the ensemble, over the year, the distribution of endpoint balances. The population of endpoints increases as the higher layers are considered. The 850-mb level is at about 1.4 km; 700 mb at 3.1 km. At the 1000-mb level, 15% of the trajectory endpoints with 1-day travel are to the north and northeast of Cape Grim, the most potentially polluted directions. Forty-three percent of the 1000-mb trajectories passed over the Australian continent. Due to the large proportion of westerly winds, most are from the western half of the continent.

TRAJECTORY STARTING POINT CLIMATOLOGY FOR CAPE GRIM, TASMANIA

Percent occurrence of trajectories in quadrant shown for period specified.

QUADRANT	ONE DAY	THREE DAYS		TEN DAYS			
	1000 mb	850 mb	700 mb	850 mb	700 mb	850 mb SUMMER	850 mb WINTER
NORTH	23	23	16	22	12	37	15
EAST	8	5	5	6	7	8	10
SOUTH	22	14	10	13	7	4	17
WEST	47	58	69	59	74	51	58

Seasonal variations are also consistent with climatological expectations. Considering only 850-mb endpoints at 10-day travel, there are

relatively small changes in the percent occurrence of east-west components. The major shift is in the north-south direction with significantly more northerly flow in December-January-February and more southerly component in June and August. There is a higher percentage of northerly winds at 850 mb than at 700 mb. During 1982, 12 trajectories were tracked to Cape Grim from New Zealand. In conclusion, there is about a 40% chance of continentally influenced flow; this percentage may increase in the summer months. This percentage does not include flow from the southeasterly sector, which may contain local contamination from the island of Tasmania itself.

REFERENCES

Harris, J. M., 1982. The GMCC Atmospheric Trajectory Program, NOAA Technical Memo. ERL/ARL-116, 30 pp.

Pack, D. H., G. J. Ferber, J. L. Heffter, K. Telegadas, J. K. Angell, W. H. Hoecker and L. Machta. 1978. Meteorology of Long-range transport. Atmos. Environ. 12:425-444.

Parrington, J. R., W.R. Zoller and N. K. Aras, 1983. Asian Dust: Seasonal transport to the Hawaiian Islands, Science, 220, 195-197.

Shaw, G. E., Transport of Asian desert aerosol to the Hawaiian Islands, J. Appl. Meteorol., 19:1254-1259, 1980.

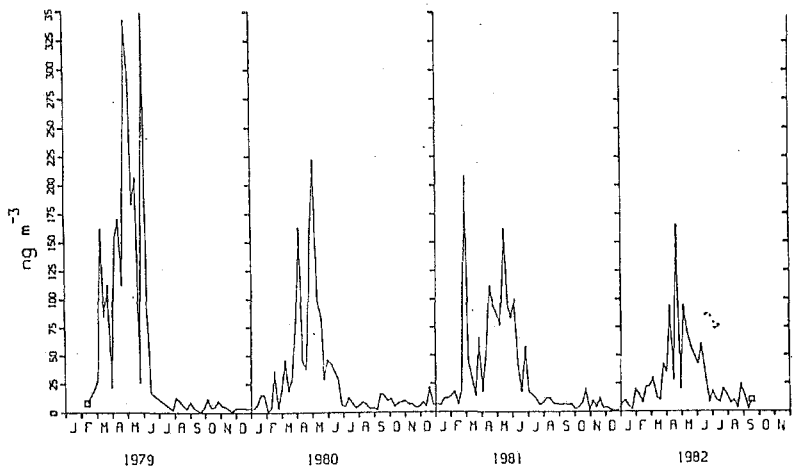


Fig. 1 Weekly filter samples of aluminum obtained during downslope wind at MLO using a high-volume aerosol sampler from Parrington, et al., 1983.

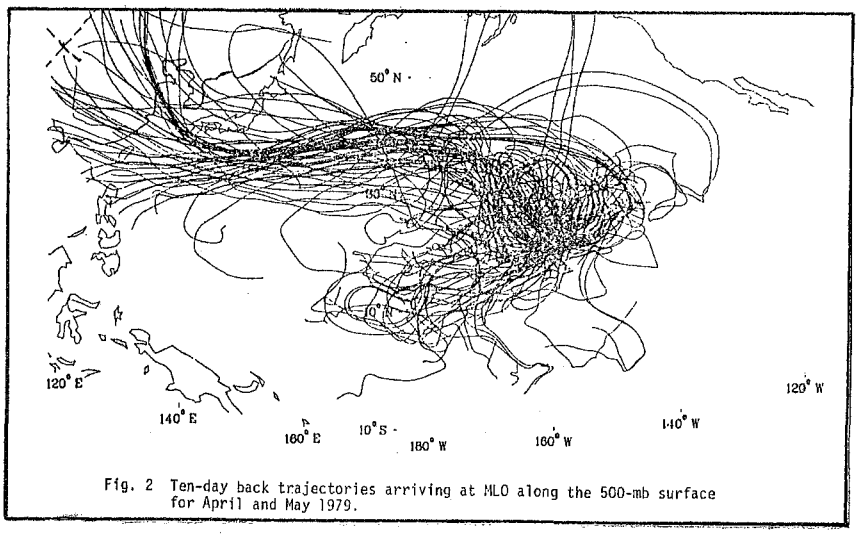


Fig. 2 Ten-day back trajectories arriving at MLO along the 500-mb surface for April and May 1979.

INTERPRETATION OF TRACE GAS MEASUREMENTS AT HIGH NORTHERN LATITUDES AND OTHER REMOTE LOCATIONS

Øystein Hov[1] and Ivar S.A. Isaksen[2]

1) Norwegian Institute for Air Research, N-2001 Lillestrøm, Norway
2) Institute of Geophysics, University of Oslo, Norway
Presently at NCAR, Boulder, Colorado 80307, U S A

SUMMARY

Air samples for determination of halocarbons and light hydrocarbons were collected at Spitsbergen in July 1982 and in March 1983 (Hov et al., 1984). With the exception of ethene and propene, which appeared to originate mainly from natural sources, hydrocarbon concentration levels were generally one order of magnitude higher for the March 1983 samples than for the summer samples. This was explained by difference in atmospheric reactivity, and particularly by direct transport of polluted air masses from the Soviet Union during March 1983. The spring samples from Spitsbergen were more abundant in alkanes and less abundant in solvents than air sampled at Barrow by Rasmussen et al. (1983) in March 1982.

Calculations with a 2-D meridional model of the chemistry and transport in the troposphere have been made (Isaksen et al., 1984). The seasonal variation in the atmospheric boundary layer concentration at high latitudes of a number of chemical species was studied. This was done for organic gases with a chemical lifetime of several weeks and longer, like C_2H_2, C_2H_6, C_3H_8, C_6H_6, C_7H_8, $CHCl_3$ and C_2Cl_4. One important part of the study was to estimate the anthropogenic sources for these species. Furthermore, the temporal and latitudinal distribution of OH and O_3 was calculated using a complex photochemical reaction system. The model analysis of the measured gas concentrations at Spitsbergen during July 1982 and March/April 1983, showed fair agreement between the calculated annual variation and the measured concentrations for C_2H_2, C_2H_6, C_3H_8, C_7H_8 and C_2Cl_4, with a distinct late winter maximum and summer minimum. This was taken as an indication that the sources are mainly determined by anthropogenic activity, and that the transport, chemical decomposition, source strength and distribution are fairly well known for these species. For $CHCl_3$ it was concluded that the anthropogenic source is minor compared to the natural sources. For benzene it was concluded that emission in car exhaust is important, but other anthropogenic sources are required to get agreement between the calculations and the measurements. Measured C_2H_4 and C_3H_6 concentrations were much higher than values calculated on the basis of anthropogenic emissions, and showed opposite seasonal trends. This indicates important biogenic sources for these compounds.

An interesting result of the model study was the calculated buildup of PAN (≈300 pptv) at high latitudes during winter. This makes it the dominant source for NOx as the temperatures increase in the spring. NOx was found to be a limiting factor for O_3 production at high latitudes during spring.

In a different application of the 2-D meridional tropospheric global model, it is shown in a long term integration (15 or 30 years) how an increase in the global emissions of methane relates to the increase in concentration. After several decades, a 1.1 %/y increase in CH_4 global flux is required for the global concentration to increase 1.5 %/y. If the global fluxes of CH_4, CO, NOx and HC go up 0.5, 3.0, 3.0 and 3.0 %/y, respectively, the global OH distribution does not change after 30 yrs of integration, indicating proportionality between

increase in source strength and concentration for a specie like CH_4. If, however, the source strengths of CH_4, CO and HC go up by 0.5, 3.0 and 3.0 %/y, respectively, while the sources of NOx decline by 3.0 %/y, there is a significant decline in the global tropospheric average OH concentration after 30 yrs, indicating a more than proportional increase in concentration of e.g. CH_4 compared to increase in flux (0.5 %/y increase in methane source gave rise to 1.2 %/y concentration increase). Further implications for the tropospheric chemistry will be discussed.

REFERENCES

Hov, Ø., Penkett, S.A., Isaksen, I.S.A. and Semb, A., 1984: Organic gases in the Norwegian Arctic, Geophys. Res. Lett. 11, 425-428.

Isaksen, I.S.A., Hov, Ø., Penkett, S.A. and Semb, A., 1984: Model analysis of the measured concentration of organic gases in the Norwegian Arctic. To be submitted for publication.

Rasmussen, R.A., Khalil, M.A.K. and Fox, R.J., 1983: Altitudinal and temporal variation of hydrocarbons and other gaseous tracers of Arctic haze, Geophys. Res. Lett. 10, 144-147.

STUDY OF BACKGROUND AEROSOLS IN THE ANTARCTIC TROPOSPHERE

Tomoyuki Ito

Meteorological Research Institute, Yatabe,Tsukuba,
Ibaraki 305, Japan.

1. INTRODUCTION

Increasing attention has been directed to the problem of global background aerosol pollution because of its possible effect on climate. Antarctica is one of important regions for the study of background aerosol pollution on a global scale. Our present knowledge of Antarctic aerosols is rather fragmentary because most of the observations have been done only in summer or only for a single item.

In order to obtain a better understanding of Antarctic aerosols, year-round observations of concentration, size distribution, and substance of Antarctic aerosols were carried out at Syowa Station (69.0°S, 39.6°E), in 1978.

On the basis of these observations, the property and origin of Antarctic submicron aerosols were examined systematically.

2. MEASUREMENT

Among aerosol particles of various size, submicron particles are of most importance in meteorology because of their essential role in cloud formation and radiation processes. The items of the observation were selected so as to obtain many-sided information about submicron aerosols.

The concentration and mean size of Aitken particles ($0.002 \leq r \leq 0.2$ μm) were measured with a Pollak counter reported by Ito (1976). The counter is equipped with a diffusion pipe to obtain information on the mean size of Aitken particles, and with an electric current balancing circuit (a kind of null method circuit) which makes precise measurements of very low concentration possible. The size distribution of Aitken particles was measured by a diffusional decay technique reported by Ito (1980). In order to obtain information on the substances of Aitken particles, the volatility of Aitken particles was examined by measuring the concentration of heated sample air. This technique is similar in principle to that used by Twomey (1968). The concentration and size distribution of Mie particles ($0.2 \leq r \leq 1$ μm) were measured with an optical particle counter (Dan Co. Ltd., Japan) which is similar in principle to the Royco light-scattering particle counter. Sequential sampling of aerosol particles was done with an impactor and an electrostatic precipitator (Thermo-System Inc., U.S.A.), and the morphology of particles were examined under electron microscope. The vertical concentration profile was also observed at Syowa Station in 1983 by use of the Aitken particle sonde reported by Ito et al. (1983).

3. RESULTS AND DISCUSSION

3.1 Aitken particles

The median value of hourly mean concentrations of Aitken particles obtained at Syowa Station from February to December 1978 was 223 cm^{-3}. This value is comparable to the values observed in the clean atmosphere outside Antarctica.

The monthly mean concentration of Aitken particles at Syowa in 1978 showed the seasonal variation characterized by the concentrations high in the sunlit months and low in the polar night months. Similar seasonal variations were observed at Mirny in 1965 (Voskresenskii, 1968), at South Pole every year from 1975 to 1978 (Murphy and Bodhaine, 1980), and at Syowa in 1977 (Ono et al., 1981). According to Ito et al. (1982), the monthly mean concentration of Aitken particles, which varies seasonally and spatially in

the Antarctic atmosphere, can be related to a single parameter, the solar zenith angle. The cosine of the solar zenith angle, when multiplied by the solar constant, represents the flux of solar photons into the earth's atmosphere. Thus it can be said that the seasonal and latitudinal variation of concentration of Aitken particles in the Antarctic troposphere are closely correlated to variation in the influx of solar photons. Similar relation between Aitken particle concentration and solar radiation flux was confirmed to be valid for further wide atmospheric regions by Bigg et al. (1984).

As a result of the volatility measurement of Aitken particles at Syowa Station, it became clear that the volatile particles which disappeared under furnace condition of 500°C existed in large fractions in summer but small in winter. Sulfate or organic aerosols as commonly seen in the atmosphere have such volatile properties, whereas sea salt or soil particles do not.

According to the morphological examination of particles under electron microscope at Syowa Station, the particles which were identified as sulfuric acid particles were abundant from summer to autumn, but disappeared from winter to spring. Although the particles identified as sulfuric acid particles were larger than 0.05 μm in radii, it seems natural to expect that the main component of volatile Aitken particles in summer is also sulfuric acid.

During the period in which local contamination was negligible, the concentration occasionally increased systematically from about 100 to 1000 cm^{-3} or more within several hours at Syowa Station as reported by Ito and Iwai (1981). This event of sudden increase took place only under the fair weather condition in sunlit months. Similar events were observed also at South Pole (Hogan and Barnerd, 1979). It was experimentally clarified that the increased particles were smaller than 0.005 μm in radii and were volatile particles which disappeared by heating of 500°C. Since such fine volatile particles can not be regarded as aged secondary particles or wind blown particles, they are probably sulfuric acid particles produced quite recently around Antarctica.

According to the vertical concentration distribution observed by an Aitken particle sonde under the cloudless condition in September in 1983, the layer containing Aitken particles in the mixing ratio of about 1000 mg^{-1} existed around 750 mb level over Syowa Station. The sudden increase in surface concentration of Antarctic Aitken particles seems to be a phenomenon that particles in such layer are brought down for instance by downdraft along the cold frontal surface. The observed vertical distribution of Antarctic Aitken particles suggests that significant portion of Aitken particles in the Antarctic troposphere are produced within the Antarctic mid-troposphere and are not those of stratspheric origin. The production rate of new particles may be estimated from the observed size distribution of submicron particles by assuming steady state.

The size distributions of submicron aerosols observed at Syowa Station were bimodal one with two modes around 0.005 μm and around 0.03 μm in radii, throughout the observation period from August to December. From these size distribution, the production rate of new particles in the sunlit period in the Antarctic troposphere was estimated as about 10^{-4} cm^{-3} s^{-1} at least (Ito, 1982).

From above considerations, it can be concluded that most of Aitken particles are sulfuric acid particles produced through the photochemical gas-to-particle conversion processes in the Antarctic troposphere and so that seasonal and latitudinal variations of Aitken particle concentration in the Antarctic troposphere mostly reflect the difference of production rate of photochemical particles. In winter, however, evidences to show that Aitken particles were also transported by maritime air, was found in seasonal variation of size distribution and mean size and day-today variation of Aitken particles.

3.2 Mie particles

The median value of hourly concentration of Mie particles obtained at Syowa Station from February to December 1978 was 0.77 cm^{-3}. The size distribution averaged for the above period can be approximated by a power low distribution of $dn/d \log r \propto r^{-\beta}$ (β=4.17). Outside Antarctica, the representative value of concentration is higher than 1.0 cm^{-3}, and that of β is as much as 3.0 or less. Thus, Antarctic Mie particles, when compared with those in the clean atmosphere outside Antarctica, can be characterized by the low concentration and by the size distribution with the large β-value which is probably resulted from the preferential loss of large particles.

From the air mass trajectory analysis, it became clear that most of Mie particles at Syowa Station were brought by maritime air coming from north.

In the scatter diagram between monthly average concentration and monthly average influx of air from north, it was found that the concentration increased as the influx increased except in summer months when the photochmical growth and cloud physical removal of particles occur effectively.

The scatter diagram between β of monthly average size distribution and the monthly average of the distance from the open sea over the sea ice regions indicated the relation in which β increased with the increase of the distance from the open sea. The relation suggests the preferential loss of larger particles during the transport of maritime air toward inland. In summer months, however, β was irregularly high due to increase of small Mie particles which grew from Aitken particles photochemically.

Thus, it can be explained that the seasonal variation of Mie particle concentration is caused mainly by that of advection of maritime air into the Antarctic atmosphere, while the seasonal variation of the size distribution of Mie particles by that of northward extension of sea ice regions. These relations are disturbed in summer because small Mie particles are produced by condensation of photochemically produced vapor on Aitken particles.

4. CONCLUDING REMARKS

Followings are concluded: Two types of aerosol originating in different sources are present in the Antarctic troposphere. With the intrusion of maritime air, mostly in polar night months, sea salt particles and ammonium sulfate particles contained originally in the clean maritime air are dominant. The size distribution of such aerosols is expected to be monomodal having a mode around 0.03 μm in radii. On the other hand, in sunlit months, sulfuric acid droplets are predominant and the size distribution is bimodal having an additional mode around 0.005 μm in radii. Those sulfuric acid aerosols are formed photo-chemically within the specific layer in the Antarctic troposphere. Thus, most of Antarctic submicron particles are tropospheric origin, but not stratospheric origin.

REFERENCE

BIGG et al.(1984): J. Atmosph. Chem, 1, 203-214./ HOGAN and BARNARD(1979): J. Appl. Meteor., 17, 1458-1465./ ITO(1976): J. Meteor. Soc. Japan, 54, 81-90./ ITO(1980): J. Meteor. Soc. Japan, 58, 81-92./ ITO(1982): Antarctic Record, No. 76, 1-19./ ITO and IWAI(1981): J. Meteor. Soc. Japan, 59, 262-271./ ITO et al.(1982): Mem. Natl. Inst. Polar Res. Spec. Issue No. 24, 289-296./ ITO et al.(1983): Mem. Natl. Inst. Polar Res. Spec. Issue No. 29, 185-189./ MURPHY and BODHAINE(1980): NOAA Tech. Memo., ERL ARL-82./ ONO et al.(1981): Mem. Natl. Inst. Polar Res. Spec. Issue No. 19, 141-151./ TWOMEY(1968): J. Rech. Atmosph., 3, 281-285./ VOSKRESENSKII(1968): Sovet. Antarkticheskaia Eksped., Trudy, No. 38, 194-198./

INFORMATION ABOUT ATMOSPHERIC AEROSOLS DORMANT IN MEASURING SERIES

- FOUR EXAMPLES -

Guillaume d'Almeida, Leni Helmes, Ruprecht Jaenicke

Institute of Meteorology, University of Mainz/Germany

1. INTRODUCTION

Networks and monitoring stations are usually initialized for a certain purpose to serve a certain goal. Typical examples are the meteorological networks maintained by most nations. They are designed for collecting data of meteorological interest and monitoring parameters of climatological importance.
Standard climatological parameters are influenced by several basic meteorological variables. So, the date of blooming, a sound phenomenological parameter, is influenced by temperature, precipitation, sunradiation, to name a few. It is possible to reveal parts of the information hidden in these observations, like temperature, under special circumstances, or with selected assumptions only. For instance, the average temperature of past centuries is deduced in this way by climatologists.
It is the purpose of this paper to show examples where information are hidden in series of aerosol - or other - observations, and how they can be revealed.

2.SUNSHINE DURATION AND ATMOSPHERIC TURBIDITY

For its own sake, the duration of sunshine is observed at most meteorological stations with a Campbell-Stokes sunshine recorder or similar devices.
Observation periods up to 100 years are available in many cases. It can be shown theoretically (Jaenicke et al, 1978) and experimentally (Helmes et al, 1984) that atmospheric turbidity can be revealed from traces of the sunshine recorder for a cloudless sunrise or sunset. Atmospheric turbidity is an important aerosol and climatological parameter, and efforts have been made in establishing special networks for its determination.
However, meteorological yearbooks do not list the sunshine duration for cloudless days separately. Therefore, a study was initialized to determine the sum S of turbidity, cloudcover, and sunshine duration empirically. The obvious assumption of S being equal to unity, is usually not valid for various reasons, and thus, S must be determined as a function of cloudcover C. First results show a possible equation for $C < .5$ with which it is feasible to evaluate sunshine observation series in terms of atmospheric turbidity. A comparison of these data with dust veil indexes of volcanic eruptions will be done.

3. STANDARD DEVIATION AND TRACE SUBSTANCE TRANSPORT

In Jaenicke (1982) a model was developed from statistical considerations connecting the standard deviation of a series of observations of any atmospheric trace substance with the residence time of this sub-

stance in the atmosphere. At that time a parameter tmax was introduced as maximum averaging time but remained unquantified for the time being.
Recently Mueller (1983) has developed an equation connecting the residence time of atmospheric trace substances with a so-called volatile point, the average of the melting and boiling temperature. It is possible to calculate the value tmax for any substance from the observed standard deviation of a measuring series with this independent determination. In Jaenicke (1982) tmax was introduced as upper limit of the time, given to a certain air parcel to age before it is inspected by the measurement.
For more than ten years measurements of chemical ions and waterinsoluble compounds in atmospheric aerosols are available at a mountain station in the Alps (Wank, 1780 m a.s.l). The evaluation shows tmax being around 6 days. This permits the conclusion that air parcels loaded with trace substances as early as 6 days before might influence the inspection of the air at a given station. For the average wind velocity of 5.5 m/s at the Wank it means a transport distance of up to 3000 km. This is a meteorological parameter and thus is not in contrast to the statement of Mueller (1983), saying that emitted substances become local, regional or long-range pollutants, depending on their votality point.

4. AIRMASS TRAJECTORIES, CONCENTRATION AND THE LOCATION OF SOURCES

If a concentration of a trace substance is monitored at a certain location, one of the first evaluations connects it to the wind direction. In the case of Cape Grim the Australian continent usually determines the "polluted" wind directions. This simple evaluation is only successfull with an extended aerea source for rather short distances. Isolated point sources cannot be singled out this way.
For a suite of surface measurements of the concentration of Aitkennuclei concentration we have calculated surface trajectories of air parcels (Jaenicke et al, 1982). If such trajectories are calculated up to two days back, the trajectories cross several times. In calculating the Aitkenparticle concentration along this way, permitting a certain ageing, a field of particle concentrations develops and permits the averaging at grid points. It is quite surprising to see an organized structure developing over the grid. In the case of the Arctic Ocean, point sources like Alert, Nord, and Danmarkshaven on Greenland, Longyearbyen on Spitsbergen, Bear Island, and Ostrov Hesja on Franz-Josef-Land, could be located up to 1000 km away from the measuring site, a Swedish icebreaker, for the summer of 1980.
It is clear that this method works successfully only in regions with a pronounced thermic stability in the vertical air column. For sophisticated trajectories the application in other regions seems feasable.

5. ATMOSPHERIC TURBIDITY AND TOTAL OZONE

As mentioned above, atmospheric turbidity is an important climatological parameter. Simple sunphotometers have been developed for measurements. These instruments work with several wavelenghts in order to cover the whole range influenced by atmospheric arosols. But the extinction of sunradiation in the atmosphere depends not only on the pre-

sence of aerosols but on permanent and trace gases too. While the effects of the permanent gases can be taken easily into account by using the Rayleigh extinction coefficient, the presence of trace gases, like water vapor and ozone, is treated separately. For a simple approach, the ozone and water content is assumed to be constant and treated accordingly. The results thus obtained are sometimes rather questionable. A more sophisticated approach uses an instrument with built-in wavelengths for the independent determination of ozone and water (d'Almeida et al, 1983).
During two years a network of sunphotometers was operated for the determination of dust transport to the four wind directions in the Sahara Desert and the Sahel Zone. When Crutzen et al (1983) proposed an increase of ozone because of volcanic SO_2 injection in the stratosphere, a separate evaluation of our network data was started. For Assekrem, a station in the center of the Sahara Desert, it turned out that the column ozone content was significantly increased from May to November 1982 compared to 1981. As an average, the optical depth of ozone was increased by .1 units (d'Almeida et al, 1983). One might take this as an indication of the influence of the El Chichon volcanic eruption in spring 1982 on the stratosphere.

6. CONCLUSIONS

The content of the results of networks and monitoring stations is not exhausted after the originally planned evaluation has been terminated. Scientists are encouraged to use their imagination to retrieve additional information. This is of great help in getting atmospheric chemistry data, even of past times without observations designed for air chemistry.

7. REFERENCES

d'Almeida, G.A., Jaenicke R., 1983, Atmospheric Turbidity over Africa - Disturbed by the El Chichon Eruption? Geoph. Res. Letters, 10, 233-235

d'Almeida, G.A., Jaenicke, R., Roggendorf, P., Richter, D., 1983: New Sunphotpmeter for Network Operation, Appl. Opt., 22, 3796-3801

Crutzen, P.J., Schmaizl, U., 1983, Chemical Budget of the Stratosphere, Planet. Space Sci., 31, 1009-1032

Helmes, L., Jaenicke, R., 1984: Experimental Verification of the Determination of Atmosheric Turbidity from Sunshine Recorders, J. Climat. and Appl. Meteorol., in press

Jaenicke, R., 1982: Physical Aspects of the Atmospheric Aerosol, In: Georgii, H.W., Jaeschke, W. (eds.), Chemistry of the Unpolluted and Polluted Troposphere, 341-373, Reidel Publishing Company

Jaenicke, R., Kasten, F., 1978: Estimation of Atmospheric Turbidity from the Burned Traces of the Campbell-Stokes Sunshine Recorder, Appl. Opt. 17, 2617-2621

Jaenicke, R., Schuetz, L., 1982: Arctic Aerosols in Surface Air, J. Hungar. Meteorol. Serv., 86, 235-241

Mueller, J., 1983: Rules in Atmospheric Behaviour of Particulate Substances, J. Aerosol Sci., 14, 212-217

SOURCES AND SINKS OF ATMOSPHERIC CARBON DIOXIDE DEDUCED FROM $^{13}C/^{12}C$ RATIO MEASUREMENTS

Charles D. Keeling

Scripps Institution of Oceanography
La Jolla, California 92093

Willem G. Mook

University of Groningen
Westersingel 34, Groningen, The Netherlands

1. INTRODUCTION

Measureable spacial and temporal differences in the concentration of atmospheric CO_2 result from combustion of fossil fuels, the metabolic activity of terrestrial plants and soils, and air-sea gas exchange. Of only the first of these processes is the source strength approximately known. It is thus impossible to distinguish oceanic and biospheric processes solely by the atmospheric CO_2 gradients which they produce. By measuring both concentrations and $^{13}C/^{12}C$ ratios, atmospheric CO_2 may be treated as though it were two different gases, one derived from plant carbon (including fossil fuel carbon) and the other from oceanic carbon. The usefulness of this approach depends, however, on the precision which isotopic measurements can attain.

Oceanic CO_2 has nearly the same isotopic composition as atmospheric CO_2, whereas plant carbon is depleted in carbon-13 by approximately 17‰. Thus, for a rise in concentration of atmospheric CO_2 of one ppm (part per million by volume) brought about by plant activity, the $^{13}C/^{12}C$ ratio decreases by approximately 0.05‰. Measurements of CO_2 concentration to a precision of 0.1 ppm are desirable to characterize global scale atmospheric CO_2 gradients, which are typically of the order of 1 ppm per 10000 km. Thus, to distinguish gradients owing to plant and oceanic carbon processes requires an isotopic precision of 0.005%, approximately 10 times that presently attainable for individual samples using mass spectrometers.

Some enhanced precision for CO_2 gradient studies is obtainable by averaging so many mass spectrometric isotopic analyses that the influence of random machine errors is significantly reduced. Pursuing this approach, Keeling et al. [1984] showed that the north-south gradient in atmospheric CO_2 over the Pacific ocean appears to be caused by an excess of plant or fossil fuel carbon emitted to the air in the northern hemisphere, whereas oceanic CO_2 causes a peak in concentration of CO_2 near the equator. This analysis depended on recognizing patterns in the mean annual $^{13}C/^{12}C$ ratio to the order of 0.01‰.

Information on sources and sinks should also be derivable from temporal variations in $^{13}C/^{12}C$ ratio. But in this case there is a need for

even larger numbers of analyses to establish short term means, and new difficulties emerge when measurements of variations over several years must be made free of systematic errors. Until now these problems have stood in the way of using isotopic time series of atmospheric CO_2 to deduce sources and sinks. In this paper we discuss a new attempt to evaluate such time series. Our data are obtained from air samples collected at the field stations where the Scripps Institution of Oceanography measures CO_2 concentrations.

2. SEASONAL VARIATIONS

From several consecutive years of isotopic measurements, we have estimated the average seasonal cycle of $^{13}C/^{12}C$ in CO_2 for specific stations, in an attempt to separate the locally observed seasonal cycle of CO_2 into plant and oceanic carbon components. Figures 1 and 2 show decompositions of the seasonal cycles for Mauna Loa Observatory, Hawaii ($19.5^{o}N$, $155.6^{o}W$) and for the geographic South Pole, based on four and six years of data, respectively. The isotopic data are evidently precise enough to establish monthly means for the cycle only to about $\pm$ 0.5 ppm. Nevertheless, even with this degree of uncertainty, some bounds can evidently be set on the magnitudes of the separated biological and oceanic seasonal cycles at these stations.

For Mauna Loa, the biospheric component of the seasonal cycle is seen to be in phase with the combined cycle, but of slightly larger amplitude. This implies an oceanic cycle in opposition to the biospheric cycle, hinted at in the plotted oceanic cycle derived by taken differences between the computed biospheric and combined cycles. For the South Pole, the amplitude of the biological cycle appears to be nearly the same as the combined cycle, but the biospheric cycle is delayed one to two months. As seen in the plots, this implies an oceanic cycle with a maximum near September and a minimum near January. The computed minimum is only about one month later than expected from a sea surface temperature driven signal, but the computed maximum occurs three months later than expected. The computed oceanic cycle for the South Pole is too noisy to attach much significance to this latter finding, however. Our main conclusion, based on isotopic data, is that the seasonal biospheric cycle has a low amplitude, not likely to exceed that of the combined cycle.

3. INTERANNUAL VARIATIONS

The $^{13}C/^{12}C$ ratio of the plant carbon perturbing the seasonal variation of CO_2 at a given station is probably not changing appreciably from year to year because storage times of plant carbon are relatively long. Thus, time series of the seasonally adjusted $^{13}C/^{12}C$ ratio of atmospheric CO_2 should reveal unambiguously what part of the interannual variation in atmospheric CO_2 is caused by land biospheric processes. Seasonally adjusted CO_2 concentration data show distinct oscillations in addition to a steady rise attributed mainly to the release of CO_2 by fossil fuel combustion. These interannual variations correlate with a large scale atmospheric circulation phenomenon called the Southern Oscillation. When an index of the Southern Oscillation attains very low values, for example, as during a so called 'El Niño' event, the CO_2

concentration rises more rapidly than when the index is high [Bacastow et al., 1983]. Especially in the tropics, sea surface temperature variations concomitate variations in southern oscillation index; a low southern oscillation index is associated there with unusually warm waters and vice versa. Since interannual variations in CO_2 correlate with the southern oscillation, they perforce correlate with tropical sea surface temperatures. It is not surprising that several attempts have been made to explain interannual CO_2 variations as owing to changes in sea water temperature. Our isotopic data suggest a different cause.

During an El Niño event of great intensity in 1982 and 1983, the CO_2 concentration at widely separated field stations rose more rapidly than usual, as expected. As shown in Figure 3, this rise appears to have been concomitated by a decrease in $^{13}C/^{12}C$ ratio at the South Pole. An additional year of data is needed to completely document this perturbation, concomitant to the 1982-1983 El Niño. The record, as far as it extends, strongly suggests, however, that the rise in CO_2 was not owing to release of CO_2 by the oceans, but to an unusually large release of plant carbon. Similar results (not shown) have been obtained at three other stations in the northern hemisphere.

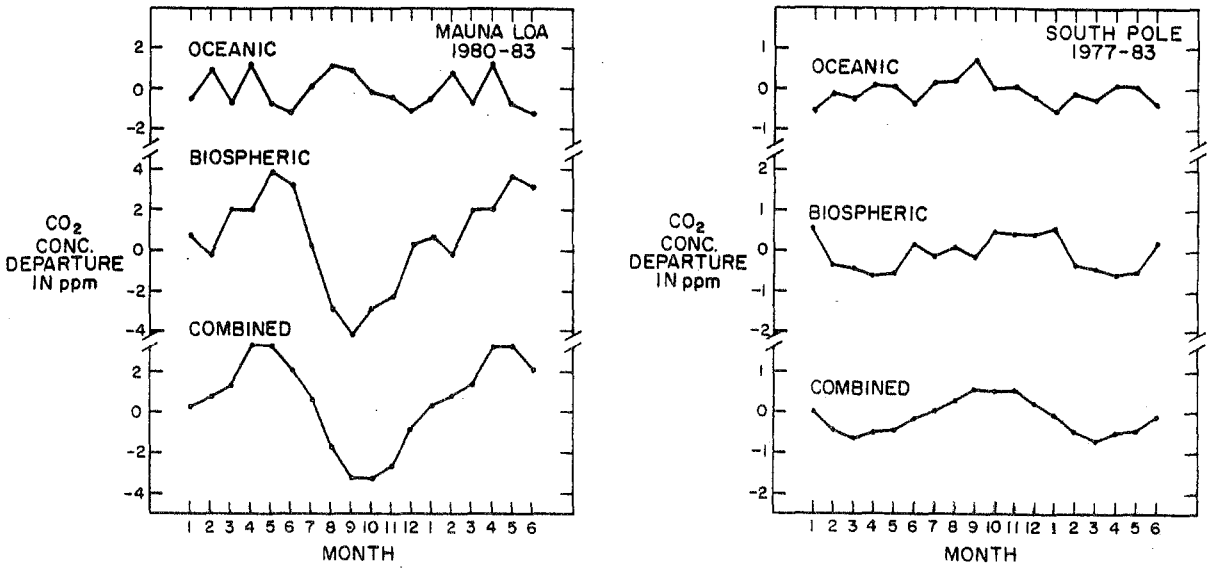
Space does not permit a full discussion of these findings here, but, as will be shown elsewhere, direct measurements in the East Pacific ocean during April, 1983 by the Scripps Institution's Benthic Expedition indicate that unusually warm surface water was at that time depleted in carbon and nutrients and could not have been an enhanced source region for atmospheric CO_2. Furthermore, when the degree of warming of ocean water needed to produce the observed interannual variations in atmospheric CO_2 is calculated, one deduces an air-sea exchange rate for CO_2 gas which is probably too large.

Thus, interannual variations in atmospheric CO_2 may generally reflect changing rates of terrestrial plant activity, possibly climatic and in origin and brought about by wide spread anomalies in the circulation of atmosphere including El Niño events.

References

Bacastow, R. B., J. A. Adams, C. D. Keeling, D. J. Moss, T. P. Whorf, and C. S. Wong, Atmospheric Carbon Dioxide, the Southern Oscillation, and the Weak 1975 El Niño, Science, 210, 66-68, 1980.

Keeling, C. D., A. F. Carter, and W. G. Mook. Seasonal, Latitudinal, and Secular Variations in the Abundance and Isotopic Ratios of Atmospheric CO_2, J. Geophys. Res., 89, 4615-4628, 1984.



Figures 1 and 2. Annual cycles of atmospheric CO_2 at Mauna Loa Observatory, Hawaii (left plots) and at the South Pole (right plots). At each station the combined cycle is as directly observed by concentration measurements. The biospheric cycle has been computed assuming that departures in $^{13}C/^{12}C$ ratio from their monthly means shift the concentration by 0.05 ‰ per ppm. The oceanic cycle has been computed by difference. January through June (months 1 to 6) as plotted twice to reveal the seasonal pattern more fully.

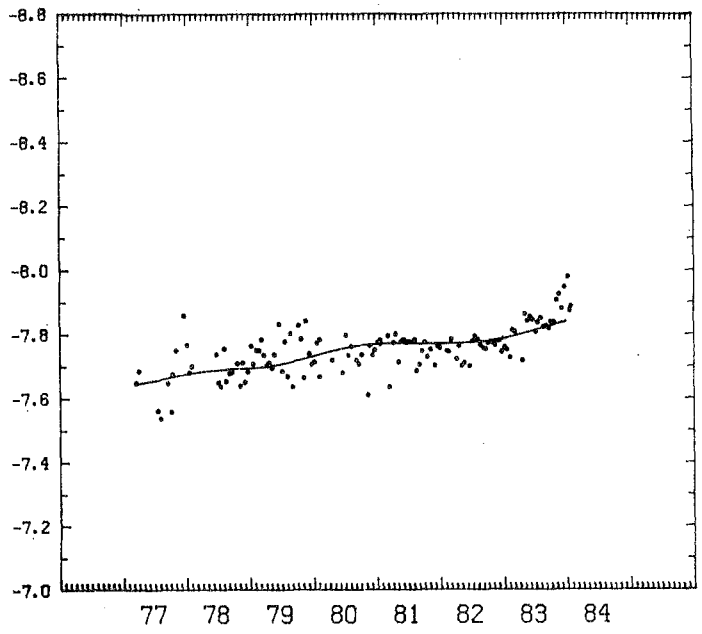


Figure 3. Trend in the per mil variation in $^{13}C/^{12}C$ ratio from an arbitrary standard at the South Pole after seasonal adjustment. The dots indicate daily isotopic averages. The smooth curve is a transformation of the concentration trend into isotopic units assuming a linear time rise owing to fossil fuel combustion by plant carbon having an isotopic ratio 27 ‰ less than the standard.

THE CHEMISTRY OF PRECIPITATION IN KATHERINE, AUSTRALIA

by

Gene E. Likens
Institute of Ecosystem Studies
The New York Botanical Garden
Mary Flagler Cary Arboretum
Millbrook, New York 12545 USA

William C. Keene
Department of Environmental Sciences
University of Virginia
Charlottesville, Virginia 22903 USA

John M. Miller
National Oceanic and Atmospheric Administration
Air Resources Laboratory
Rockville, Maryland 20852 USA

James N. Galloway
Department of Environmental Sciences
University of Virginia
Charlottesville, Virginia 22903 USA

The Global Precipitation Chemistry Project has been collecting data on precipitation chemistry since 1979 at various sites to determine what natural factors control the composition of precipitation in continental and marine areas remote from industrial and agricultural influences (Galloway et al. 1982). In general, the study is designed to evaluate the background or natural composition of rain and snow, and to infer what precipitation chemistry may have been in the Northern Temperate Zone prior to major influences of fossil-fuel combustion. Currently, precipitation is being collected at Amsterdam Island; Katherine, Australia; Tores del Paine, Chile; Cape Point, South Africa; and Kruger National Park, South Africa. Volume-weighted averages for sites in the Southern Hemisphere ranged from 9.4 to 20.4 μeq H^+/liter, 2.6 to 5.9 μeq excess $SO_4^=$/liter and 1.5 to 4.9 μeq NO_3^-/liter during 1980-84 (Galloway et al. 1984).

Katherine, Australia

One-hundred seventy-seven samples of precipitation were collected at the CSIRO Katherine Research Station in Katherine, Australia during 18 November 1980 and 8 April 1983. Annual precipitation averages about 92 cm at Katherine with a distinct wet (November - April) and dry (May - October) season. The dry season is characterized by southeasterly trade winds and the wet season by northwesterly equatorial winds.

The chemical composition of precipitation at Katherine is given in Table 1. Data are reported only for those samples with sufficient volume, with acceptable ion balances and that were treated with chloroform immediately after collection (120 samples for inorganic and 74 for organic analysis). Approximately 81% of the total rainfall was collected and analyzed. Concentrations of Mg^{++}, Na^+, $SO_4^=$ and Cl^- were 23 - 31% higher in the set of 120 samples than in the set of 74. The other ions had essentially the same concentration in both sets.

Organic acids comprised 65% of the measured acidity in the 74 samples measured. Formic and acetic acids predominated (> 95%) in most samples. Concentrations of organic acids were generally greater during the early part of the wet season (November and December) when storm trajectories suggested a continental source, and were markedly lower during the latter part of the wet season (January - March) when amounts of precipitation were greater and storm trajectories suggested a marine origin. Organic acids contributed some 93% of the measured acidity in one sample collected in April.

Based on an average precipitation of 92 cm/yr, the average deposition at Katherine would be 19 mg/m^2-yr for H^+, 41 for Ca^{++}, 18 for Mg^{++}, 36 for K^+, 108 for Na^+, 44 for NH_4-N, 63 for NO_3-N, 69 for SO_4-S and 293 mg/m^2-yr for Cl^-.

The average chemical composition of precipitation at a relatively remote forested site in New Hampshire, U.S.A. is considerably enriched relative to Katherine (Table 2). In particular, the enrichment of sulfur, nitrogen and hydrogen ion in the northeastern U.S. results from the combustion of fossil fuels.

REFERENCES CITED

Galloway, J. N., G. E. Likens, W. C. Keene and J. M. Miller. 1982. The composition of precipitation in remote areas of the world. J. Geophys. Res. 87(11):8771-8786.

Galloway, J. N., G. E. Likens and M. E. Hawley. 1984. Acid precipitation: natural versus anthropogenic components. Science (In Press)

Likens, G. E., F. H. Bormann, R. S. Pierce and J. S. Eaton. 1984. The Hubbard Brook Valley. Chapter II. In: G. E. Likens (ed.). An Ecosystem Approach to Aquatic Ecology: Mirror Lake and its Environment. Springer-Verlag New York Inc. (In Press)

Table 1. Volume-weighted means (VWM) standard errors, minimums and maximums, for 120 samples of precipitation from Katherine, Australia during 1980-83. Values in μeq/liter.

	H^+	Ca^{++}	Mg^{++}	Na^+	K^+	NH_4^+	NO_3^-	$SO_4^=$	Cl^-	Organic Anions*
Volume-weighted means	20.5	2.2	1.6	5.1	1.0	3.4	4.9	4.7	9.0	12.6
Standard error**	2.1	0.3	0.2	0.6	0.2	0.4	0.5	0.5	0.9	1.8
Minimum	4.1	< 2	< 0.3	< 0.4	< 0.5	0.2	0.3	< 0.4	1.1	< 0.8
Maximum	72.4	50.3	15.4	64.9	60.3	28.5	25.1	24.6	84.9	38.9

*74 samples

**standard error of VWM calculated according to Galloway et al. 1984

Table 2. Volume-weighted mean (VWM) concentration of dissolved substances in precipitation at Katherine, Australia and the Hubbard Brook Experimental Forest, New Hampshire, U.S.A. Values in μeq/liter.

Substance	Katherine*	Hubbard Brook**	HB/K
H^+	20.5	70	3.4
Ca^{++}	2.2	6.5	3.0
Mg^{++}	1.6	3.3	2.1
Na^+	5.1	4.8	0.9
K^+	1.0	1.5	1.5
NH_4^+	3.4	11	3.2
NO_3^-	4.9	24	4.9
$SO_4^=$	4.7	54	11.5
Cl^-	9.0	11	1.2
$PO_4^{\equiv}$	—	0.31	—
organic anions	12.6	—	—

*1980-83; VWM pH = 4.68; average annual precipitation = 92 cm

**1963-80; VWM pH = 4.15; average annual precipitation = 131 cm

TROPOSPHERIC OZONE: SEASONAL PATTERNS AND TRENDS

Jennifer A. Logan

Center for Earth and Planetary Physics
Harvard University

We will present results of an analysis of data for tropospheric ozone derived from both ozonesonde and surface instruments. Our focus is on spatial and temporal variations.

Surface Ozone

Surface ozone at mid-latitudes displays two modes of seasonal behavior. A broad summer maximum in ozone is associated with well populated and industrialized regions, Europe and the central and eastern U.S., while a summer minimum is associated with sparsely populated regions remote from industrial activity, Canada and Cape Grim. We will argue that the summer maximum is due to photochemical production of ozone, associated with anthropogenic sources of NO_x, CO and hydrocarbons. Furthermore, we will propose that ozone in summer in the U.S. and Europe may have increased by 30-100% during this century, as a result of increasing anthropogenic emissions.

The difference in seasonal patterns for surface ozone cannot be ascribed simply to a latitudinal gradient or to differences between the hemispheres. We emphasize in this context first the summer maximum found in surface ozone at 53^{o}-55^{o}N in Europe and the summer minimum found at the same latitude in Canada. The Canadian sites experience surface air flow from the Arctic in summer and are unlikely to be influenced by industrial sources of trace gases. Second, we note that the seasonal cycles of ^{90}Sr, a tracer of stratospheric air, are exactly in phase at 52^{o} and 40^{o} in North America (Staley, 1982). This suggests that the contrasting seasonal cycles found for ozone, a summer minimum at 53^{o} and a summer maximum at 38^{o}, cannot be due to latitudinal variations in the source of ozone from the stratosphere. Third, we note the summer-autumn maximum in ozone at Aspendale (38^{o}S) and the summer minimum at Cape Grim (41^{o}S). Aspendale is affected by air pollution from Melbourne, 30 km away (Galbally, 1971) while Cape Grim is usually under the influence of pristine marine air masses.

There is good evidence for a long term increase in concentrations of surface ozone in Europe and for a concurrent change in the seasonal distribution. Measurements from Arkona on the Baltic coast show that ozone concentrations in summer have doubled since the 1950s, while winter values have increased by 50% (Warmbt, 1979). Comparison of measurements from Arosa in 1951-53 (Junge, 1962) with recent results from Alpine stations also suggests a larger increase in ozone in summer than in other seasons. Measurements from Hohenpeissenberg for 1970 to 1983 indicate an increase in ozone of perhaps 20%, with evidence for a larger change in summer and autumn than in other seasons.

Comparison of ozone measurements from Michigan in the 1870s (Linvill et al., 1980) with contemporary data suggests that there has been a significant change in the seasonal cycle of ozone in the United States also. The early measurements are less reliable than more recent results, but we emphasize

that the maximum in surface ozone in Canada (53°) occurs today in the same months as it did in Michigan (42°) in the 1870s (April and May), and that the ratio of spring to summer concentrations is similar (∿1.6). It appears that average summer concentrations of ozone may have increased by as much as 10ppb in the mid west, and possibly by as much as 15-20ppb in highly impacted environments, such as the Ohio River Valley.

There is evidence for an increase in surface ozone only in regions with significant sources for NO_x, CO and HC from fossil fuel combustion. No trend is apparent in surface ozone at remote sites in Canada, or on the islands of Hawaii and Samoa (GMCC, 1983), locations which display a summer minimum in ozone.

Ozone in the middle troposphere

A broad summer maximum in ozone in the middle troposphere is found only at northern midlatitudes. The seasonal cycle at 700 mb and 500 mb over Europe, the U.S. and northern Japan is very similar to that at the surface, but it is quite different from that at 300 mb. There is good evidence for an increase in ozone in the middle troposphere over Europe, and weaker evidence for an increase over North America and Japan. The data from mid-latitudes do not show a strong seasonal variation in the trend, unlike the surface observations. We caution that period of observation is rather short ∿13 years, and that the quality of data is somewhat variable. Data from Resolute show that ozone may be increasing at high latitudes also, in spring and summer. Measurements of sulphate and particulates indicate that the Canadian Arctic is most likely to be influenced by air masses from mid-latitudes between December and May. The trend in ozone over Resolute may therefore result from long range transport of ozone from mid-latitudes, since the photochemical lifetime of ozone at high latitudes should be much longer than at mid-latitudes.

It is extremely difficult to rationalize the summer maximum or the observed trends in ozone without invoking a photochemical source associated with surface emissions of ozone precursors. Stratosphere-troposphere exchange is most effective during late winter and spring when stratospheric ozone concentrations are highest. Since the lifetime of tropospheric ozone is less than a month in summer, a production mechanism other than stratospheric injection is required to explain the persistence of high concentrations from April to August, as emphasized recently by Fishman (1984). Results from a recent 3-dimensional model study also suggest that photochemical sources of ozone are required to explain the observed seasonal distribution (Levy et al., 1984).

Ozone in the tropics

There is a significant seasonal cycle in ozone at Natal, Brazil (6°S). Average concentrations are about a factor of two higher in September and October than in February to April. Minimum ozone values at Natal correspond to annually averaged values at Panama (9°N), while maximum values in the middle troposphere at Natal correspond to those found at mid-latitudes in summer. We speculate that high values of ozone over Natal may result from emission of NO_x and hydrocarbons from agricultural burning. Concentrations of ozone in the southern tropics are similar to and sometimes exceed values in the northern tropics. Interhemispheric gradients in ozone vary significantly with season and longitude.

Acknowledgements

I would like to thank Ian Galbally for generously providing unpublished measurements of ozone at Cape Grim. I would also like to acknowledge useful discussions with Steven Wofsy and Chip Levy. Rose Yevich and Clarisa Spivakovsky assisted with the data analysis.

References

Fishman, J. The importance of photochemistry on the seasonal cycle of ozone in the troposphere. J. Geophys. Res., submitted, 1984.

Galbally, I.E. Surface ozone observations at Aspendale, Victoria, 1964-1970. Atmos. Environ., 5, 15-25, 1971.

GMCC, 1983. Geophysical Monitoring for Climatic Change. No. 11. Summary Report, 1982. U.S. Dept. of Commerce, 1983.

Junge, C.E. Global ozone budget and exchange between stratosphere and troposphere. Tellus, 14, 363-377, 1962.

Levy, H., J.D. Mahlman, W.J. Moxim, and S.C. Liu. Tropospheric ozone: the role of transport. J. Geophys. Res., submitted, 1984.

Linvill, D.E., W.J. Hooker, and B. Olson. Ozone in Michigan's environment 1876-1880. Mon. Wea. Rev., 108, 1883-1891, 1980.

Warmbt, W. Results of long-term measurements of near surface ozone in the GDR. Zeit. fur Met., 29, 24-31, 1979.

ATMOSPHERIC TRANSMISSION DECREASES AND STRATOSPHERIC WARMING AT MAUNA LOA DURING THE TWO YEARS AFTER THE EL CHICHON VOLCANIC ERUPTION

Bernard G. Mendonca, John J. Deluisi, Ellsworth G. Dutton

Geophysical Monitoring for Climatic Change Division, NOAA
325 Broadway
Boulder, Colorado 80303 U.S.A.

INTRODUCTION:

Mauna Loa Observatory is one of four baseline observatories operated by the Geophysical Monitoring for Climatic Change division of NOAA to monitor atmospheric trace constituents to assess their impact on climate change. It is located on the island of Hawaii (19.5^{o} N Lat. and 153.8^{o} W Long.) on the north slope of Mauna Loa volcano at 3.4 km elevation. The observatory is surrounded by barren lava flows and is above a persistent subtropical trade wind inversion that enables sampling of air last in continental contact 2000 miles upstream.

Stratospheric dust clouds injected into the stratosphere by explosive volcanic eruptions have been indirectly detected from Mauna Loa by measuring decreases in incoming solar irradiances at the surface and more recently by direct measurements using lidar (Ellis and Pueschel 1971; Mendonca et al. 1978; Coulson et al. 1982). These measurements have been linked with other measurements taken from different points around the world to deduce the life times as well as latitudinal, hemispherical, and global spreading of volcanic dust clouds after they have been ejected into the stratosphere.

Until March 28 and April 4 and 5 of 1982, when El Chichon (17.3^{o} N 93.2^{o} W) erupted in Mexico, Mount Agung (8.5^{o} S 115.5^{o} W) in Indonesia was the largest and longest-lived dust cloud detected at Mauna Loa since measurements began in 1958. Other notable volcanic dust clouds detected over Mauna Loa have been Awu 1966, De Fuego 1974, and the mystery cloud of 1982. After both Mt. Agung and El Chichon erupted, stratospheric heating and deficits in incoming solar irradiance at the surface were observed and documented globally. In the case of Mt. Agung, fractional backscattering of solar energy to space by aerosols ejected into the stratosphere was attributed by several authors as a causal factor to an ongoing global cooling trend at the surface of the earth from the sixties to the seventies (Newell 1984).

This study will examine a unique set of measurements made at Mauna Loa Observatory following the eruption of El Chichon. The detection of the dust cloud, the subsequent stratospheric warming, and the reduction in short wave solar irradiance at the surface will be reviewed.

MEASUREMENTS:

Measurements of the direct beam and total hemispheric solar irrandiance, light detection and ranging (Lidar) observations, and temperature and wind profiles from a rawindsonde station 56 km east of Mauna Loa Observatory on the coast of the island of Hawaii were used to detect and examine the effects of the El Chichon dust cloud in the stratosphere over Mauna Loa.

The technique described by Ellis and Pueschel (1971) and Mendonca et al. (1978) was used to measure the apparent transmission of the atmosphere by converting the direct beam measurements of solar irradiances at relative air masses of 5, 4, 3, and 2 into an indirect measurement of aerosol loading in the stratosphere after explosive volcanic eruptions. Direct beam and total

hemispheric irradiance observations were used to detect decreases in irradiance fluxes at the surface following the passage of the El Chichon volcanic cloud over the Observatory.

Lidar observations, described by Coulson et al. (1982) were used to measure the relative strength of the volcanic dust cloud as it passed over the observatory as well as the height of the dust cloud in the stratosphere. Lidar observations measures the amount of light in a laser pulse that is scattered back to the surface by the atmosphere and aerosols in the atmosphere. The amount and height of the aerosols can be determined by comparing the amount of light backscattered by the air molecules and residual aerosols under normal conditions (without aerosol loadings from a volcanic eruption) from a given altitude to the amount of backscatter received during a volcanic episode. The lidar observations identified stratified layers of volcanic dust in the stratosphere and monitored the vertical evolution of the dust cloud with time.

Rawindsonde measurements gave a twice daily profile of temperature and air flow in the stratosphere over Mauna Loa. From these measurements, stratospheric temperatures were compared to earlier temperatures when no volcanic cloud was present in the stratosphere.

DISCUSSION:

After the El Chichon eruptions on March 28 and April 4 and 5, the first detection of the cloud over Mauna Loa was observed on April 4 by a decrease in normal incident irradiance measured at the surface of Mauna Loa. The first lidar observation taken after the eruption was on April 10 and it detected the El Chichon cloud and showed a 222 times above normal backscatter return over Mauna Loa that peaked at 26 km altitude.

Table 1 gives a summary of the measurements made after the initial detection of the El Chichon dust cloud over Mauna Loa. The data are broken up into northern hemisphere seasons starting with spring of 1982 (March, April, and May). Radiation decreases observed are most pronounced in the three seasons following the eruption, with the normal incident irradiance decreasing as much as 30% and the total irradiance 7% during the summer of 1982. The apparent transmission measurements for this period showed the largest decreases in transmission at the observatory since the record began in 1958. This coincides with lidar measurements showing the maximum spreading of the dust cloud vertically as well as horizontally during that period, with most of the volcanic debris still confined to a band between 15^{o} S and 40^{o} N. After the autumn of 1982, the dust cloud was no longer concentrated in a latitudinal band and spread globall (Pollack et al. 1983). Lidar measurements over Mauna Loa showed a sharp decrease in backscatter return during this period, and the effects are immediately seen in the solar radiation fluxes measured at the surface. After the autumn of 1982, there was an abrupt increase in the downward irradiance fluxes, which coincides with a significant drop in lidar backscatter at the 25-30 km and 20-25 km levels. This is particularly true at the higher level between 25-30 km.

The decay of the El Chichon dust cloud over Mauna Loa after the winter of 1982 to the summer of 1984 was gradual. The normal incident flux increased only 5%, the total irradiance flux increased back to normal, and the lidar backscatter decreased to 3 to 2 times normal values at all levels as early as the winter of 1984.

Table 1

	1982			1983				1984		
	S	S	A	W	S	S	A	W	S	S
Percentages Below Normal										
Normal Incidence Irradiance	16	29	19	8	9	6	5	4	6	3
Total Irradiance	3	7	4	2	2	2	.5	.5	--	--
Apparent Transmission	7	13	9	4	5	4	3	2	3	1.5
Stratospheric 31km	2.7	3.9	3.8	2.6	2.2	2.7	1.3	-1.1	1.7	
Temperatures 27km	2.1	2.9	3.2	2.3	2.2	1.9	1.5	1.7	.3	
Departures 24km	2.0	3.0	3.4	1.0	.9	1.2	1.4	1.7	0.0	
from Normal °C 20km	1.9	3.0	1.7	.4	-.7	1.1	1.5	1.5	-.2	
Lidar 25-30km	133	56	27	3	4	3	2	2	3	2
Backscatter 20-25km	33	37	23	11	7	5	5	3	2	3
Intensity 15-20km	4	3	2	2	5	4	5	3	2	2

Table 1. A summary of measurements made at Mauna Loa after the El Chichon eruption of 1982. Normal incident solar irradiances were obtained with a tracking Epply pyrheliometer during cloudless mornings from sunrise to solar noon. Total irridance measurements (sun plus sky) were obtained from an Epply pyranometer coinciding with the normal incident measurements. Values at solar zenith angle 30^{o} were used for the comparisons in the table. Both measurements were compared with similar measurements made in 1981 before El Chichon erupted and when the stratosphere was relatively free of volcanic aerosols. Apparent transmission data were obtained from the normal incident data according to Ellis and Pueschel (1971) and Mendonca et al. (1978). The values obtained after El Chichon were compared to a background value determined by Mendonca et al. (1978) when the stratosphere was free of volcanic aerosols. The stratospheric temperatures were obtained from rawindsonde observations taken at the National Weather Service Station in Hilo, Hawaii and were compared to a ten year average (1979-1981 inclusive) of stratospheric temperature above Mauna Loa. The lidar data were obtained from a lidar system operated on Mauna Loa on a twice weekly schedule according to Coulson et al. (1982). The lidar backscatter values given is the relative strength of the signal after the eruption to the normal signal measured before the eruption when little or no volcanic aerosols were present in the stratosphere.

The stratospheric temperatures over Mauna Loa during the two-year period following the eruption are all greater, with a few exceptions, than the average of the previous 10 years--1979 to 1981, inclusive. Even allowing for the biennial swing to higher temperature in the stratosphere in 1982 and 1983, stratospheric warming is evident. Table 1 shows that the maximum temperature increases occurred above the 24 km level. This is elevation where the cloud was detected and measured during the first three seasons after the El Chichon eruption. By the autumn of 1983 and winter of 1984, the temperatures, while still mostly positive, are well within the normal fluctuations of stratospheric temperatures over Mauna Loa. The positive departures in stratospheric temperatures measured from the spring of 1982 to the autumn of 1983 were greater than 2 standard deviations from the 10-year mean measured over Mauna Loa between 21 km and 30 km for 40% of the time.

CONCLUSION:

The El Chichon volcanic dust cloud was detected over Mauna Loa several days after the El Chichon eruption ejected debris into the stratosphere.

The volcanic dust and gases were carried by zonal stratospheric winds directly over Mauna Loa.

Normal incident solar irradiances, total hemispheric irradiances, and apparent atmospheric transmission decreased to the lowest levels measured under cloudless skies at Mauna Loa since observations began in 1958. The maximum decreases were measured in the summer of 1982, one season after the eruption.

Stratospheric warming was as great as that observed over the Pacific after the Agung eruption and reached its maximum during the three seasons that followed the eruption (Angell and Korshover 1983).

Lidar observations pinpointed the elevation of the dust cloud over Mauna Loa and reached backscatter intensities more than 100 times above normal backscatter values immediately after the eruption. By the fall of 1982 the dust cloud was more uniform vertically and horizontally, and by the winter of 1982 the lidar measurements indicated that a large portion of the cloud had moved away from the latitude of Mauna Loa.

Up to the summer of 1984, normal incident irradiances and lidar backscatter have not returned to normal values. Stratospheric temperature departures from the mean, while still mostly positive, were not significantly positive by the summer of 1984. Total hemispheric irradiances have returned to normal values after the winter of 1984.

REFERENCES:

Angell, J.K., and J. Korshover: Comparison of stratospheric warmings following Agung and El Chicho. Monthly Weather Review, Vol. III, No. 10, Oct. 1983; pp.2129-2135.

Coulson, K.L., T.E. DeFoor, and J. DeLuisi: Lidar and optical polarization measurements of the stratospheric cloud in Hawaii. Presented at the fall AGU meeting, San Francisco, Dec. 7-15, 1982; EOS, 63, 897.

Ellis, H.T., and R.F. Pueschel: Solar radiation: absence of air pollution trends at Mauna Loa. Science, Vol. 172, pp. 845-846, 1971.

Mendonca, B.G., K.J. Hanson, and J.J. DeLuisi: Volcanically related secular trends in atmospheric transmission at Mauna Loa observatory, Hawaii. Science, Vol. 202, pp. 513-515, Nov. 3, 1978.

Newell, R.E.: Volcanism and Climate. 1985 Yearbook of Science and the Future. Published by Encyclopedia Britannica, Inc., Chicago, pp. 206-225, 1984.

Pollack, J.B., O.B. Toon, E.F. Danielsen, D.J. Hofmann, and J.M. Rosen: The El Chichon volcanic cloud: an introduction. Geophysical Research Letters, Vol. D, No. 11, pp. 989-992, Nov. 1983.

ACIDITY OF RAINFALL IN THE ALLIGATOR RIVERS REGION NORTHERN TERRITORY, AUSTRALIA

B.N. Noller, N.A. Currey, P.J. Cusbert, M. Tuor, P.F. Bradley
Office of the Supervising Scientist, Alligator Rivers Region Research Institute, Jabiru, N.T. 5796. Australia.

G.P. Ayers and R. Gillett
CSIRO Division of Atmospheric Research, Aspendale, Vic. 3195. Australia

A. Harrison
Environmental Section, Water Division, N.T. Department of Transport and Works, Darwin, N.T. 5794.

Rainfall in the Alligator Rivers Region is restricted to the period October to April. This study of rainwater composition at the township of Jabiru and surrounding sites during the 1982/83 wet season has shown that the pH was consistently between 4.0 and 5.0 Examination of independent measurements of pH at Katherine and Groots Eylandt has revealed the widespread occurrence of acidic rainwater across the northern parts of Northern Australia.

Measurements of anions (sulphate, nitrate, chloride, phosphate) and weak organic acids (formate and acetate) in rainfall, together with pH and conductivity have shown the presence of free acidity in excess of that attributed to dissolved carbon dioxide. Most acidity was associated with the presence of weak acids but acidity due to sulphate in excess of that derived from sea-salt was real and of large magnitude (≈75% of sulphate). No significant differences were found between collection sites (apart from rainfall volume) but significant differences arose during the wet season from climatic events associated with differences between the "transitional" and monsoonal periods of the wet season. Possible natural and anthropogenic sources of acidity are discussed. The impact of sulphur emissions from the Ranger Uranium Mine/Mill Complex (sulphuric acid plant and electricity generating station) on rainwater acidity in the surrounding Jabiru area were examined but the fate of the sulphur dioxide emissions was not known.

Difficulties in establishing the significance of contributions from anthropogenic sources against this background of natural acidity are outlined. This study points to a lack of information concerning rainwater chemistry in tropical regions, particularly those of Australia.

* * *

THE GLOBAL TRANSPORT AND INTER-RESERVOIR EXCHANGE OF CARBON DIOXIDE WITH PARTICULAR REFERENCE TO EFFECTS ON CONCENTRATION AND STABLE ISOTOPIC DISTRIBUTIONS

G.I. Pearman and P. Hyson
CSIRO Division of Atmospheric Research
Private Bag No. 1, Mordialloc, 3195, Australia

Further studies are made using a global 2-dimensional atmospheric transport model coupled to oceanic and biospheric exchange models. The transport model is updated with new wind data and calibrated with recent CCl_3F distributions and release. The biosphere is incorporated as 3 reservoirs of carbon for each latitudional zone (20) of the model, representing carbon with turn-over times on average of 2.6 , 25 and 100 years respectively with respect to the gross primary production, (Table 1, Figure 1). Biomass and productivity are estimated for each zone from a recent 10 x 10 global map of major ecosystems.

All transport and inter-reservoir exchanges treat the isotopic species $^{13}CO_2$ and $^{12}CO_2$ independently and fractionation effects are taken into account. Seasonal variations in gross primary production and respiration are simulated as a function of seasonal temperature variation, while the seasonal imbalance of these, net ecosystem production, is determined such that the model generates surface CO_2 concentration fluctuations which agree with observations. The variation of the seasonal concentration variation with altitude is compared with observations as a validation of the vertical transport (Figure 2).

The relationship between concentration and isotopic variations in the annual cycle are examined in light of the main forcing functions and the future use of isotopic data to refine our general understanding of these cycles is discussed.

The annual average meridional distribution of concentration and isotopic abundance as influenced by fossil fuel combustion and oceanic exchange is compared with observations (Figure 3). Simulations involving hypothetical tropical releases of carbon with oceanic or temperate forest uptake are used to suggest that tropical deforestation can not be a source of atmospheric CO_2 of the magnitude of fossil fuel CO_2.

Simulations of equatorial sea-surface temperature and wind-stress variations and their effects on atmospheric CO_2 concentration and isotopic composition are described.

Table 1.

Meridional distribution of the proportion of land area and fossil fuel CO_2 release, biomass and annual net primary production (NPP) subdivided into latitude zones appropriate for the atmospheric transport model. Estimates for the standing biomass, litter, and soil components are presented. The latter become the third biospheric reservoir of the current model. The sum of the standing and litter biomasses is subdivided to give the first and second biospheric reservoirs of the model.

Latitude Zone	Land area!	Fossil Fuel Release *	Biomass (Gt C)#				NPP ($Gtyr^{-1}$)$	
			Standing	Litter	Soil Res.1	Res.2 Res.3	Matthews	Leith
1 90-64 N	0.32	0.005	21.9	7.6	8.9	20.6 136.3	1.59	1.69
2 64-53 N	0.62	0.141	103.0	16.6	35.9	83.7 207.5	5.00	4.01
3 53-44 N	0.56	0.226	66.9	9.3	22.9	53.3 159.5	4.66	4.61
4 44-37 N	0.46	0.226	30.0	3.3	10.0	23.3 84.0	2.71	3.98
5 37-30 N	0.44	0.205	29.3	2.9	9.7	22.5 79.8	2.77	3.90
6 30-24 N	0.39	0.048	33.8	1.6	10.6	24.8 48.5	2.18	3.14
7 24-18 N	0.33	0.036	29.4	0.8	9.1	21.1 32.4	1.73	3.14
8 18-12 N	0.26	0.018	21.0	0.9	6.6	15.3 48.9	1.81	3.36
9 12- 6 N	0.25	0.013	33.1	1.2	10.3	24.0 65.6	2.53	4.26
10 6- 0 N	0.23	0.012	75.1	1.5	23.0	53.6 88.6	3.78	5.02
11 0- 6 S	0.24	0.011	97.0	1.7	29.6	69.1 108.7	4.64	5.43
12 6-12 S	0.23	0.009	52.2	1.3	16.1	37.4 71.7	2.98	4.78
13 12-18 S	0.23	0.004	25.8	1.2	8.1	18.9 56.4	2.12	3.63
14 18-24 S	0.24	0.009	21.2	1.1	6.7	15.6 51.1	1.84	2.78
15 24-30 S	0.21	0.012	13.1	0.7	4.1	9.7 37.3	1.19	1.99
16 30-37 S	0.13	0.014	7.2	0.6	2.3	5.5 27.0	0.75	1.42
17 37-44 S	0.05	0.008	6.2	0.5	2.0	4.7 9.1	0.33	0.68
18 44-53 S	0.02	0.003	2.9	0.3	1.0	2.2 4.3	0.14	0.25
19 53-64 S	0.02	0.000	0.7	0.1	0.2	0.6 0.1	0.03	0.08
20 64-90 S	0.72	0.000	0.0	0.0	0.0	0.0 0.0	0.0	0.05
Totals			669.8	53.2	217.1	505.9 1316.8	42.78	58.20

! Ratio of land to ocean area for each latitude zone based on Defant (1963). Each zone has the same surface area of 25.5×10^6 km².

* Proportion of total CO_2 production released at each latitude zone averaged over one year, based on Rotty (1983).

\# Biomass of each latitude zone based on the distribution of various ecosystems by Matthews (1983) and the standing biomass of the broad ecosystems by Whittaker and Likens (1973), the litter density by Ajtay et al. (1979) and soil organic carbon densities by Post et al. (1982).

$ Annual Net Primary Production (NPP) of each latitude zone based on the distribution of various ecosystems by Matthews (1983) and the NPP of broad ecosystems by Whittaker and Likens (1973). For comparison the NPP estimates of Lieth (1981) have been converted from units to CO_2 mass to carbon and integrated over the appropriate latitude zones.

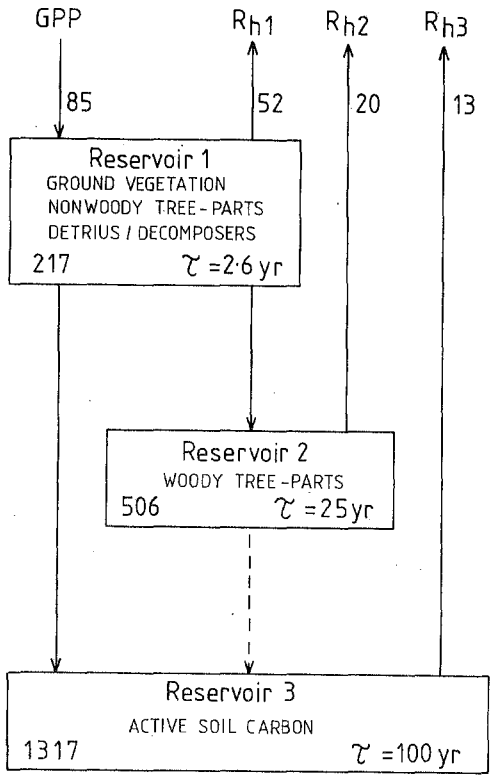


Figure 1.
Carbon reservoirs of the biosphere.

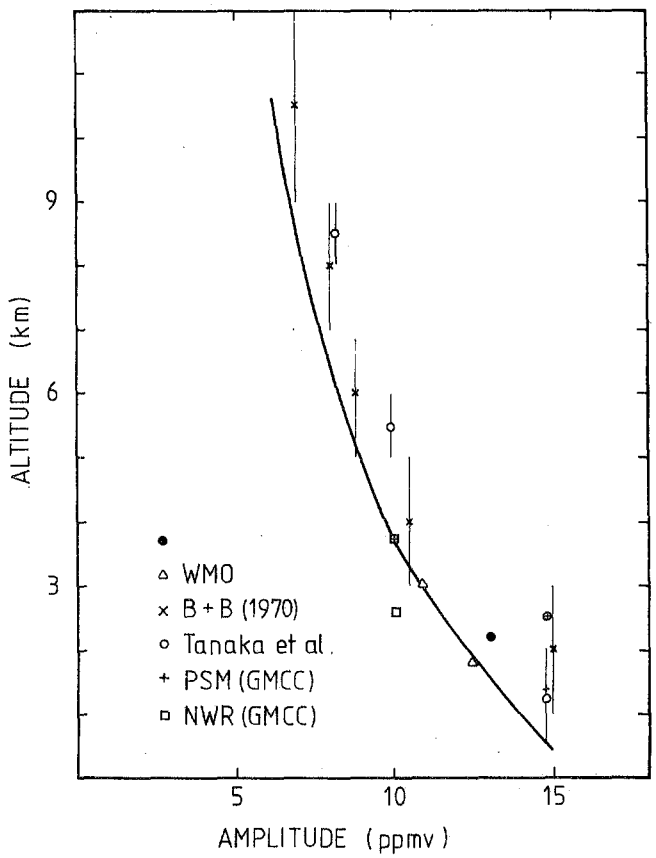


Figure 2.
Amptitude of the seasonal variation of CO_2 concentration versus altitude.

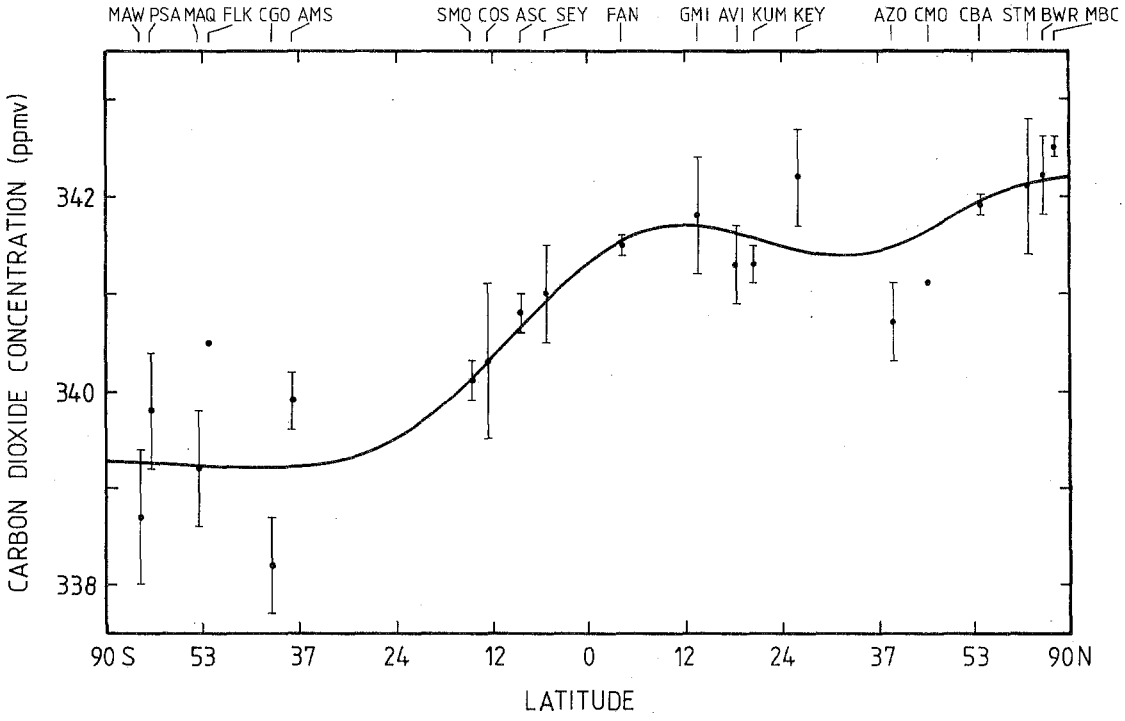


Figure 3.
Observed meridional distribution of CO_2 concentrations.

INTERANNUAL VARIATION OF ATMOSPHERIC CO_2 CONCENTRATION

G.I. Pearman*, M.L. Thompson†, I.G. Enting* and P. Hyson*.

* Division of Atmospheric Research, CSIRO, Private Bag 1, Mordialloc, Vic., 3195 Australia.

† Division of Mathematics and Statistics, CSIRO, Private Bag 10, Clayton, Vic., 3168 Australia.

Baseline CO_2 records have been analysed in order to investigate the interannual variability of the secular increase and the seasonal cycle. An analysis in the frequency domain has been used to investigate records from Mauna Loa, Barrow, the South Pole, Bass Strait, Cape Kumakahi, Samoa, Niwot Ridge and Key Biscayne, each record spanning more than 8 years. This allowed us to check the degree of consistency between different sites more extensively than has been done in previous studies.

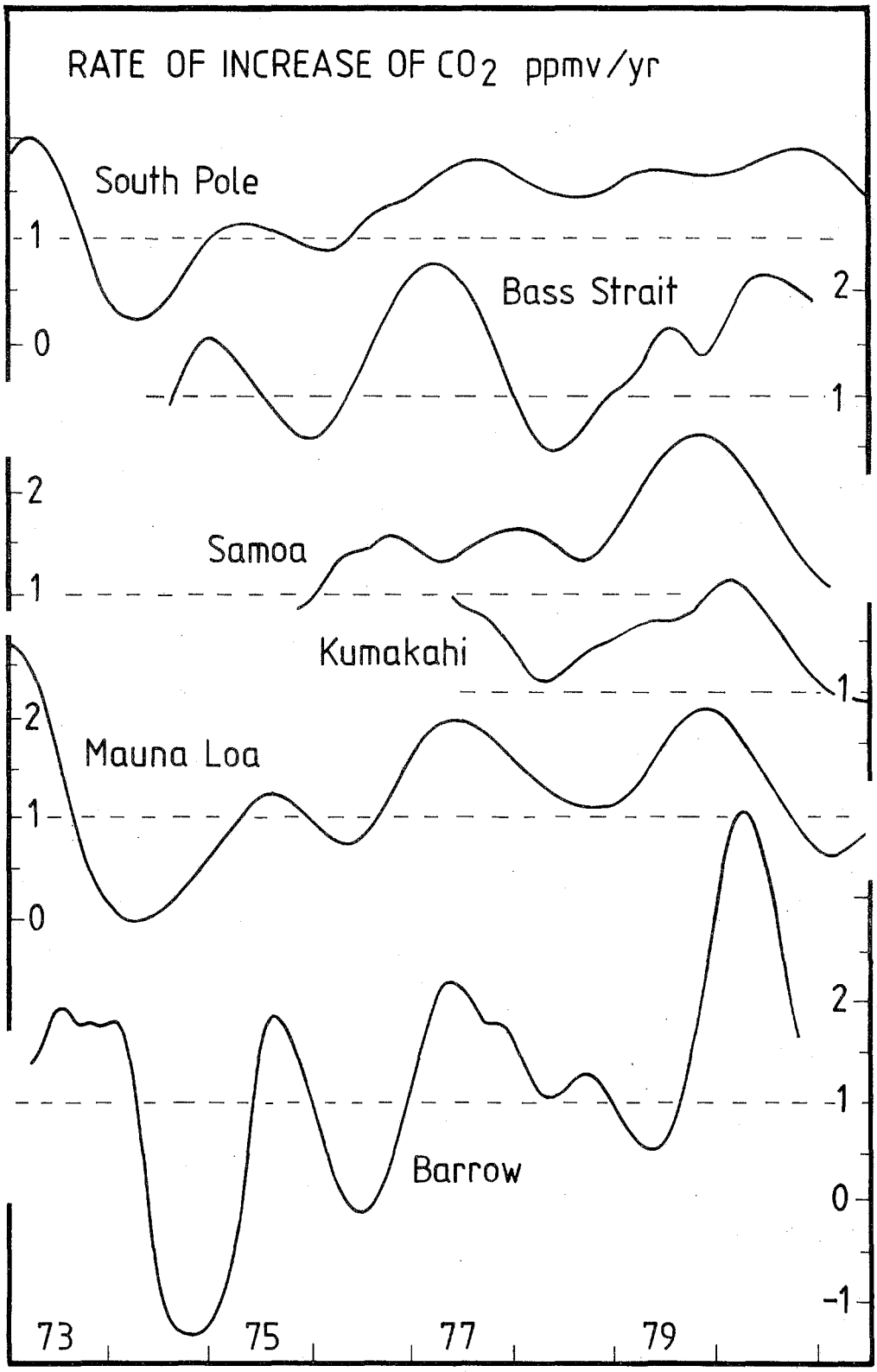
For each series, the rate of change of CO_2 concentration has been obtained by estimating a varying seasonal cycle, removing this cycle, applying a low-pass filter to the series and then finally constructing differences. In these rate of change records we find a consistent signal for five of the sites, (in order of decreasing amplitude) Bass Strait, Barrow, Kumakahi, Mauna Loa and South Pole. The same signal (with marginal statistical significance at the 95% level) is found at Samoa while Niwot Ridge and Key Biscayne were inconsistent with the other sites. The lags between the signals were of order 0 to 6 months. Since these lags had to be estimated from series which had been low-pass filtered they were subject to relatively large uncertainties. The general pattern was Bass Strait and Mauna Loa leading with the South Pole 2 or 3 months behind and Barrow a further 2 to 3 months behind. The signal at Samoa appeared to be in phase with Bass Strait and Mauna Loa but estimates of the phase lag for Samoa were very uncertain because of the small amplitude of the signal. The intercomparison between the various rate-of-change series was undertaken by using a regression analysis defined in the frequency domain. The reason for this was to enable us to carry out a correlation analysis that properly allowed for the fact that the series were autocorrelated.

The same technique has also been used to relate the rate-of-change series to series characterising the Southern Oscillation, Northern hemisphere surface air temperatures and the quasi-biennial oscillation. For each of these series, significant correlations were found with the rate-of-change series for the South Pole, Barrow, Bass Strait, Mauna Loa and Kumakahi. The relative lags deduced from this analysis were generally consistent with those obtained by direct intercomparison of the CO_2 series.

Some possible mechanisms for the interannual variation have been investigated using a two-dimensional atmospheric transport model coupled to an ocean surface mixed layer. It is found that possible sea-surface temperature changes are inadequate as a cause of the observed variations in the CO_2 signal.

A possible mechanism for the interannual variation is an imbalance between the annual photosynthetic uptake of CO_2 and the release of CO_2 through respiration. The observed interannual variations correspond to about 1 to 2 Gt of carbon which represents about 1% of the annual net primary production. There is no indication of any significant correlation between the rate of change series and the series representing the amplitude of the seasonal cycle. Such a correlation would have been one indication of a

biospheric influence on the interannual variability. The amounts of carbon involved imply that a biospheric origin for the interannual variability of CO_2 should give observable changes in $^{13}C:^{12}C$ ratio in the atmosphere if the precision of the most recent records can be maintained over sufficiently long periods.



MEASUREMENTS OF ATMOSPHERIC CO_2 AT BARROW, ALASKA FROM THE U.S. NOAA/GMCC PROGRAM

James T. Peterson

U.S. Department of Commerce/NOAA
325 Broadway
Boulder, CO 80303 U.S.A.

1. INTRODUCTION:

The NOAA/GMCC baseline observatory at Barrow, Alaska is located near the northernmost point of the United States. The village of Barrow, some 7 km to the southwest of the observatory, has a population of about 2500. The Naval Arctic Research Laboratory (NARL), about 2 km west, currently has a population of less than 100 people.. The prevailing winds are from north through east, directions from which there is very little local influence on the measurments.

We present in this paper an overview of the Barrow, Alaska, CO_2 data set obtained from a continuously operating in situ analyzer along with a brief look at the flask sample data set from the same location. A complete discussion of the flask sample data has been prepared by Komhyr et al. (1984). The general characteristics of the data are similar to those described in our earlier paper (Peterson et al., 1982). The secular trend from 1974 through 1982 averages nearly 1.3 ppm/yr.

A description of the GMCC CO_2 measurement program at Barrow, Alaska, has been published previously (Peterson et al., 1982). Therein, we described the CO_2 analyzer setup, surrounding terrain, experimental method, data reduction, and other logistical and historical aspects of the CO_2 measurement program at Barrow. The CO_2 data were presented in the SIO 1959 Adjusted Index Scale and as mole fractions with a pressure-broadening correction applied.

Recently, we have reprocessed our complete CO_2 histrocial record. the data are now on a new WMO-endorsed mole fraction scale, namely the Scripps Institution of Oceanography (SIO) 1981X scale, which incorporates the latest manometric calibration information developed by SIO. The updated CO_2 values presented here, now on the SIO 1981X scale, are similar to the mole fractions presented in our 1982 article. The differences between the two data sets stem largely from a more carefully derived pressure-broadening correction as well as updated calibration values of our secondary standard tanks provided by the SIO central laboratory.

2. THE DATA:

The results of our extensive reprocessing effort are shown in Figure 1. Monthly averages of selected data from the Barrow Observatory are presented from the beginning of the record in mid 1973 through 1982. Similar data are shown from our baseline observatory at Mauna Loa, Hawaii. They are presented for general comparison to the Barrow data and will not be discussed in any detail. The Barrow data have been selected to screen out those hours where the measurements are not representative of larger scale background conditions. That is, if the hour-to-hour CO_2 change exceeded 0.25 ppm, those 2 hours were screened out from the record. The philosophy behind this method is that air masses with homogeneous CO_2 concentrations representative of large scale atmospheric processes will exhibit small hour-to-hour changes of CO_2. Conversely, large hour-to-hour changes would be indicative of locally contaminated measurements.

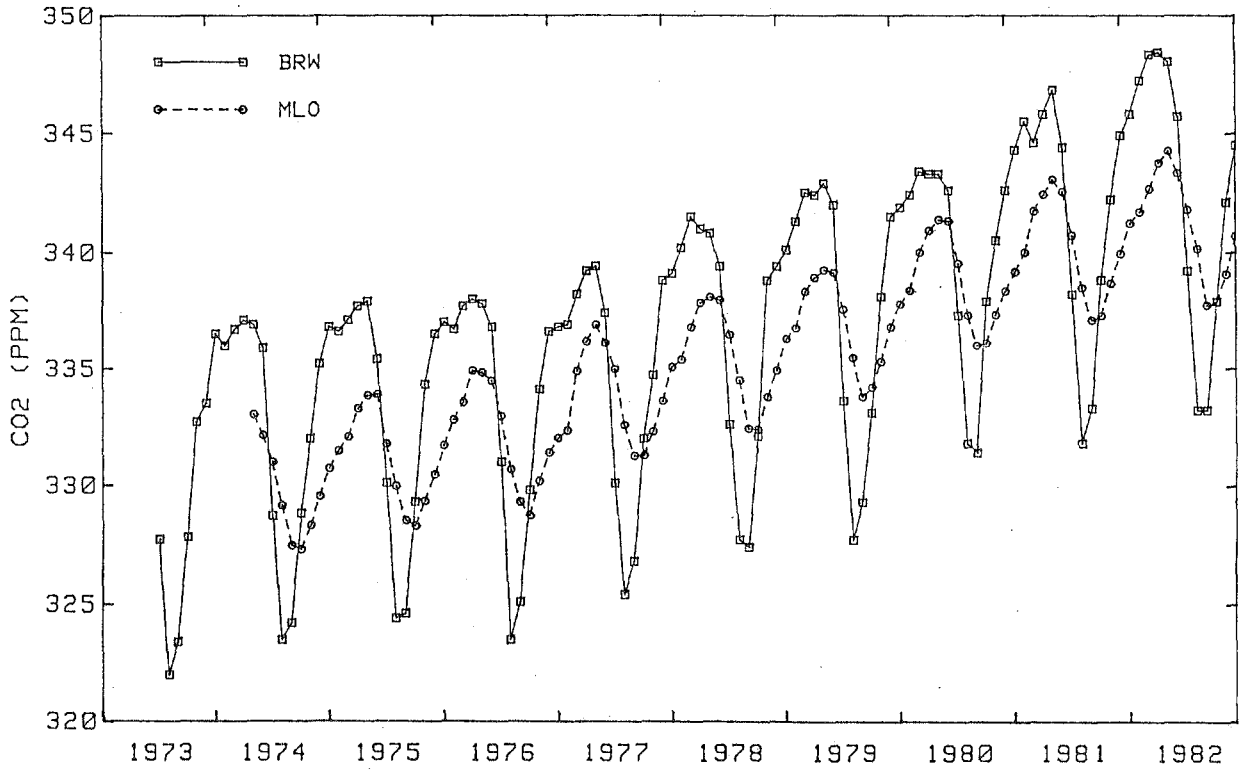


Figure 1. Monthly average CO_2 concentration at Barrow, Alaska, and Mauna Loa, Hawaii, 1973-1982. Selected data for background values are presented on the Scripps 1981X manometric scale.

The obvious features of the Barrow record are the large amplitude annual cycle and the long-term increase. The annual cycle of about 15 ppm amplitude exhibits a minimum in August-September and an April-May maximum. In contrast, the Mauna Loa annual cycle has an amplitude of only about 6 ppm with the maximum occurring slightly later and the minimum averaging about 2 months later. The general features of the Barrow annual cycle are quite repeatable from year to year, but variations with timescales less than a month can be quite different from year to year.

Recently, there has been interest in the amplitude of the CO_2 annual cycle over the globe and its possible changes with time. For example, Bacastow and co-workers at SIO (1984) have determined that a significant increase in amplitude has occurred over the nearly 25 year record of Mauna Loa. At Barrow, over the quite shorter record, there is a suggestion of increasing amplitude with time, but the results are not statistically significant.

Mean annual concentrations and year-to-year changes are shown in table 1. The growth rate in recent years has been much greater than that during the first 3 years of the record. The 8-year CO_2 increase was 10.2 ppm, yielding an average growth rate of nearly 1.3 ppm/yr. The mean nearly reached 343 ppm by 1982. The year-to-year change (shown in column 3), however, was quite variable, ranging from only 0.3 (1975-1976) to 2.0 ppm/yr on two occasions.

The low values of 1982 were affected by the very pronounced El Nino/ Southern Oscillation (ENSO) event of that year. During the last one-third of the year the CO_2 concentrations at Barrow were actually less than those of the previous year. This (temporary) reversal of the CO_2 trend at Barrow was likely associated with very warm sea surface temperatures in the eastern equatorial Pacific. Moreover, upwelling of naturally CO_2 rich water in this

region was significantly reduced along with the strength of the tradewinds. Consequently, this natural CO_2 source was significantly lessened during 1982. We can now report, however, that during 1983 the CO_2 growth rate clearly rebounded from the negative values of late 1982. The CO_2 measurements during the latter part of 1983 are some 2-3 ppm greater than those of the previous year.

Table 1. Annual average CO_2 concentrations at Barrow, Alaska, and year-to-year changes. Data are expressed in the SIO 1981X manometeric scale.

Year	Mean CO_2 Concentration	Year-to-Year Change
1974	332.6	
		0.8
1975	333.4	
		0.3
1976	333.7	
		1.0
1977	334.7	
		2.0
1978	336.7	
		1.2
1979	337.9	
		2.0
1990	339.9	
		1.8
1981	341.7	
		1.1
1982	342.8	

In addition to the continuously operating in situ nondispersive infrared analyzer at the observatory, we also collect 0.5-liter glass flasks of air for a subsequent analysis at our central facility in Boulder. Typically, a pair of these flasks are filled with ambient air twice a week. While the flask record cannot reveal very short term variability, it does clearly show the annual cycle and long-term trend. The two data sets do show good general agreement. Annual averages over the 9 years of record agree within ±0.4 ppm.

Other data sets from high Northern Hemisphere latitudes are available for comparison to the Barrow record. CO_2 measurements from Ocean Station P (50°N) conducted by C. S. Wong and C. D. Keeling reach back to 1969. the Canadian government program at Alert (82.5°N) began in 1975. NOAA flask samples from Cold Bay, Alaska (55°N) are available from 1978. Integration of these data sets shows CO_2 time and space variability in response to regional/global scale CO_2 sources and sinks and atmospheric transport.

REFERENCES

Bacastow, R. B., C. D. Keeling, and T. P. Whorf, 1984: Seasonal amplitude increase in atmospheric CO_2 concentration at Mauna Loa, Hawaii, 1959-1982. (draft manuscript).

Komhyr, W. D., R. H. Gammon, T. B. Harris, L. S. Waterman, T. J. Conway, W. R. Taylor, and K. W. Thoning, 1984: Global atmospheric CO_2 distribution and variations from 1968-1982 NOAA/GMCC CO_2 flask sample data. J. Geophys. Res., (submitted).

Peterson, J. T., W. D. Komhyr, T. B. Harris, and L. S. Waterman, 1982: Atmospheric carbon dioxide measurements at Barrow, Alaska, 1973-1979. Tellus, 34, 166-175.

THE INTERPRETATION OF ATMOSPHERIC TURBIDITY MEASUREMENTS

C. M. R. PLATT

CSIRO, Division of Atmospheric Research
Private Bag 1, Mordialloc, Vic. 3195 Australia.

The atmospheric turbidity, or aerosol optical depth, of the atmosphere is a mandatory requirement at Baseline Stations. The main concern about aerosols is based on their widespread occurrence globally, and partially anthropogenic origin, leading to a potential influence on climatic change. Aerosols scatter and absorb both solar visible and terrestrial infrared radiation thus affecting the radiation balance.

The turbidity or optical depth, gives the integrated effect of aerosols in an atmospheric column at the wavelength measured, which is related directly to the solar albedo and infrared emittance. However, the detailed effects of aerosols depend on several quantities. The single scattering albedo ωo determines how much radiation is absorbed and how much is scattered in an aerosol volume. The asymmetry parameter $\langle \cos\theta \rangle$ determines the amount of radiation scattered in the back hemisphere which is related directly to the albedo. Moreover, the radiative interaction in the atmosphere depends on the altitude distribution of aerosols, and furthermore the total effect is a spectrally integrated one over all wavelengths.

Thus the detailed knowledge of aerosols, which is required for a proper assessment of their climatic effects, can only be obtained by a number of different measurements. A sunphotometer can measure the optical depth at a number of wavelengths across the solar spectrum and as the optical depth is normally a smoothly varying function of wavelength, a measurement at about six wavelengths is probably sufficient. Continuous measurement with such an instrument will indeed determine whether there is an increase in aerosol optical loading in time, provided that the effects of local aerosol sources, such as urban areas, are excluded. But is this increase due to solar absorption, or scattering, and at what height in the atmosphere are the aerosols increasing? For instance, volcanic eruptions can cause considerable increases in aerosol loading in the atmosphere, aerosols which are then diffused rapidly in the upper troposphere and stratosphere by high winds. Moreover, the stratospheric aerosol layer can remain there for several years. How is this layer to be considered? Should only 'background' periods in stratospheric aerosol be used in assessing increases in turbidity? The volcanic outbreaks can cause appreciable perturbations to the radiative balance thereby perturbing the upper winds for several years, so that they re indeed a climatic effect in that timescale.

The presence and mass volcanic aerosols can only be assessed unambiguously by balloon sonde, lidar or aircraft flights. The solar absorbing and scattering properties similarly can only be obtained by a detailed investigation of the composition of aerosols and their size distribution, or by optical methods which investigate small volumes of aerosols. The infrared effects of aerosols, perhaps of less importance because of the small aerosol size, can still be significant, at times.

How are all these effects to be measured? South the Baseline program aim to have a more comprehensive set of aerosol measurements at each Station? This is a question which needs discussion.

Turbidity measurements at Aspendale over an extended period and at Cape Grim over the last few years illustrate trends and annual variations which are not immediately explainable. The availability of measurements of aerosol number, composition and size distribution at Cape Grim highlights the utility of such measurements in the interpretation of atmospheric turbidity and the desirability of an integrated program.

THE ZONALLY- AVERAGED TRANSPORT CHARACTERISTICS OF A GCM AND A TEST OF THE VALIDITY OF "K-THEORY" AS A PARAMETERIZATION OF EDDY TRANSPORT.

R. Alan Plumb

CSIRO Division of Atmospheric Research.
Private Bag 1, Mordialloc, Vic. 3195 Australia.

Two-dimensional (zonally-averaged) modelling has become an established technique for the simulation of the global structure of trace constituents. Such models are much simpler to formulate and cheaper to operate than three-dimensional general circulation models while avoiding some of the gross (and theoretically ill-founded) simplifications of one-dimensional models. Nevertheless, the parameterization of eddy fluxes required in a 2-D model is not a trivial problem. Indeed, this fact has apparently led some to interpret the shortcomings of existing 2-D models as indicating that the parameterization procedure is wrong in principle. There are grounds to believe, however, that these shortcomings result primarily from incorrect implementations of the predictions of eddy transport theory and that a properly based parameterization may provide a good basis for atmospheric constituent modelling.

In most 2-D models the unresolved eddies are parameterized on the basis of "K-theory", i.e. the eddy flux u'q' of a tracer of zonally-averaged mixing ratio q is specified via a flux-gradient relationship

$$\underset{\sim}{\overline{u'q'}} = - \underset{\sim}{\underset{\sim}{K}} . \underset{\sim}{\nabla} \overline{q}$$

where K is a four-component transport tensor. The symmetric part of this tensor is a representation of diffusive transport, while the antisymmetric part is advective (i.e. it represents a correction that must be applied to the mean wind field in order to obtain the velocity distribution which determines the total advective transport).

While the flux-gradient relation has been in use for some years, it is only relatively recently that it has been formally justified, under the assumption of small-amplitude eddies. Even if it is assumed that this validity extends to realistic flows, the determination of K is a not a simple task. Direct application of the results of small-amplitude theory is impracticable, since this would require knowledge of Lagrangian statistics which are not available from observations. Some attempts have been made to estimate K from Eulerian statistics (on the basis of ill-founded assumptions) or from observed tracer distributions (which yield insufficient information to determine K uniquely).

Given these difficulties and uncertainties in the determination of the transport coefficients from atmospheric data, it seems appropriate to calculate them for a general circulation model; the advantages of a truly objective derivation almost certainly outweigh the shortcomings of the models. In collaboration with J.D. Mahlman, the GFDL general circulation/tracer model was used to generate eddy flux statistics in artificial tracer experiments; K was then derived by inversion of the flux-gradient relation.

In the first part of this talk, the transport characteristics of the GCM

will be described, and related to dynamical processes in the (model and real) atmosphere. The effective transport circulation differs substantially from the Lagrangian mean and residual circulations and is the simplest representation of the model circulation. The diffusive component is coherently structured, comprising the following components:

1) Strong quasi-horizontal mixing ($K_{yy} \sim 1 \times 10^6$ m^2 s^{-1}) in the midlatitude lower troposphere, apparently associated with fronts and the occlusion of synoptic systems.

2) A band of strong quasi-horizontal mixing ($K_{yy} \sim 2 \times 10^6$ m^2 s^{-1}) stretching across the tropical upper troposphere and the subtropical upper troposphere and the subtropical winter stratosphere. This band follows the band of weak zonal mean winds and is a manifestation in the model of the "surf zone" recently identified by McIntyre and Palmer as a region of breaking planetary waves.

3) Intense vertical mixing ($K_{zz} \sim 30$ m^2 s^{-1}) in the troposphere at and near the latitudes of the intertropical convergence zone.

4) Vertical mixing ($K_{zz} \sim$ 5-10 m^2 s^{-1}) through much of the troposphere, associated with subgrid-scale mixing (e.g. model convective processes).

Implications of the results for transport modelling will be discussed.

The existence of these GCM-derived coefficients affords an unprecedented opportunity to test the validity of the flux-gradient parameterization. To this end, a zonally-averaged (2-D) model was developed, using these coefficients in the transport parameterization. Results from this model for a number of contrived tracer experiments were compared with the zonally averaged results from identical experiments with the parent GCM. In the second part of the talk, these results will be presented and discussed; the generally very good agreement substantially validates the flux-gradient parameterizaton and thus the basic principle of 2-D modelling.

SIMULATIONS OF CHLOROFLUOROCARBONS WITH A THREE-DIMENSIONAL MODEL

Michael Prather
Center for Earth & Planetary Physics
Harvard University
Cambridge, Massachusetts 02138, USA.

The results from three-dimensional model studies of trace gases in the troposphere are presented. Calibration and verification of these tracer models require an observational database of global extent such as that provided by NOAA's GMCC network and by the Atmospheric Lifetime Experiment. Emphasis will be placed on model simulations of the chlorofluorocarbons 11 and 12 and comparisons, where possible, with measurements (e.g., the ALE data).

The 3-D tracer model is based on the general circulation model developed at Goddard Institute for Space Studies by Hansen and co-workers (see Fig. 1-2). The simulation of CFC concentrations from 1970 through 1981 is based on a time-dependent pattern for CFC emissions, on mixing and transport from GCM, and on photochemical losses in the stratosphere. The GCM is designed as a global climate model, not for use in simulating any specific period of weather.

The modelled CFC distribution indicates notable gradients not only with latitude but also with longitude and altitude within the troposphere (see Fig. 3-4). Furthermore, the model shows synoptic scale variability for locations near source regions as shown in Fig. 5. Comparison of the high frequency ALE measurements at different stations with tracer model results (8-hour resolution) verifies that the model may be used, in some circumstances, to predict the variability at an observing station. However, caution must be exercised in such analyses in that (i) considerable noise is often found in the data and (ii) the current tracer model cannot resolve scales less than 500 km.

Three-dimensional tracer models are developed now to the extent that they may aid in planning measurement strategies or interpreting observations from a sparse global network. Indeed, some key results of the model for CFCs must be verified: for example, the predicted decline above the boundary layer of northern continents, and the increase with altitude over much of the Southern Hemisphere. Similarly, the details of the CFC distribution in the Southern Tropics is essential to understanding the meteorological mechanisms responsible for interhemispheric exchange.

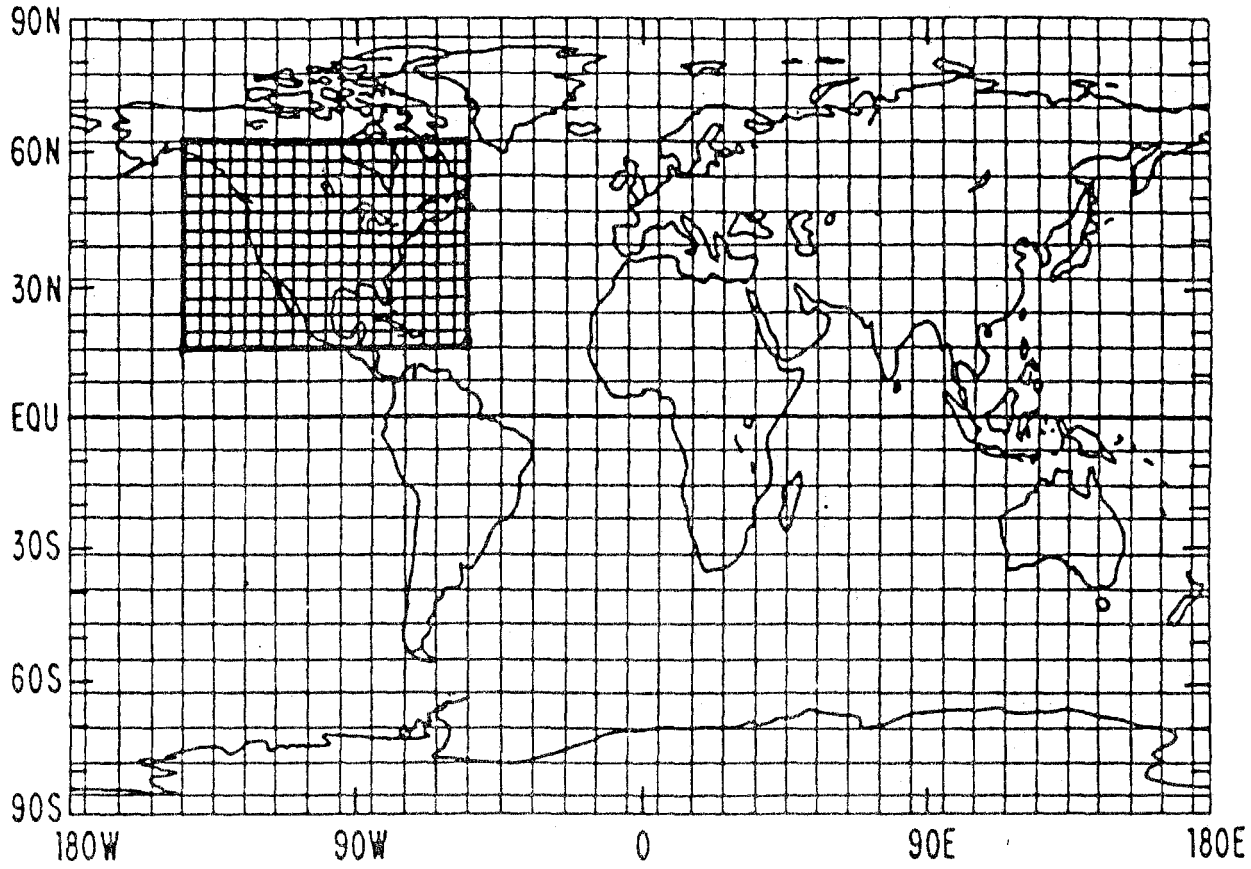


Figure 1. Horizontal resolution of the GCM and tracer model $8^{o}x10^{o}$ grid squares and (inset) $4^{o}x5^{o}$ grid squares.

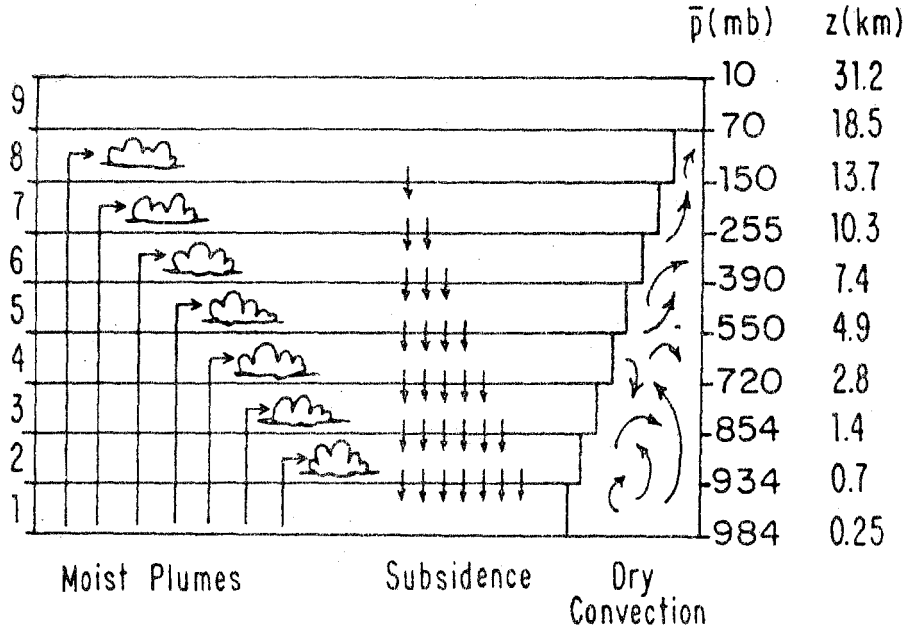


Figure 2. Schematic depiction of vertical structure of the GCM and the subgrid-scale vertical transport processes.

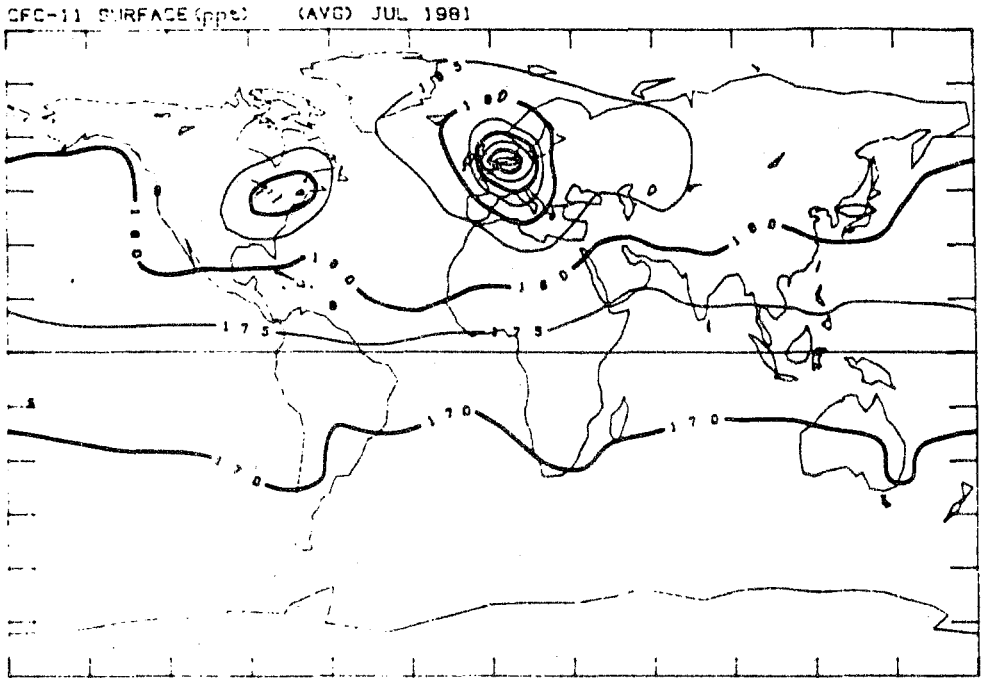


Figure 4. Same as Figure 3 for July, 1981.

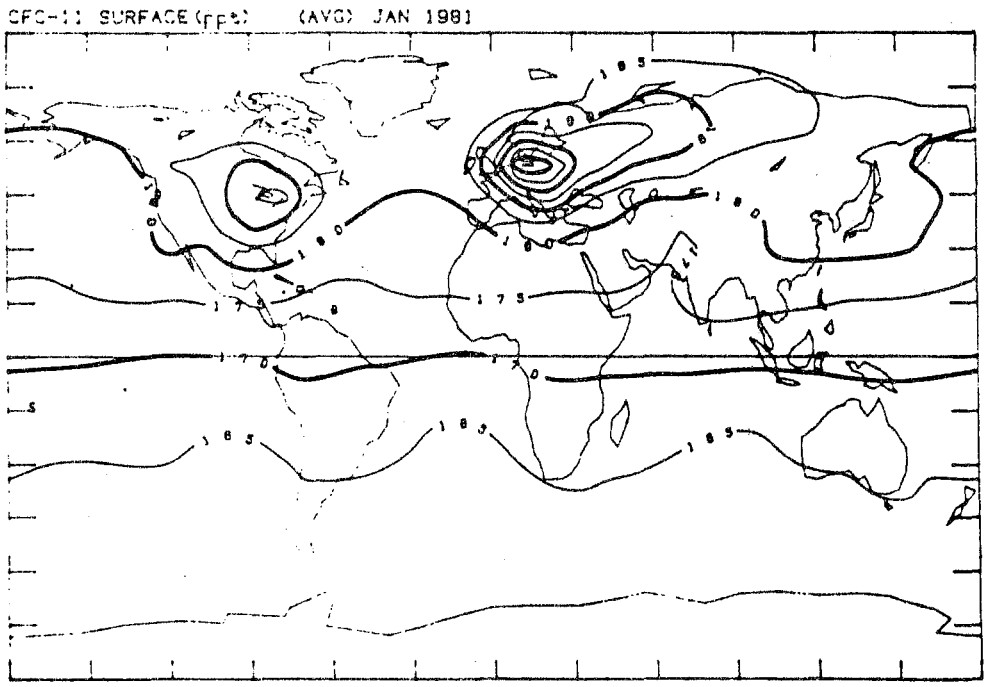


Figure 3. Calculated surface layer concentrations of CFC-11 averaged for January 1981.

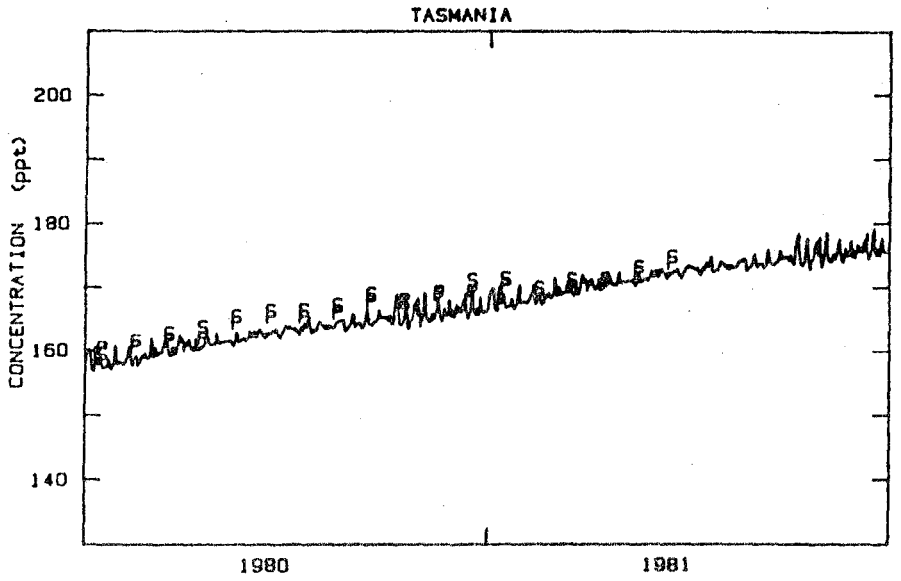


Figure 5. Calculated concentrations for CFC-11 at Tasmania for 1980-1981. Monthly means of data from the ALE network are shown by the symbols S and P.

A GLOBAL THREE DIMENSIONAL MODEL OF THE CIRCULATION AND CHEMISTRY OF $CFCl_3$, CF_2Cl_2, CH_3CCl_3, CCl_4 and N_2O

Ronald G. Prinn and Amram Golombek

Center for Meteorology and Physical Oceanography
Massachusetts Institute of Technology
Cambridge, Massachusetts 02139

An efficient three-dimensional spectral model is used to investigate the circulation, chemistry, and photochemistry of the long-lived atmospheric species $CFCl_3$, CF_2Cl_2, CH_3CCl_3, CCl_4, and N_2O.

The model uses pre-calculated three-dimensional spectral fields of vorticity, vertical velocity, temperature, and ozone concentration and current estimates of the magnitudes and distributions of industrial and natural sources of the various species. Explicit calculations of instantaneous photodissociation rates for each species are carried out and reactions with atmospheric OH and $O(^1D)$ and dissolution in the ocean are also included in the model where relevant. Available measurements of the horizontal, vertical, and temporal distribution of the modelled atmospheric species generally compare favourably with our calculations. However, there are some disagreements, in particular between the observed and calculated global surface distributions of CH_3CCl_3 and global trends and vertical distributions of CCl_4, which are critically discussed. Assuming that their destruction is dominated by photodissociation and reaction with $O(^1D)$, the calculated present-day atmospheric lifetimes of $CFCl_3$, CF_2Cl_2, CCl_4, and N_2O are respectively 78, 232, 49, and 185 years.

Decreasing the O_2 absorption cross-sections in the Schumann-Runge continuum (2000-2200Å) by 40% results in a decrease of the $CFCl_3$ lifetime to 45 years. The calculated atmospheric lifetime of CH_3CCl_3 due to photodissociation and reaction with OH and $O(^1D)$ is 12 years. The latter calculation utilizes a seasonally-dependent zonally-invariant OH distribution with an annual-average tropospheric OH concentration of 7×10^5 molecule cm^{-3}.

RADON MEASUREMENTS AS AN AID TO INTERPRETATION OF ATMOSPHERIC MONITORING

by S. Whittlestone

The predominant sources of radon in the atmosphere are the continents. Thus the presence of radon in an air stream indicates that at least some of the air has recently been over a continent, thereby affecting the concentrations of some of the constituents, such as ozone, carbon dioxide or particles.

This paper describes the radon measurement program at Cape Grim, Tasmania, where radon has been measured for several years. The low levels of radon, about 0.5 Bq m^{-3}, and variability of concentration over periods of a few hours, have required development of a highly sensitive detector capable of operating continuously.

Radon levels which can be expected from a purely continental air have been established from measurements in South Australia and Sydney. The annual average of 3.8 Bq m^{-3} in northerly air streams at Cape Grim is considerably less than the 9.3 Bq m^{-3} average for continental air in Sydney. Reasons for this difference are discussed.

The origin of radon in maritime air is shown to be almost entirely continental. The contribution of the ocean to radon concentration is probably less than 10% of the lowest levels observed at Cape Grim (0.3 Bq m^{-3}). This result is supported by strong radon/particle and radon/ozone correlations in maritime air. The data suggest that most of the particles at Cape Grim are of continental origin. This is difficult to reconcile with strong evidence from Antarctic stations that the annual variations of particle concentrations are due to photo-chemical reactions over the ocean. Clarification of this phenomenon will require extension of the radon measurement program to other stations.

It is concluded that radon is able to provide a continuous record of continental influence down to a few percent in maritime air. This would not be possible using air trajectory analysis. With its simple source and loss mechanisms, radon can provide much less equivocal evidence of the past history of an air stream than can other atmospheric constituents. When measurements of several constituents are combined it is possible to clarify the mechanisms affecting each constituent separately.